2019

Modulation of inflammatory process and tissue regeneration in calvaria mouse models

BOSTON UNIVERSITY

HENRY M. GOLDMAN SCHOOL OF DENTAL MEDICINE

DISSERTATION

MODULATION OF INFLAMMATORY PROCESS AND TISSUE REGENERATION IN CALVARIA MOUSE MODELS

by

JACOB YOUSEF KHADUM AL-HASHEMI

B.D.S, Al-Mustansiriyah University, 2006
M.S. Biomaterials, SUNY at Buffalo, 2013

Submitted in partial fulfillment of the requirements for the degree of

Doctor of Science in Dentistry in Endodontics
In the Department of Molecular and Cell Biology

2019

Approved by:

First Reader _____

Salomon Amar, Ph.D., D.M.D.

Professor of Molecular and Cell Biology

Second Reader_____

Eva Helmerhorst, Ph.D.

Associate Professor of Molecular and Cell Biology

Committee Member _____

Phillip Trackman, Ph.D.

Professor of Molecular and Cell Biology

Committee Member_____

Frank Oppenheim, Ph.D., D.M.D.

Professor of Molecular and Cell Biology

DEDICATIONS

To my Son,

To my live companion and lovely wife

Without her love, encouragement, support, and sacrifice this work would have not seen the light of day.

To my adoring parents,

Who taught me to live life to the fullest, believe in hard work and doing much with little.

To my beloved brother

To my cute sisters,

Who were my guardian during my education.

ACKNOWLEDGEMENTS

The present work was carried out at the Department of Melocular and Cell Biology, Henry M. Goldman School of Dental Medicine, Boston University, Boston, Massachusetts, USA, with a scholarship of the Higher Committee for Education development in Iraq (HCED in Iraq) as well as the generous financial support from the Dean's scholarship.

First and foremost, I would like to express my sincere appreciation and gratitude to my advisor, Dr. Salomon Amar, for his excellent guidance, constant support, and continuous encouragement throughout my research. For the past year, his enthusiasm for research, positive attitude toward work, and appreciation for science have motivated me. None of my present work would have been seen the light of day without his advice and instruction.

I also appreciate Dr. Sami Chogle, Chairman of the Department of Endodontics, for providing such an excellent educational environment.

I would like to extend my thanks to Dr. Abdulsalam Al-Shamarri, Jayesh Petal and Marina Burkatovskaya, who worked with me in the same laboratory, for their expertise and assistance.

MODULATION OF INFLAMMATORY PROCESS AND TISSUE REGENERATION IN CALVARIA MOUSE MODELS

JACOB YOUSEF KADHUM AL-HASHEMI

Boston University**,** Henry M. Goldman School of Dental Medicine, 2019

Major Professor: Salomon Amar, Professor of Molecular and Cell Biology

ABSTRACT

MicroRNAs (miRNAs) are short, non-coding RNAs involved in the regulation of several processes associated with inflammatory diseases and infection. Bacterial infection modulates miRNA expression to subvert innate immune response. In this study, we analyzed bacterial modulation of miRNAs in bone-marrow-derived macrophages (BMMs), in which activity was induced by infection with *Porphyromonas gingivalis* (*Pg)* through a microarray analysis. Several miRNA expressions levels were modulated 3 hours post infection (at a multiplicity of infection (MOI) of 25). A bioinformatics analysis was performed to further identify pathways related to the innate immune host-response pathways that are under the influence of the selected miRNAs. To assess the effects of the identified miRNAs on cytokines secretion (pro-inflammatory TNF-α and anti-inflammatory IL-10), BMMs were transfected with selected miRNAs mimics or inhibitors. Transfection with mmu-miR-155 and mmu-miR-2137 did not modify TNF-α secretion while their inhibitors increased it. Inhibitors of mmu-miR-2137 and mmu-miR-7674 increased the secretion of the anti-inflammatory IL-10. In *Pg*-infected BMMs, mmu-miR-155-5p significantly decreased TNF-α secretion while inhibitor of mmu-miR-2137 increased IL-10 secretion. *In vivo,* in a *Pg*-induced calvarial bone resorption mouse model, injection of mmu-miR-155-5p or anti-mmu-miR-2137 reduced the size of the lesion significantly. Furthermore, anti-mmu-miR-2137 significantly reduced inflammatory cell infiltration, osteoclast activity and bone loss. Bioinformatics analysis demonstrated that

pathways related to cytokines and chemokines related pathways but also osteoclast differentiation may be involved in the observed effects. The study highlights the potential therapeutic merits of targeting mmu-miR-155-5p and mmu-miR-2137 to control inflammation induced by *Pg* infection.

To assess the regenerative process in the same animal model, we aimed to compare the effect of Bone Morphogenic Protien 2 (BMP2), Platelets Rich Plasma (PRP), Leukocyte-Platelets Rich Fibrin (L-PRF), and Polygucosamine (PGIcNAc) on bone formation in critical size bone defects in mice. One-hundred-thirty-eight mice were divided into 23 groups (n=6), negative control, different combinations of the PGIcNAc with or without of BMP2, Collagen Sponge (SurgiFoam), PRP, and L-PRF. The 5mm defect, then, was allowed to heal. After six weeks, samples were analyzed for bone formation utilizing radiographs, H&E staining, alkaline phosphatase staining. Our results show that BMP2 were able to produce 90-95% healing of critical size defects after six weeks histologically and radiographically. However, SurgiFoam, PRP and L-PRF with or without PGIcNAc were able to close 60% of the original defect. This study supports that BMP2 is more effective for bone regeneration than SurgiFoam, PRP, L-PRF and PGIcNAc.

TABLE OF CONTENTS

LIST OF TABLES

LIST OF FIGURES

LIST OF ABBREVIATIONS

BMMs	Bone-marrow-derived macrophages
BMP2	Bone Morphogenic Protein 2
cBone	Crushed Homologous Bone
CSD	Critical Size Defect
cTM	Crushed Poly-N-Acytel-glucosamine placed inside the defect
IL-10	Interleukin 10
IL-6	Interleukin 6
L-PRF	Leukocyte-Rich-Platelets-Fibrin
LPS	lipopolysaccharides
miRNA	MicroRNA
mRNA	Messenger RNA
PD	Periodontitis
Pg	*Porphyromonas gingivalis*
PGIcNAc	Poly-N-acetyl glucosamine
PRP	Platelet-Rich-Plasma
TGF-β	Transforming Growth Factor Beta
TLR	Toll-like receptor
TM out	Poly-N-Acytel-glucosamine sheets outside the defect

TMgel	Poly-N-Acytel-glucosamine gel
TNF-α	Tumor Necrosis Factor Alpha

1. INTRODUCTION

1.1.Modulation of Inflammation

Periodontitis (PD) is a common chronic inflammatory disease which can induce the destruction of tooth-supporting tissues (Pihlstrom *et al.*, 2005; Hajishengallis & Lamont, 2014) and has been linked to several systemic diseases, such as cardiovascular diseases (Zhou & Amar, 2007; Hajishengallis, 2015). The pathogenesis of PD is associated with a dysbiosis of periodontal microbiota. This dysbiosis is characterized by a shift from a symbiotic microbial community to a pathogenic one which is mainly composed of anaerobic bacteria, resulting in an alteration of the host-microbe cross-talk (Hajishengallis, 2015). *Porphyromonas gingivalis* (*Pg*) is a gram-negative anaerobic bacterium, considered as a keystone-pathogen in PD (Hajishengallis, 2015). It produces several virulence factors such as lipopolysaccharides (LPS) and fimbriae, the later facilitating the invasion of different cell types, such as endothelial (Rodrigues *et al.*, 2012) and epithelial cells (Kato *et al.*, 2014; Morandini *et al.*, 2014). Several mechanisms are induced by *Pg* such as modulation of gene and protein expression, thereby compromising immune function at the periodontal level (Zhou *et al.*, 2007; Hajishengallis *et al.*, 2014). For instance, in endothelial cells, *Pg*, through its LPS, not only increases secretion of several pro-inflammatory cytokines including TNF-α and IL-6 but also of anti-inflammatory cytokines such as IL-10 demonstrating the complexity of the cell's response to infection (Bugueno *et al.*, 2016). These inflammatory processes and immune responses activated after bacterial infection are also responsible for tissue destruction.

Macrophages are pivotal cells in the host-response due to their direct contact with infectious agents or their byproducts (Giannobile, 2008; Kebschull & Papapanou, 2015). These cells are often found in chronic periodontitis diseased tissues (Gemmell *et al.*, 2001) and represent an important fraction of the total inflammatory cell population (Okada & Murakami,

1998). *Pg* has been demonstrated to activate macrophages (Yu *et al.*, 2010; Kebschull *et al.*, 2015), known to be able to invade macrophages (Olczak *et al.*, 2015) and to induce an important modulation of gene expression resulting in the synthesis of several mRNAs related to signaling, apoptosis, cytokine receptors, and chemokine pathways (Zhou *et al.*, 2007; Yu *et al.*, 2010). Post-transcriptional regulation may occur specifically through microRNAs (miRNAs). It is important to note that it is not known if the miRNA modulations induced by *Pg* have biological consequences.

Recognized as critical mediators in gene expression, miRNAs are short, non-coding RNAs involved in many physiological and pathological processes (Zhou *et al.*, 2007; Hajishengallis *et al.*, 2014; Hosin *et al.*, 2014). In recent years, several roles have been described for miRNAs in numerous inflammatory diseases, such as cardiovascular diseases, diabetes, obesity, arthritis and PD (Marques-Rocha *et al.*, 2015). Partially complementary to the sequence of mRNAs in the 3' UTR region, miRNAs could down-regulate gene expression at the post-transcriptional level (Simo *et al.*, 2015). However, the identification of miRNA expression and the roles of miRNAs in inflammatory and infectious diseases are not fully understood. The analysis of the modulation of miRNA expression in infectious and inflammatory diseases may lead to the identification of new potential biomarkers and therapeutics (Marques-Rocha *et al.*, 2015).

It is important to note that even though natural miRNA possess short half-life. Synthetic miRNA has been successfully developed to be more stable and able to avoid the activation of endogenous RNase. The added stability to the synthetic miRNA has been obtained through a chemical modification in the backbone. Such chemical modifications of the antisense includes 2′-O-oligonuclmethyl, methoxyethyl nucleotides, 2′-F nucleotides and phosphorothioate

backbone). Modified oligonucleotides have been shown to effectively interfere with natural miRNA expressions (Lennox & Behlke, 2011; Baumann & Winkler, 2014).

In the context of PD, the impact of infection-induced miRNA expressions with common periodontal pathogens, like *Pg*, has been evaluated mostly on gingival tissue samples. Several miRNAs which are differentially expressed between healthy and diseased tissues have been identified (Stoecklin-Wasmer *et al.*, 2012). However, a precise correlation between specific pathogens and the different cell types involved in periodontal tissue destruction has not been made.

1.2. Bone Regeneration

One of the most significant clinical manifestation of PD is bone loss due to inflammation (Grossi *et al.*, 1995; Baker, 2000; Cochran, 2008). Inflammatory mediators such as IL-1, TNF-α and many others have been associated with this bone loss (Assuma *et al.*, 1998; Jämsen *et al.*, 2017). Inflammation modulations is a fundamental contributor to the bone regeneration (Mountziaris & Mikos, 2008; Thomas & Puleo, 2011). Bone regeneration is a composite, physiological process of bone formation that can be observed during fracture healing and other clinical scenarios. Often, a high degree of bone regeneration is required in the reconstruction of large bone defects such as those due to infection, tumor resection, and skeletal abnormalities. In some cases, bone formation can be compromised via avascular necrosis, atrophic non-unions and osteoporosis. In most of these situations, bone induction is necessary to allow for a desirable healing process, There are currently many different strategies to augment the impaired or 'insufficient' bone-regeneration process, including the 'gold standard' autologous bone graft, allograft implantation, and use of growth factors (Dimitriou *et al.*, 2005).

Clinically, any bone defect that does not heal completely without intervention is defined as being a Critical Size Defect (CSD) (Spicer *et al.*, 2012). This concept has been created in animal models to evaluate alternative regimens to adjunct bone regeneration process (Cowan *et al.*, 2004; Spicer *et al.*, 2012; Cordova *et al.*, 2014). The mouse model is widely accepted for bone regeneration studies (Cowan *et al.*, 2004). Many researchers report 3-4mm circular calvaria bone defects as being a CSD (Cordova *et al.*, 2014).

1.3. Material with osteogenic potentials

Poly-N-acetyl glucosamine (PGIcNAc) is a chemical compound that is extracted from microalgae (Maus, 2012). It is commercially available as a thin 5x5 cm white sheet that is FDA approved for the treatment of impaired skin lesions such as venus leg ulcers.

Platelet-Rich-Plasma (PRP) is source of platelet-derived growth factor that has been advocated as an adjunct to bone regeneration (Marx *et al.*, 1998). PRP can easily be prepared by sequestering and concentrating platelets via gradient density centrifugation. This technique produces a sufficient concentration to induce bone formation (Marx *et al.*, 1998). It is reported that PRP-thrombocyte increases bone formation in the dento-alveolar region (Weibrich *et al.*, 2002). Other studies also show evidence that PRP can induce skin healing and reduces scar formation at graft-donor sites (Marx, 2004). A recent study by Joshi Jubert *et al.* asserts that single intra-articular PRP-injection can improve daily activities and reduce pain in late stage osteoarthritis patients (Joshi Jubert *et al.*, 2017).

Leukocyte-Rich-Platelets-Fibrin (L-PRF), a widely used product in dental surgery, has been described as a second generation PRP product. The main difference between PRP and L-PRF is the lack of anti-coagulant use during preparation, thus allowing for clot formation during L-PRF preparations (Dohan *et al.*, 2006; Di Lauro *et al.*, 2015). Research has indicated that L-PRF, similar to PRP, improves epithelial tissue healing and enhances tissue growth in

the dental region (Dohan *et al.*, 2006; Di Lauro *et al.*, 2015). Kim *et al.* demonstrated that L-PRF can reduce inflammation and induces osteoblast differentiation of dental pulp cells exposed to lipopolysaccharide (Kim *et al.*, 2017). In a human study, Varghese *et al.* notes better osseous formation and faster healing associated with L-PRF use (Varghese *et al.*, 2017).

Bone Morphogenic Protein 2 (BMP2) is an FDA approved drug for bone regeneration in humans. BMP2 is a member of the TGF-β superfamily, a group of proteins known to enhance bone growth (Hoodless *et al.*, 1996). Zara *et al.* reported, in a rat study, that BMP2 not only produces bone, but also can induce irregular bone formation at high doses with undesirable soft tissue swellings (Zara *et al.*, 2011). It is also well documented that activation of the BMP2 gene in skeletal muscles is a strong activator for ectopic bone formation (Kawai *et al.*, 2003). Furthermore, applying low doses of BMP2 at any site using collagen sponge was found to be sufficient to produce ectopic bone (Tachi *et al.*, 2011). More importantly, BMP2 is a cancer promoting factor at high does; it has been shown to promote cell invasion in oral squamous cell carcinoma (Kim *et al.*, 2014).

2. Aims of the Study

The aim of this study was to identify miRNAs differentially expressed by macrophages in response to *Pg* infection and to assess their impact at the cytokine level. Furthermore, we wanted to evaluate, *in vitro* and *in vivo*, the ability of miRNAs with anti-inflammatory properties to reduce inflammatory effects associated with *Pg* infection. Secondly, this study aimed to find a reliable alternative to BMP2 for bone regeneration in CSD. The study utilized a mouse calvaria model because it provides a highly controlled environment for bone formations. The tested materials were collagen Sponge (SurgiFoam), PRP, L-PRF, and PGIcNAc.

AIM I: MODULATION OF INFLAMMATION

3. MATERIALS AND METHODS

3.1. Bacterial strain

The *Pg* (ATCC 33277) (kindly provided by Dr R. Lamont, University of Louisville, KY, USA) was cultured and maintained on enriched trypto-soy agar plates containing a mixture of defibrinated sheep blood, 5 mg/ml hemin, and 1 mg/ml menadione, at 37°C in anaerobic conditions. Then, bacterial colonies were transferred into a Brain Heart Infusion medium (Becton, Dickinson and Company, Sparks, MD, USA) supplemented with the hemin and menadoine as indicated previously. On the day of infection, bacteria were centrifuged, washed with PBS and the number of bacteria was determined by measuring the optical density at 600nm.

3.2. Macrophage cultures

Bone-marrow-derived macrophages (BMMs) were harvested as described in a previous study (Zhang *et al.*, 2008). Briefly, bone marrow cells from femora of donor mice were incubated for 7 d at 37°C in a RPMI medium supplemented with L929. BMMs were cultured in a RPMI medium supplemented with 100,000 U/l of penicillin, 100 mg/l of streptomycin and 10% of FBS in a humidified atmosphere with 5% CO_2.

3.3. Infection of BMMs with *Pg*

$1x10^6$ BMMs were plated in 6-well plates. Adherent BMMs were infected with live *Pg* at a multiplicity of infection of 25 (Zhou *et al.*, 2007). Cells and supernatants were harvested 3 h after infection with live bacteria.

3.4. RNA extraction and microarray analysis

BMMs were washed with cold PBS 3h after infection and the total RNAs were extracted using a miRNeasy Mini Kit (Qiagen, Valencia, CA, USA) according to the manufacturer's instructions. Collected RNA was verified using RNA 6000 Nano Assay RNA chips run in an Agilent 2100 Bioanalyzer (Agilent Technologies, Palo Alto, CA, USA). The RNAs, a total of 300μg from each sample, were then labeled with a FlashTag HSR Kit (Genisphere Inc., Hatfield, PA, USA) according to the manufacturer's protocol. The labeled RNAs were hybridized with the miRNA 4.0 arrays (Affymetrix, Santa Clara, CA, USA) for 16h in the GeneChip Hybridization Oven 640 at 48^{o}C with rotation (60 rpm). The hybridized samples were washed and stained using the Affymetrix Fluidics Station 450. The first stain with streptavidin-R-phycoerythrin was followed by signal amplification using a biotinilated goat anti-streptavidin antibody and another streptavidin-R-phycoerythrin staining (Hybridization, Washing and Staining Kit, Affymetrix, Santa Clara, CA, USA). Microarrays were immediately scanned using the Affymetrix GeneArray Scanner 3000 7G Plus (Affymetrix, Santa Clara, CA, USA). The Affymetrix Expression console software was used for summarization, normalization and quality control of the resulting CEL files. All experiments were performed in triplicate.

3.5. Data processing

Raw Affymetrix CEL files (GeneChip miRNA version 4.0 array) were normalized to produce probeset-level expression values for all mouse and control probesets using the Affymetrix Expression Console (version 1.4.1), Robust Multiarray Average (Irizarry *et al.*, 2003) and Detection Above BackGround Analysis was limited to 1,908 mature mouse miRNAs assessed by the array. A Principal Component Analysis was performed using the 'prcomp' R function with expression values that had been normalized across all samples to a

mean of zero and a standard deviation of one. Analyses of variance were performed using the 'f.pvalue' function in the *sva* package (version 3.4.0). Pairwise differential miRNA expression was assessed using the moderated (empirical Bayesian) *t*-test implemented in the *limma* package (version 3.14.4) (i.e., creating simple linear models with *lmFit*, followed by empirical Bayesian adjustments with *eBayes*). Correction for multiple hypotheses testing was accomplished using the Benjamini-Hochberg false discovery rate (Benjamini & Hochberg, 1995). All statistical analyses were performed using the R environment for statistical computing (version 2.15.1).

3.6. Identification and analysis of predicted target genes of differentially expressed miRNAs

MiRWalk 2.0 (http://www.umm.uni-heidelberg.de/apps/zmf/mirwalk/) (Dweep *et al.*, 2014) was used to identify putative target genes from 8 identified miRNA with a predicted *p*-value <0.05. Interactomics data were extracted from the STRING 10 database (Szklarczyk *et al.*, 2015), which contains known and predicted physical and functional protein-protein interactions (PPI) from diverse sources. Only interactions with the highest confidence were selected (combined score >= 0.9). The open source software platform Cytoscape 3.2.1 (Shannon *et al.*, 2003) was used to visualize and analyze PPI networks. The clusterMaker2 0.9.5 plugin (Morris *et al.*, 2011) from Cytoscape and in particular, the Markov Clustering algorithm (MCL) (Enright *et al.*, 2002) (granularity parameter = 2.5) was applied to identify topological modules. KEGG pathway enrichment analysis was performed with DAVID release 6.8 (Huang *et al.*, 2008), in order to study the functional significance of the modules.

3.7. Transient miRNA transfections

The miScript miRNA mimics used were syn-mmu-miR-155-5p (miR-155), syn-mmu-miR-2137 (miR-2137), syn-mmu-miR-7674-5p (miR-7674) and syn-mmu-miR-8109 (miR-

8109) and the miScript miRNA inhibitors used were anti-mmu-miR-155-5p (anti-miR-155), anti-mmu-miR-2137 (anti-miR-2137), anti-mmu-miR-7674 (anti-miR-7674), anti-mmu-miR-8109 (anti-miR-8109). All were purchased from Qiagen (Valencia, CA, USA). For control, AllStar Neg. siRNA AF 546 was used (Qiagen). One day prior to the transfection, $4x10^5$ cells were seeded in a 24-well plate. Transfection was performed using a HiPerfect Transfection Reagent (Qiagen), according to the manufacturer's protocol. BMMs were transfected with miRNA mimics or inhibitors at a final concentration of 50 nM and infected with *Pg* (MOI=25).

3.8. Cytokine analysis

The supernatants of the *Pg*-infected BMMs that were transfected with the miRNA mimics or inhibitors were collected after 24 h of treatment. The levels of TNF-α and IL-10 (Life Technologies Corporation, Carlsbad, CA USA) were evaluated using ELISA kits according to the manufacturer's protocol.

3.9. Calvarial bone resorption mouse model

The 8 to 12 weeks-old wild-type C57BL/6J mice used in this study were purchased from The Jackson Laboratories (600 Main Street, Bar Harbor, ME, USA). All experiments involving animals were approved by the Boston University Institutional Animal Care and Use Committee and were performed in compliance with relevant animal care and use laws. Regular mice chow and water were provided *ad libitum*. The mice (n=4) were separated into the following four groups: (I) *Pg*-infected mice as the control; (II) *Pg* and 8μg miR-155 and 8μg anti-miR-2137 inhibitor (herein, this group is referred to as combination group); (III) *Pg* and 16μg miR-155; and (IV) *Pg* and 16μg anti-miR-2137. The final volume of each individual injection was 100μl in PBS.

All of the procedures were done under anesthesia as previously described (Graves *et al.*, 2005). Anesthesia was obtained after an intraperitoneal injection of ketamine-xylazine.

First, the heads of mice were shaved, then subcutaneous injections of *Pg* ($5x10^8$ CFU in 100 µl of PBS) along with either the mmu-miR 155 mimic, or mmu-miR 2137 inhibitor, or both were injected at the same site. Injections were carried out with a 30.5-gauge needle at a point on the midline of the skull between the ears and eyes. Mice were sacrificed 7 days after the injection. The size of the lesion resulting from injection in each animal (area in mm^2) was analyzed using ImageJ.

3.10. Histological analysis

The calvarium of each mouse was fixed in 2% paraformaldehyde in PBS (Affymetrix, Inc. Cleveland. OH, USA) for 2h at room temperature and refrigerated in PBS until further processing. Samples were embedded in an optimum-cutting-temperature-compound (Fisher HealthCare, Houston, TX, USA), frozen and then sectioned. Sections of 5-8µm were stained with hematoxylin and eosin (H&E) and prepared for further analysis. To analyze osteoclast activity, a Tartrate-resistant acid phosphatase (TRAP) assay was performed according to an already established protocol (Chiang *et al.*, 1999). To quantify the histological sections, samples were evaluated by double blinded examiners according to three different scoring protocols: a) calvarial bone resorption was assessed using a scoring of 0 through 4 with 0: corresponding to no calvarial bone resorption, 1: ¼ of calvarial bone was affected but no through and through penetration; 2: ½ of calvarial bone was affected but no through and through penetration, 3: half of calvarial bone with through and through bone penetration less than 1mm in width; 4: more than ½ of the calvarial bone was affected with through and through bone penetration greater than 1mm; b) osteoclast activity was assessed using a score of 0 through 3, 0: corresponding to no osteoclast with no sign of bone resorption; 1: presence of some osteoclasts lacunae with minimal bone resorption; 2: presence of 5-10 osteoclast lacunae with bone resorption and 3: presence of more than 10 osteoclasts with lacunae and severe

bone resorption; c) inflammatory cell infiltration (ICI) was assessed using a scoring of 0 through 5; 0: corresponding to no sign of inflammation; 1: incipient inflammatory cells infiltration (ICI) in derma/subderma; 2: mild ICI in derma/subderma; 3: moderate ICI in derma/subderma and scarce inflammation in bone surroundings, 4 advanced ICI in derma, subderma and mild inflammation in bone surroundings, and 5: severe ICI in derma, subderma and advanced inflammation in bone surroundings.

3.11. Statistical analysis

Data were analyzed for statistical significance using XLStat (Addinsoft, New York, USA). *P*-values were calculated using the Mann-Whitney's *t*-test.

4. RESULTS

4.1. Differentially expressed miRNAs between control and infected cells

To evaluate the effects induced by *Pg* infection on the miRNAs expression profile in BMMs, the expression profile of 1,908 mouse miRNAs was analyzed by a microarray analysis. 203 miRNAs showed a differential expression with a false discovery rate, corrected *p*-values (*q*) at <0.25, and clustering trends appeared between the groups (Figure 1). The analysis was restricted to the most differentially expressed miRNAs identified with higher stringency parameters (a threshold of fold-change (≥ or ≤ 2), *p* and *q* (≤0.001) values). Therefore, eight miRNAs were differentially expressed between BMMs and the *Pg*-infected BMMs. Five miRNAs were up-regulated (mmu-miR-7674-5p, mmu-miR-6975-5p, mmu-miR-155-5p, mmu-miR-347-3b, mmu-miR-347-3e) and 3 were down-regulated (mmu-miR-2137, mmu-miR-8109, mmu-miR-211-3p) (Table 1). The results obtained with the microarray analysis were validated by RT-qPCR for all the identified miRNA except for mmu-miR-6975-5p and mmu-miR-8109 due to primer GC content and technical issues (Table 1).

miRNA differentially expressed upon *P. gingivalis* infected Macrophages	
Up-regulated	Fold change
mmu-miR-7674-5p	(27.3)
mmu-miR-6975-5p	(4.4)
mmu-miR-3473b	(2.7)
mmu-miR-3473e	(2.7)
mmu-miR-155-5p	(5.4)
Down-regulated	
mmu-miR-8109	(-3.3)
mmu-miR-2137	(-3.2)
mmu-miR-211-3p	(-2.4)

Table 1 Differential Expression of miRNA between Bone Marrow Macrophages infected with P. gingivalis and control (uninfected)

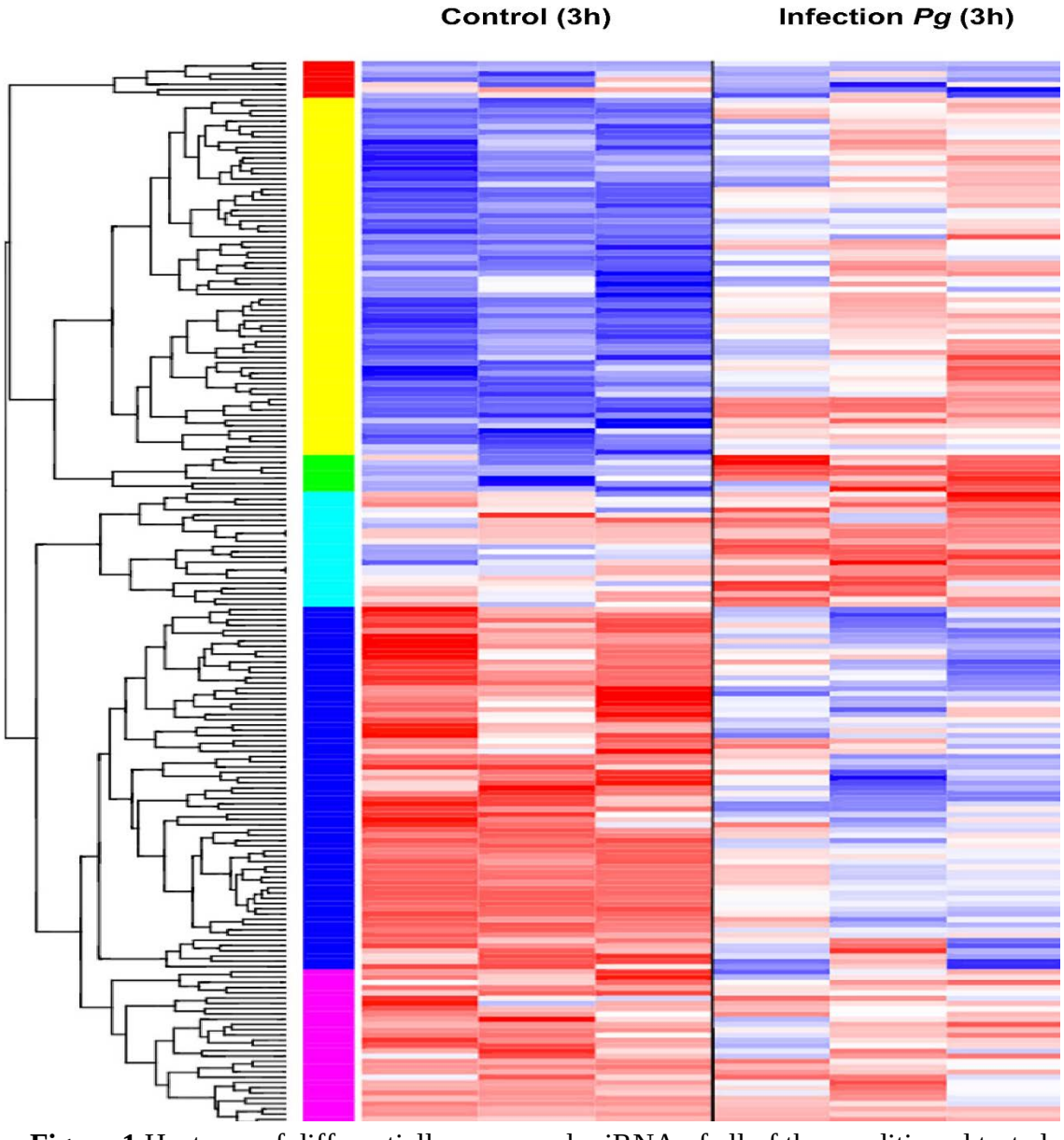

Figure 1 Heatmap of differentially expressed miRNA of all of the conditioned tested. Red and Blue indicate z-score of ≥2 or ≤ -2, respectively, and white indicate z-score of zero (row-wise mean), p and $q < 0.25$. Experiment performed in triplicate.

4.2. Predicting the targets of differentially expressed miRNAs

To assist in the selection of miRNAs with potential impact on host-response and identify the biological pathways that may be affected by these miRNAs, a bioinformatics analysis was performed. Therefore, after having analyzed the putative mRNA targets of the differentially expressed miRNAs between naïve BMMs and *Pg*-infected BMMs, 3796

potential target genes were predicted. The number of predicted target genes varied from 44 (mmu-miR-8109) to 1262 (mmu-miR-6975-5p). Interactions of target genes were extracted from the STRING database and the resulting protein-protein interaction (PPI) network was visualized using Cytoscape. To facilitate analysis, only proteins with at least two interactions with identified targets were considered. The network contains 6746 nodes and 51470 edges, where nodes represent target genes and edges represent interactions between target genes. Topological modules (densely connected regions) were identified by the MCL clustering algorithm. 639 modules were identified, among which 211 modules contained more than 5 nodes and the largest module contained 613 nodes. Pathway analysis led to the identification of miRNAs target genes in several pathways related to the inflammatory response including chemokine signalling pathway and cytokine-cytokine receptor interaction (Table 2). Interestingly, even though several pathways related to cell's life were identified, such as cell cycle, ribosome, spliceosome, from the 10^{th} largest identified topological modules, 3 of them were linked to pathways related to the inflammatory response highlighting the potential involvement of identified miRNAs on the modulation of inflammatory response in BMMs *Pg* infected.

Topological module and predicted pathways	Benjamini-corrected *P* value
Olfactory transduction	0.0E0
Neuroactive ligand-receptor interaction	1.2E-107
Taste transduction	4.9E-36
Calcium signaling pathway	1.5E-19
Chemokine signaling pathway	2.7E-17
Cytokine-cytokine receptor interaction	4.3E-8
Complement and coagulation cascades	5.7E-6
CyclicAMP signaling pathway	6.6E-6
Ribosome	1.2E-141
Protein export	1.3E-19
Cell cycle	3.0E-86
Progesterone-mediated oocyte maturation	1.7E-25
Oocyte meiosis	1.7E-24
HTLV-I infection	1.8E-13
p53 signaling pathway	6.8E-12
Viral carcinogenesis	20.7E-11
Ubiquitin-mediated proteolysis	8.7E-11
Small-cell lung cancer	2.3E-9
Hepatitis B	1.2E-8
FoxO signaling pathway	3.5E-8
Pathways in cancer	2.3E-7
PPAR signaling pathway	2.4E-21

Thyroid hormone signaling pathway	1.2E-19
Adipocytokine signaling pathway	3.6E-7
Bile secretion	4.3E-5

Table 2 Predicted pathways of the identified target genes of 155-5p miRNAs. The predicted pathways of the largest topological modules are presented. Only pathways with a Benjamini-corrected p value of < 0.00001 were considered. Boldface type indicates pathways related to immune and inflammatory response.

4.3. Impact of identified miRNAs on TNF-α and IL-10 secretion in BMMs

To evaluate the effect of identified miRNAs on the inflammatory response, BMMs were transfected with mimics and inhibitors of the most differentially expressed miRNAs (mmu-miR-155-5p, mmu-miR-2137, mmu-miR-7674, mmu-miR-8109). This experiment aimed at evaluating the specific effect of each miRNA to assess their role on the inflammatory response to *Pg* infection and especially on pro-inflammatory TNF-α and anti-inflammatory IL-10 secretion.

Transfection of BMMs with miR-155 and miR-2137 did not modify significantly TNF-α secretion. Their respective inhibitors, on the other hand, increased significantly its secretion level. Regarding miR-7674 and miR-8109, transfection induced an increase of TNF-α to a lesser extent than transfection with their respective inhibitors (Figure 2A and Table 3). Regarding IL-10 secretion, only a few of the tested miRNAs modified its secretion profile significantly. Mimic of mmu-miR-7674 and inhibitors of mmu-miR-2137 and mmu-miR-8109 induced a significant increase of IL-10 release in comparison with control ($p<0.05$) (Figure 2B and Table 3). However, even though statistical significance was reached, the increase was small. Therefore, it appears that some of the identified miRNAs and inhibitors are able to modulate the secretion rate of these two cytokines.

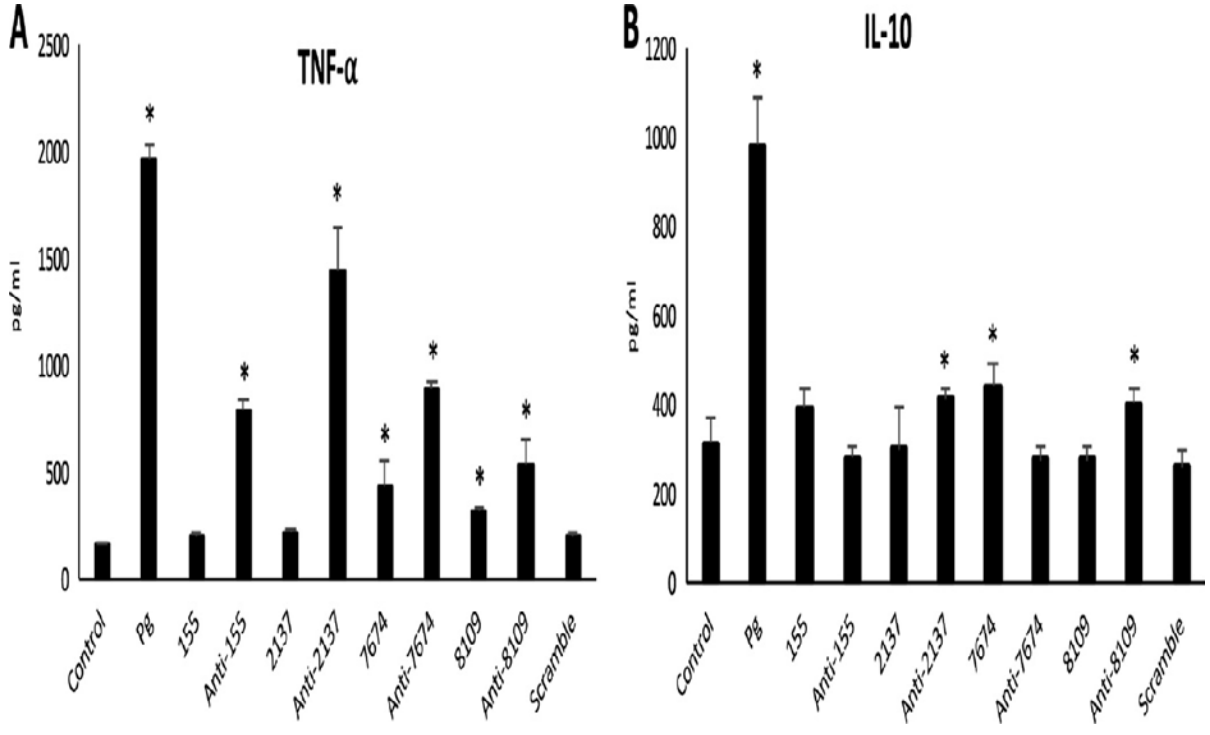

Figure 2 (A) TNF-α secretion in transfected BMMs with selected miRNAs and their inhibitors (*, $p<0.05$). (B) IL-10 secretion in transfected BMMs with selected miRNAs and their inhibitors (*, $p < 0.05$).

4.4. BMMs transfection with selected miRNAs modulates cytokines secretion induced by *Pg* infection

To evaluate if a concomitant exposure to selected miRNAs is able to modulate cell's response to *Pg* infection, transfected BMMs were infected and TNF-α/IL-10 secretion were evaluated. Interestingly, transfection with miR-155 significantly decreased TNF-α secretion by 30% (Figure 3A and Table 3). In contrast, this effect was not observed for other mimics or inhibitors. Regarding IL-10 secretion, the transfection of anti-miR-2137 increased significantly IL-10 secretion (Figure 3B and Table 3) while miR-155 and anti-miR-7674 decreased it significantly ($p<0.05$).

Taken together, these data showed that the transfection with miRNAs especially miR-155 or anti-miR-2137 modulates the host-response to *Pg* infection.

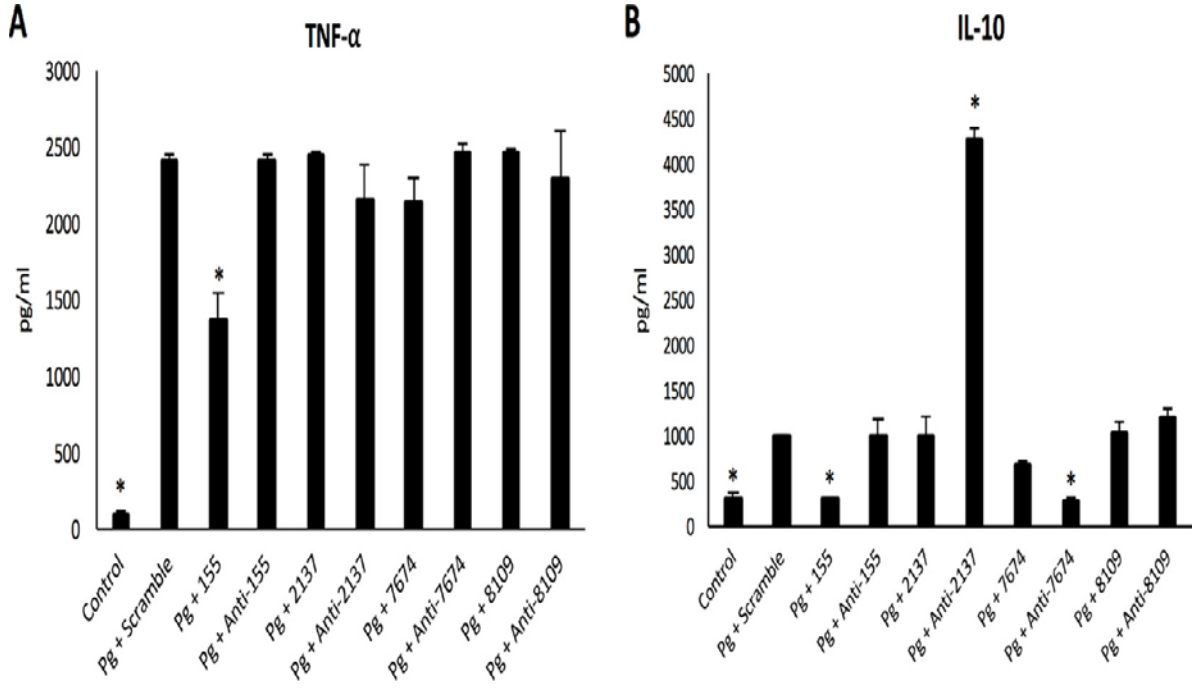

Figure 3 (A) Dosages of TNF-α in supernatants of transfected BMMs infected with *P. gingivalis* (*Pg*) at 24h. *, $p < 0.05$ versus *P. gingivalis* plus scramble. (B) Dosages of IL-10 in supernatants of transfected BMMs infected with *P. gingivalis* at 24h. *, $p < 0.05$ versus *P. gingivalis* plus scramble.

	miRNA effect with no *Pg*		**miRNA effect with presence of *Pg***	
miRNA	IL-10	TNF-α	IL-10	TNF-α
Scramble	none	none	none	none
155	none	none	(+)	(-)
Anti- 155	none	(+)	none	none
2137	none	none	none	none
Anti-2137	(+)	(+)	(+)	none
7674	(+)	(+)	none	none
Anti-7674	none	(+)	(+)	none
8109	none	(+)	none	none
Anti-8109	(+)	(+)	none	none

Table 3 the effect of over expression or inhibition of selected miRNA on the levels of IL-10 and TNF-α at the presence or absence of *Pg* infection to BBMs. When (+) denotes statistically significant increase, (-) denotes statistically significant decrease, and (none) indicates no statistical significant change.

4.5. Effects of miR-155 and anti-miR-2137 *in vivo*

In this context, an *in vivo* proof of concept experiment was conducted to assess the potential effects of miR-155 and anti-miR-2137 in a calvarial bone resorption mouse model induced by *Pg* infection. To determine their potential role on the inflammatory response and bone resorption, selected miRNAs were injected concomitantly with *Pg* in mice calvaria. After 7 days, the area of the induced lesion was measured for each mouse (Figure 4A), having a mean area of 11.08 mm^2 (+/- 1.47). The injection of miR-155 alone or anti-miR-2137 alone concomitantly to *Pg* injection significantly decreased the size of the lesion (7.55 mm^2 (+/-1.6) and 6.42 mm^2 (+/-1.4) respectively), *in vivo*.

Histological examinations showed some degree of ICI (leukocytes, lymphocytes and macrophages) in all groups (Figure 5) in comparison with untreated mice (Figure 6). However, animals infected with *Pg* and treated with anti-miR-2137 showed a reduced amount of inflammation (Figure 5 G-H), in comparison with *Pg*-infected group (Figure 5A and 5B) supported by quantitative analysis (Figure 4B). Regarding bone resorption, *Pg* infection induced bone resorption (Figure 4C) which correlated with an increased osteoclast activity as evidenced by resorption lacunae. When anti-miR-2137 was injected concomitantly to the infection, a significant reduction of calvarial bone loss and osteoclast activity were observed (Figures 4C and 4D), while mice injected with miR-155 did not show significantly reduction in ICI, bone loss, or osteoclast activity. However, regarding the combination group, while no significant reduction in ICI was observed, a trend for reduction of bone loss and osteoclast activity could be observed (Figures 4C and 4D).

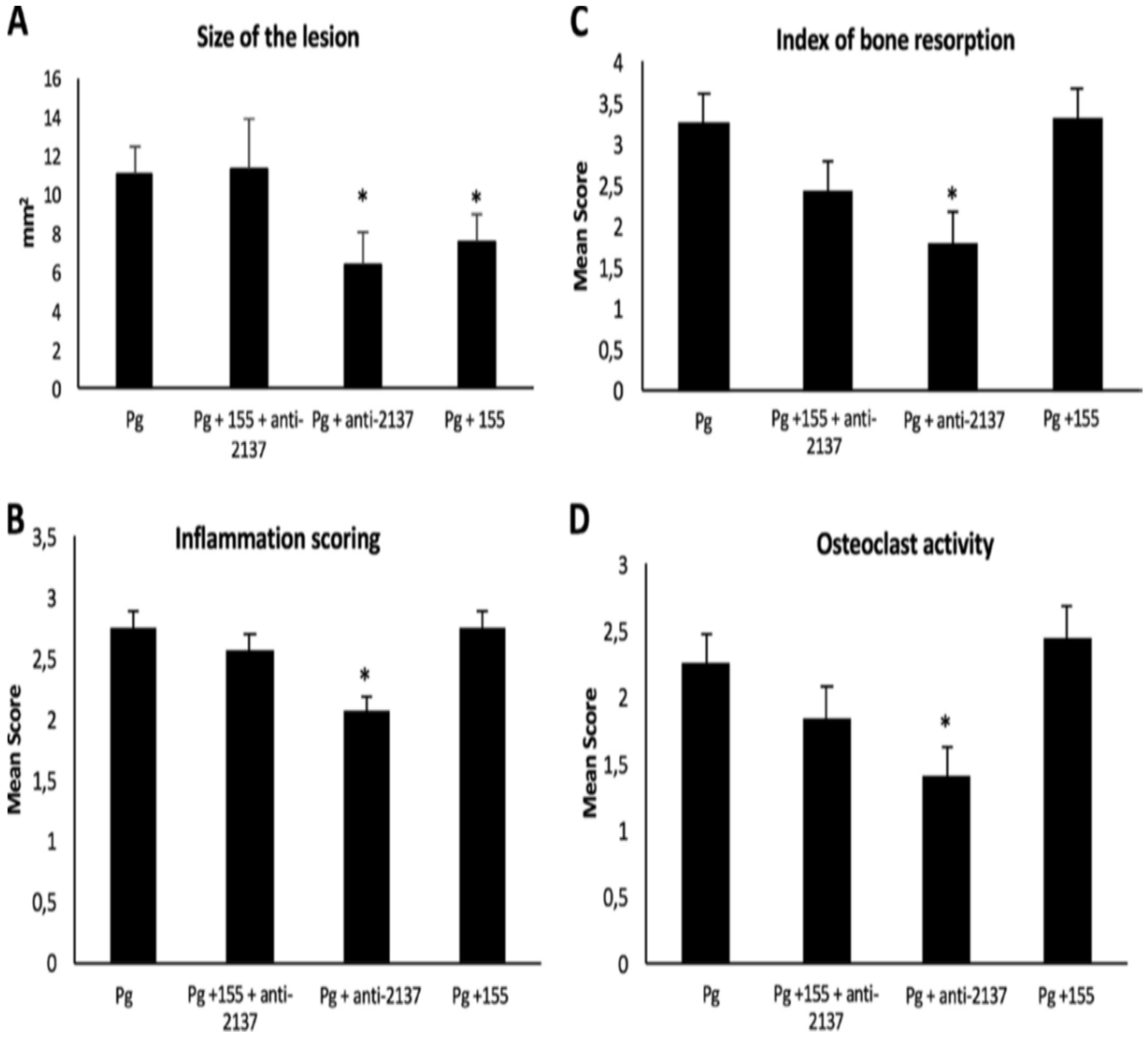

Figure 4 (A) Sizes of calvarial lesions 7 days after *P. gingivalis* (Pg; 5 x 10^8 CFU) infection and the injection of miR-155 and anti-miR-2137. *, $p< 0.05$, $n=4$

(B) Quantitative analysis of the index of ICI in each of the following groups: *P. gingivalis*-only infected, combination group (*P. gingivalis* and 8μg of anti-miR-2137 plus 8μg of miR-155), *P. gingivalis* and 8μg of anti-miR-2137, and *P. gingivalis* and 8μg of miR-155. *, $p< 0.05$.

(C) Quantitative analysis of calvarial bone resorption in each of the following groups: *P. gingivalis*-only infected, combination group (*P. gingivalis* and 8μg of anti-miR-2137 plus 8μg of miR-155), *P. gingivalis* and 8μg of anti-miR-2137, and *P. gingivalis* and 8μg of miR-155. *, $p< 0.05$.

(D) Quantitative analysis of osteoclast activity in each of the following groups: *P. gingivalis*-only infected, combination group (*P. gingivalis* and 8μg of anti-miR-2137 plus 8μg of miR-155), *P. gingivalis* and 8μg of anti-miR-2137, and *P. gingivalis* and 8μg of miR-155. *, $p< 0.05$.

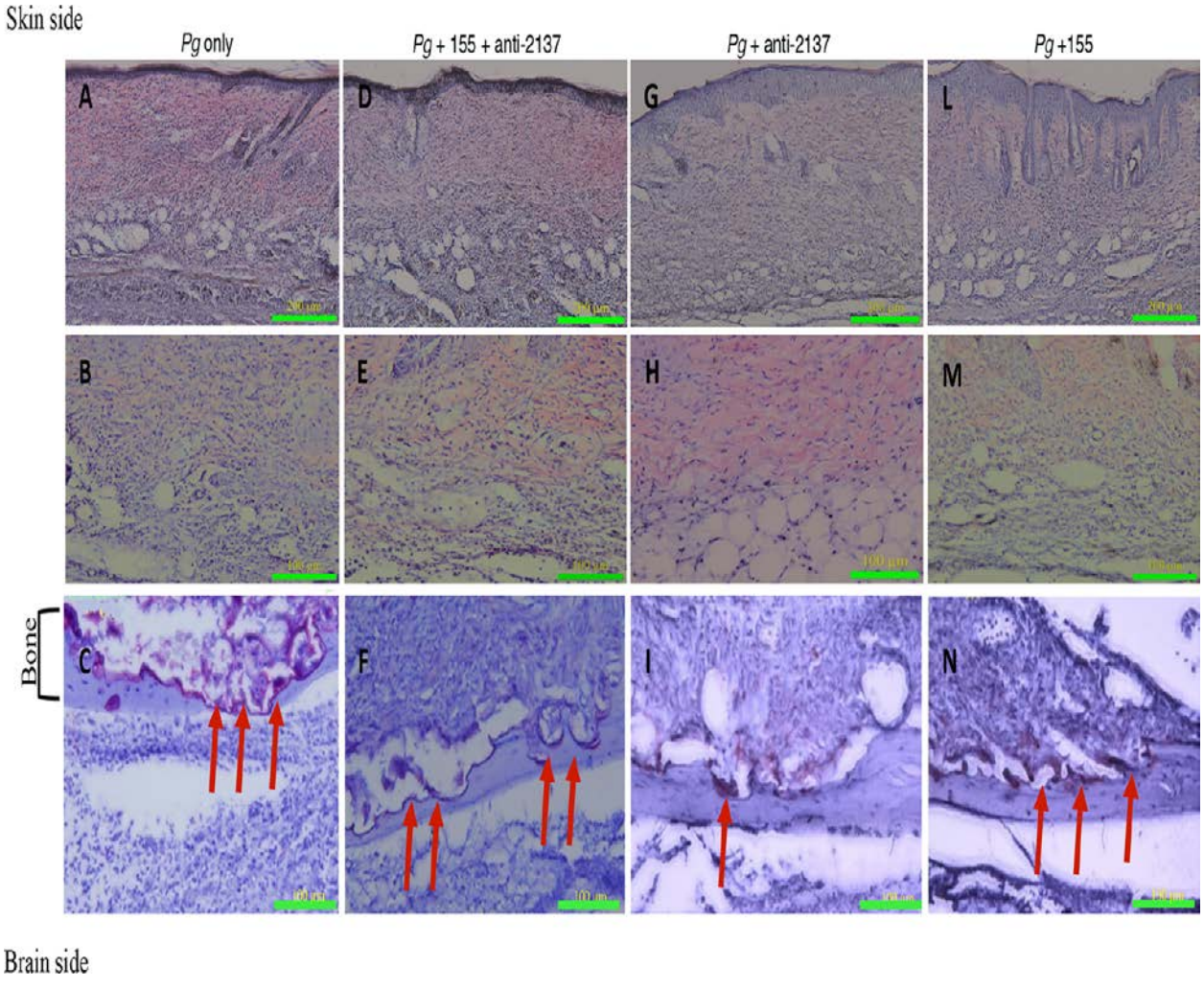

Figure 5 Histological sections. Shown are representative samples of skin and underlying calvarial bone at the middle of the lesion from each of the following groups: *P. gingivalis* (*Pg*) (A to C), combination (*P. gingivalis* and miR-155 plus anti-miR-2137) (D to F), *P. gingivalis* and anti-miR-2137 (G to I), and *P. gingivalis* and miR-155 (L to N). TRAP staining of bone (bottom row, x200 magnification) and hematoxylin-and-eosin staining of skin (top row, x100 magnification; middle row, x200 magnification) are shown. Arrows indicate TRAP-stained multinucleated osteoclasts attached to bone and bone resorption lacunae.

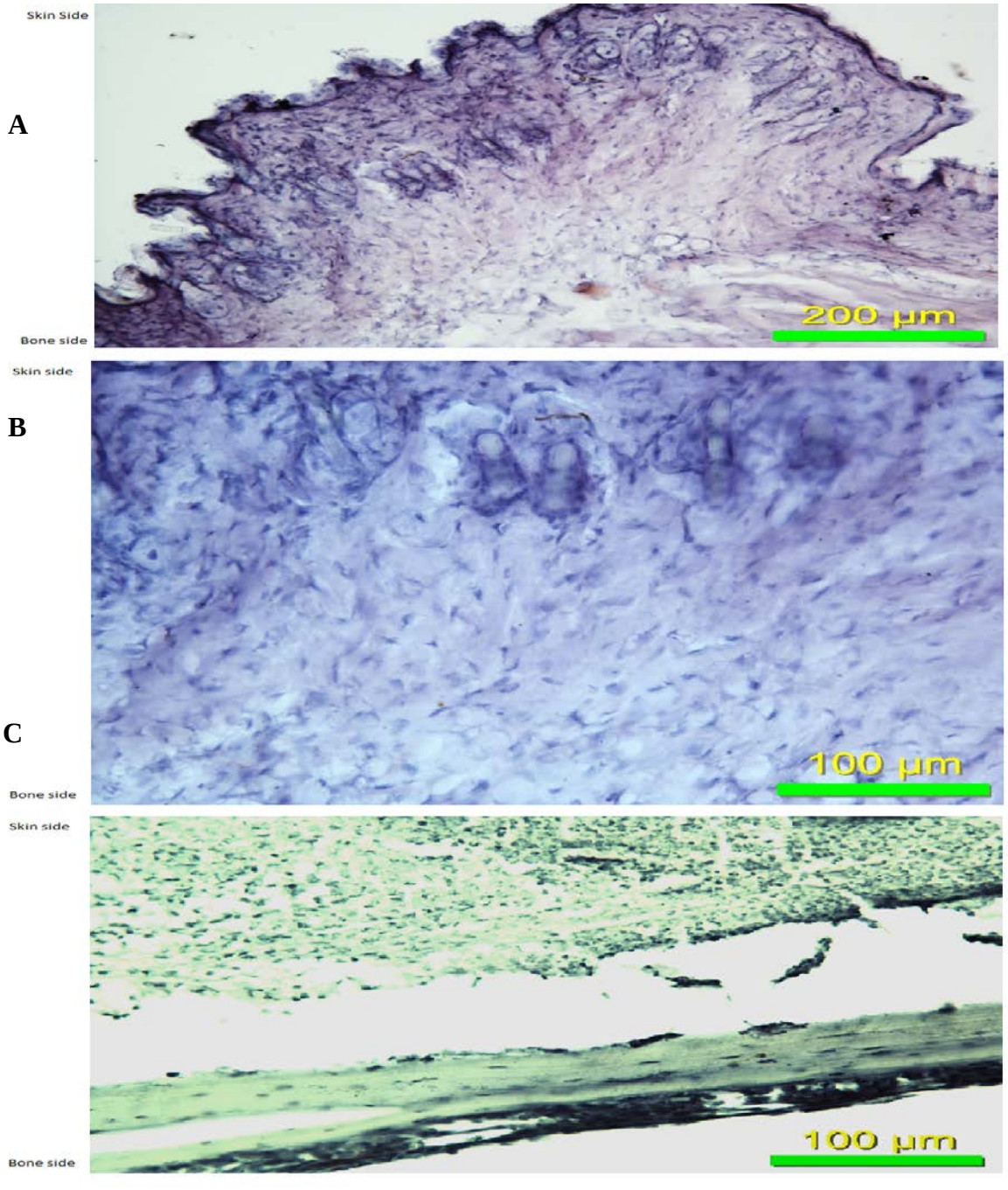

Figure 6 Representative samples for skin (A-B) & underlying calvarial bone (C) at the middle of the calvaria in an uninfected mouse. TRAP staining for bone (bottom row, 200x) and H&E staining for the skin (Top row, 100x; middle row, 200x).

4.6. Identification of potential pathways targeted by mmu-miR-155 and mmu-miR-2137

As some biological effects have been observed *in vitro* and *in vivo,* a new set of bioinformatics analysis regarding mmu-miR-155 or mmu-miR-2137 was been performed to determine which molecular pathway could be linked to the observed results.

Regarding mmu-miR-155, 130 topological modules were identified by the MCL clustering algorithm, amongst which 52 modules contained more than 5 nodes. When the largest topological modules (Figure 7) were considered, several pathways related to the inflammatory response but also pathogen recognition were identified as potential targets including cytokines and chemokines related pathways, the Toll-like receptor signalling pathway and also osteoclast differentiation pathways. Furthermore, gene ontology analysis confirmed a potential involvement of this miRNAs on the genes associated with the inflammatory response (Benjamini corrected *p*-value =1.3^{E}-24). Interestingly, one other topological module (Figure 8) was related to the Jak-STAT pathway, a well-described pathway related to apoptosis but also to pro-inflammatory cytokines production notably through the targeting of TNF and NF-kappa B signalling pathways. Furthermore, associations with pathways related to epithelial cells invasion and osteoclasts differentiation have also been underlined for this module especially through the direct targeting of PI3k-AKT pathway.

Regarding mmu-miR-2137, 10 topological modules were identified among which 4 modules contained more than 5 nodes. The largest module was associated with the cell cycle (Benjamini corrected *p*-value = 2.1^{E}-12). However, no pathway related to inflammation for mmu-miRNA-2137 has been identified yet, even though our study showed the clear effect on IL-10 production.

Pathway	Benjamini corrected *p*-value
Chemokine signalling pathway	1.3^{E}-27
Cytokine-cytokine receptor interaction	2.4^{E}-8
TNF signalling pathway	1.9^{E}-1

Pathway	Benjamini corrected *p*-value
Osteoclast differentiation	5.3^{E}-8
T cell receptor signalling pathway	6.7^{E}-7
Toll-like receptor signalling pathway	4.6^{E}-6
MAPK signalling pathway	7.5^{E}-6
Chemokine signalling pathway	2.0^{E}-5

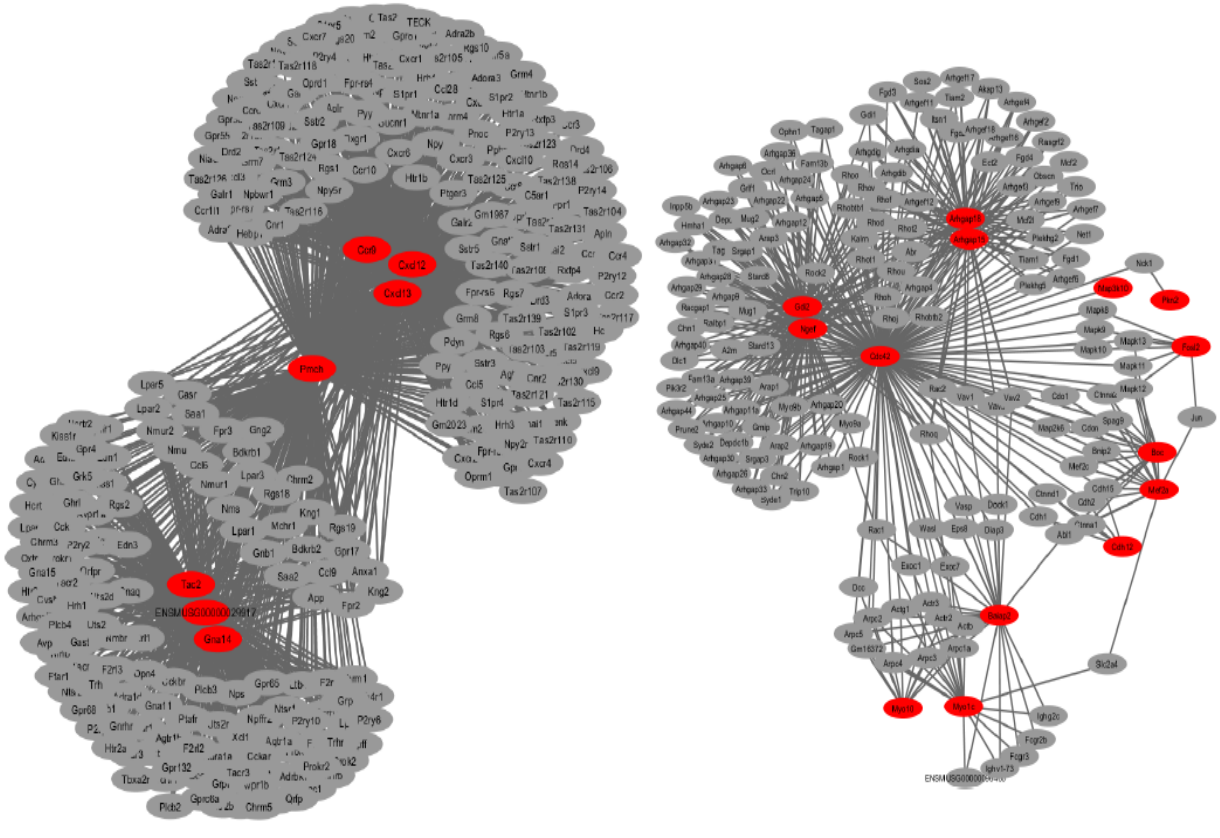

Figure 7 Representative topological modules related to mmu-miR-155 target genes and identified pathways associated to innate immune response. In red, genes identified as directly affected by mmumiR-155.

Pathway	Benjamini corrected *p*-value
T-cell receptor signalling pathway	6.6^{E}-12
Osteoclast differentiation	2.2^{E}-11
B-cell receptor signalling pathway	1.9^{E}-11
Bacterial invasion of epithelial cells	7.4^{E}-11
Chemokine signalling pathway	2.6^{E}-10
Jak-STAT signalling pathway	1.1^{E}-8
NF-kappa B signalling pathway	1.4^{E}-5
Apoptosis	3.0^{E}-5
PI3-Akt signalling pathway	1.0^{E}-4
Toll-like receptor signalling pathway	2.5^{E}-4
TNF signalling pathway	3.1^{E}-4

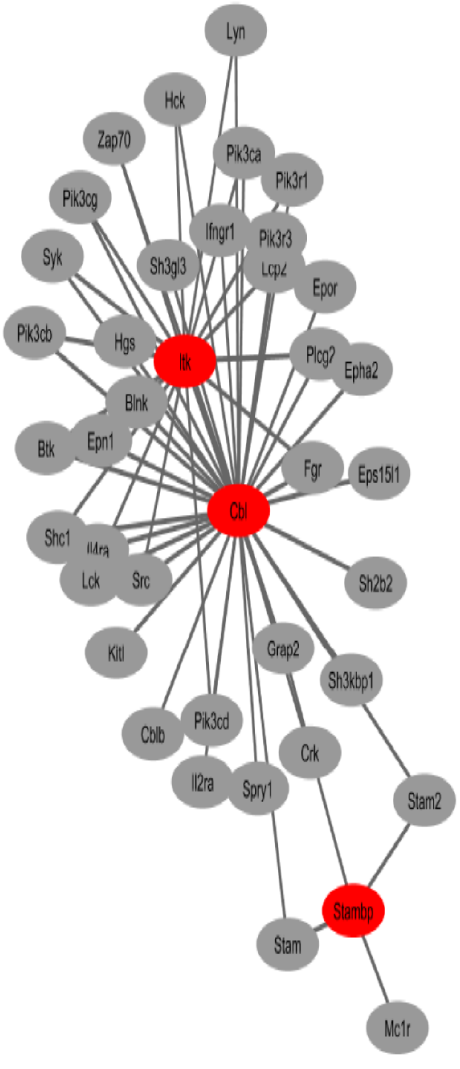

Figure 8 Topological module related to mmu-miR-155 target genes and identified pathways associated to innate immune response. In red, genes identified as directly affected by mmu-miR-155.

AIM II: BONE REGENRATION

5. MATERIALS AND METHODS

5.1. Mice

One-hundred-thirty-eight pathogen-free male C57BL/6J twelve weeks old mice purchased form Jackson Laboratory (10 Discovery Dr, Farmington, CT 06032) were used in this study. Mice were fed sterile food and distilled water *ad libitum* and were randomly assigned into group of six (*n*=6 per group) in one of the following twenty-three experimental groups:

1. Negative control
2. Poly-N-Acytel-glucosamine (PGIcNAc) sheets only (TM out)
3. Crushed PGIcNAc (cTM)
4. Crushed PGIcNAc and PGIcNAc sheet outside (cTM+TM out)
5. Crushed Bone (cBone)
6. Crushed Bone and crushed PGIcNAc (cBone+cTM)
7. Crushed Bone and crushed PGIcNAc and PGIcNAc sheet (cBone+cTM+TM out)
8. PGIcNAc gel only (TMgel)
9. PGIcNAc gel and PGIcNAc sheet (TMgel+ TM out)
10. Low concentration of BMP2 (0.3 µg per animal) and SurgiFoam (lBMP2+SurgiFoam)
11. Low concentration of BMP2 (0.3 µg per animal) and SurgiFoam and PGIcNAc sheet (lBMP2+SurgiFoam+TM out)
12. PGIcNAc gel and SurgiFoam (TMgel+SurgiFoam)
13. SurgiFoam only (SurgiFrom)
14. High concentration of BMP2(1.4 µg per animal) and SurgiFoam (1.4 µg per animal) (hBMP2+SurgiFrom)

15. High concentration of BMP2 (1.4 µg per animal) and SurgiFoam and PGIcNAc sheet (hBMP2+SurgiFoam+TM out)
16. High concentration BMP2 and SurgiFoam and PGIcNAc gel (hBMP2+TMgel+SurgiFoam)
17. High concentration BMP2 and PGIcNAc gel and PGIcNAc sheet (hBMP2+TMgel+TM out)
18. Platelets-Rich-Plasma only (PRP)
19. Platelets-Rich-Plasma and PGIcNAc gel (PRP+TMgel)
20. Platelets-Rich-Plasma and PGIcNAc gel and PGIcNAc sheet (PRP+TMgel+TM out)
21. Leukocyte-Rich-Platelets-Fibrin only (L-PRF)
22. Leuckocytes-Rich-Platelets-Fibrin and PGIcNAc gel (L-PRF+TMgel)
23. Leucocytes-Rich-Platelets-Fibrin and PGIcNAc gel and PGIcNAc sheet (L-PRF+TMgel+TM out)

The animals were allowed to heal for 6 weeks. After that, they were sacrificed and calvaria samples were collected and processed.

5.2. Poly-N-acetyl glucosamine (PGIcNAc)

The Poly-N-acetyl glucosamine preparation was supplied by Marine Polymer Technologies, Inc., Danvers, MA 01923 in two forms: 5x5cm sheets, and gels. During surgeries, groups denoted with TM out received 7x7mm of PGIcNAc sheet to cover the entire outer surface of the 5mm defect completely.

Groups indicated to have TM gel received 14µL of the PGIcNAc gel preparation. The concentration of the supplied gel was 20mg/mL. The gel was placed inside the 5mm circular defect in the middle of the mouse calvaria.

Groups that received crushed PGIcNAc (cTM) were treated, in fact, with crushed PGIcNAc sheet. The PGIcNAc sheet of 5x5cm was manually crushed using a mortar and pestle until a powder form was obtained. Then enough powder to full the 5mm circular defect was used in each animal treated with cTM.

5.3. Crushed Bone (cBone)

Homologous calvaria bone were collected from C57BL/6J mice and crushed into a sterile mortar and pestle manually. Bone powder was filled into the entire 5mm defect for groups scheduled to receive cBone.

5.4. Reagents and recombinant Bone Morphogenic Protein 2 (BMP2)

Recombinant Bone Morphogenic Protein 2 (BMP2) utilized in this study was purchased form R&D system Catalogue# 355-BM-10 (R&D Systems, Inc. 614 McKinley Place NE, Minneapolis, MN 55413). Either a low amount (0.3µg) or high amount (1.4µg) of BMP2 per animal were used as indicated in the groups.

Homologous Platelet-Rich-Plasma of C57BL/6J mice was prepared in BioreclamationIVT (123 Frost St, Westbury, NY 11590) and used fresh, within 72h of preparation. Each animal treated with PRP received a PRP gel that was prepared at the time of surgery. The PRP gel contains 25µL of fresh PRP and 5µL of mouse alpha-thrombin (Cat #MCT-5020, Haematologic Technologies, Inc., VT, USA). The combination of PRP-throbmin was allowed to form a jel for 10 minutes before insertion into the 5mm defect of the mouse calvaria.

Homologous Leukocytes-Rich-Platelets-Fibrin (Munoz *et al.*, 2016) (L-PRF) was prepared at the BioreclamationIVT facility and used within 72h of preparation. A 7x7mm

section of the L-PRF was placed over the 5mm defect with an addition of 5µL of mouse thrombin per animal.

5.5. Surgical Procedure

Each animal was first weighed and an analgesic (i.p. Buprenorphine at dose range of 0.05-0.1 mg/kg) was injected 30 minutes prior to the procedure. General anesthesia was obtained via a 50-100mg/kg Ketamine + 10-15mg/kg Xylazine by i.p. injection. Once the animal was fully anesthetized, the hair covering the area of interest was shaved using an electrical hair clipper. The surgical site was prepared and disinfected as indicated in the BU IACUC protocol #15544. Using surgical grade Betadine (Purdue Pharma L.P., Stamford, CT 06901-3431), the incision site was wiped three times and allowed to completely dry. A 15mm incision was created at the middle of the mouse-calvaria using surgical blade size 15c (ThermoFisher Scientific, Inc., MA). A full thickness of skin-muscle-periosteum flap was raised to allow space for the drilling process. A 5mm bi-cortical bone defect was created using surgical trephine (Trephines for Micro Drill, catalogue#18004-50, Fine Science Tools, Inc., Foster City, CA 94404-1139) attached to surgical handpiece under copious irrigation. Bleeding was controlled using surgical gauze and manual pressure for 10 seconds. Subsequently, the materials of interest were inserted in the defect as indicated in each group. Figure 9 illustrates the procedure.

The incision was then closed using a single interrupted suturing technique using resorbable suture (ACE 5-0 Plain Gut Sutures, DSM13, 18", ACE Surgical Supply Co., Inc., Brockton, MA). Animals were kept warm during the entire procedure and until they were fully awake and able to walk. Postsurgical analgesic i.p. Buprenorphine injections was administered at 12-hours intervals for 3 days and animals were monitored daily for 6 weeks.

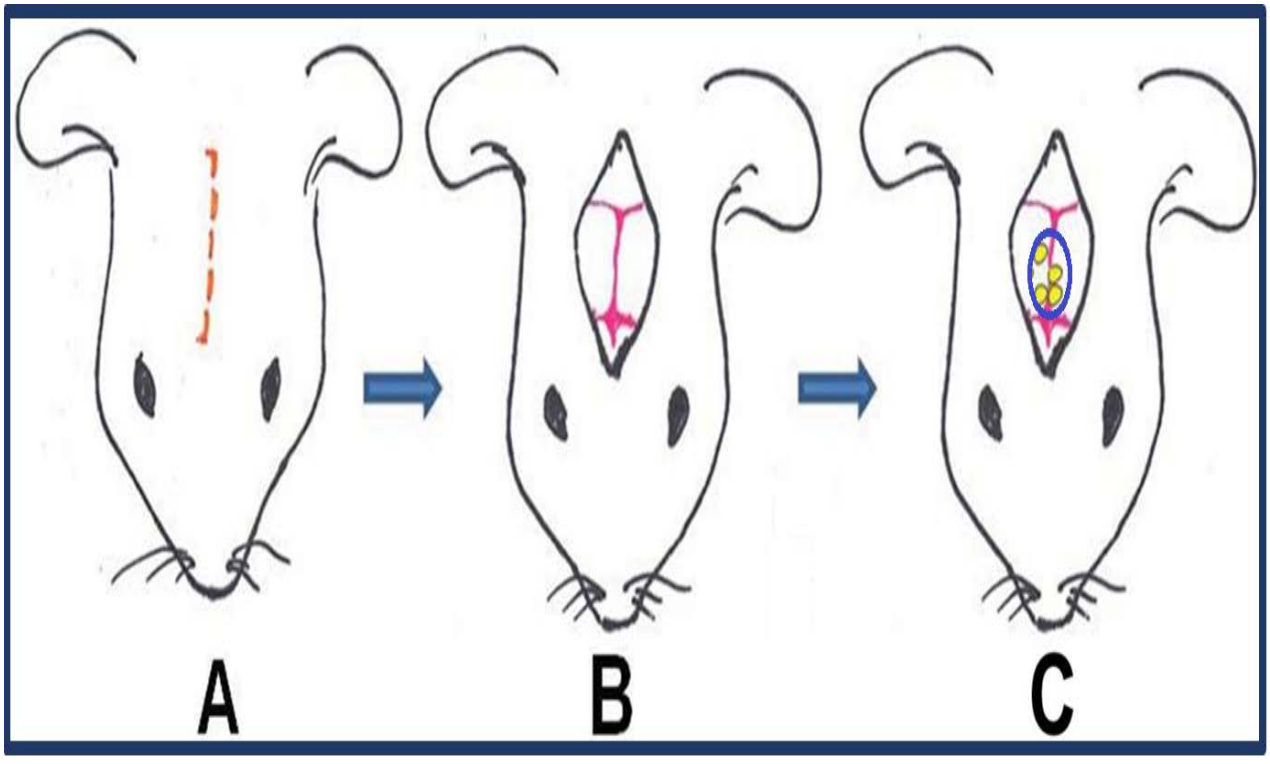

Figure 9 Illustration of the surgical procedure steps

5.6.Specimen Preparation.

Mice were sacrificed at 6 weeks and the calvarium of each mouse was harvested and fixed in 2% Paraformaldehyde in PBS (Affymetrix, Inc. Cleveland. OH, USA) for 2hrs. at room temperature and refrigerated in PBS until ready for further processing. Samples were embedded in an O.C.T. compound (Fisher HealthCare, Houston, TX, USA) and frozen at the time of sectioning. Sections of 5-8 µm were stained with hematoxylin and eosin and prepared for further analysis. Sections were collected at the middle of the 5mm defect as shown in Figure 10.

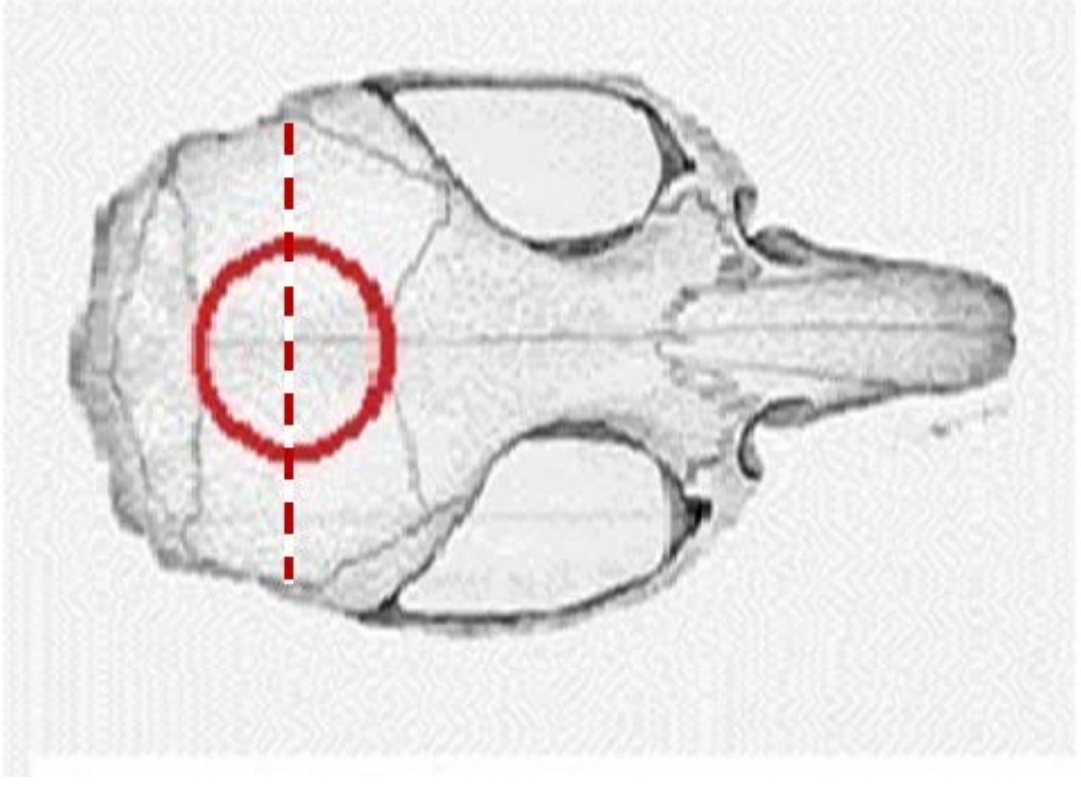

Figure 10 illustrate the place where histological sections collected form each mouse calvaria

5.7.H&E Staining protocol and Histological analysis

The following H&E staining protocol was followed to stain the prepared frozen samples for histological examinations. H&E sections were first allowed to thaw at room temperature for 30 minutes. Slides were then rehydrated in 1x PBS solution for 1 minute. Then slides were covered for 10 seconds with few drops of Fisher Chemical™ Harris Modified Method Hematoxylin Stains (Fisher Chemical, 168 3rd Ave, Waltham, MA 02451) and wash three times in tab water for 10 second each. Quickly immersed the slides for 5 times in blueish solutions (100% Li_2O_3) and immediately check of the Hematoxylin stain under microscope. Following that immersed slide in fresh 100% ethyl alcohol in quick motion. The slide then stained in Eosin for 20 seconds (Eosin Y, Fisher Chemical, 168 3rd Ave, Waltham, MA 02451) and dehydrated by quick immersion in following alcohol series: 95%, 95%, 100%, and 100%. Finally, slides were bathed in Xylene (Fisher Scientific, Pit, IL) twice 20 seconds each, and then cover-slipped with Permount (Fisher Scientific, Pit, IL).

Once staining was completed, images were taken using a digital camera attached to light microscope in ImagePro Premier Software at 20x magnification for histological measurements. Each image was pre-calibrated and the measurement for the remaining (unclosed) defect was measured in mm as illustrated in Figure 11.

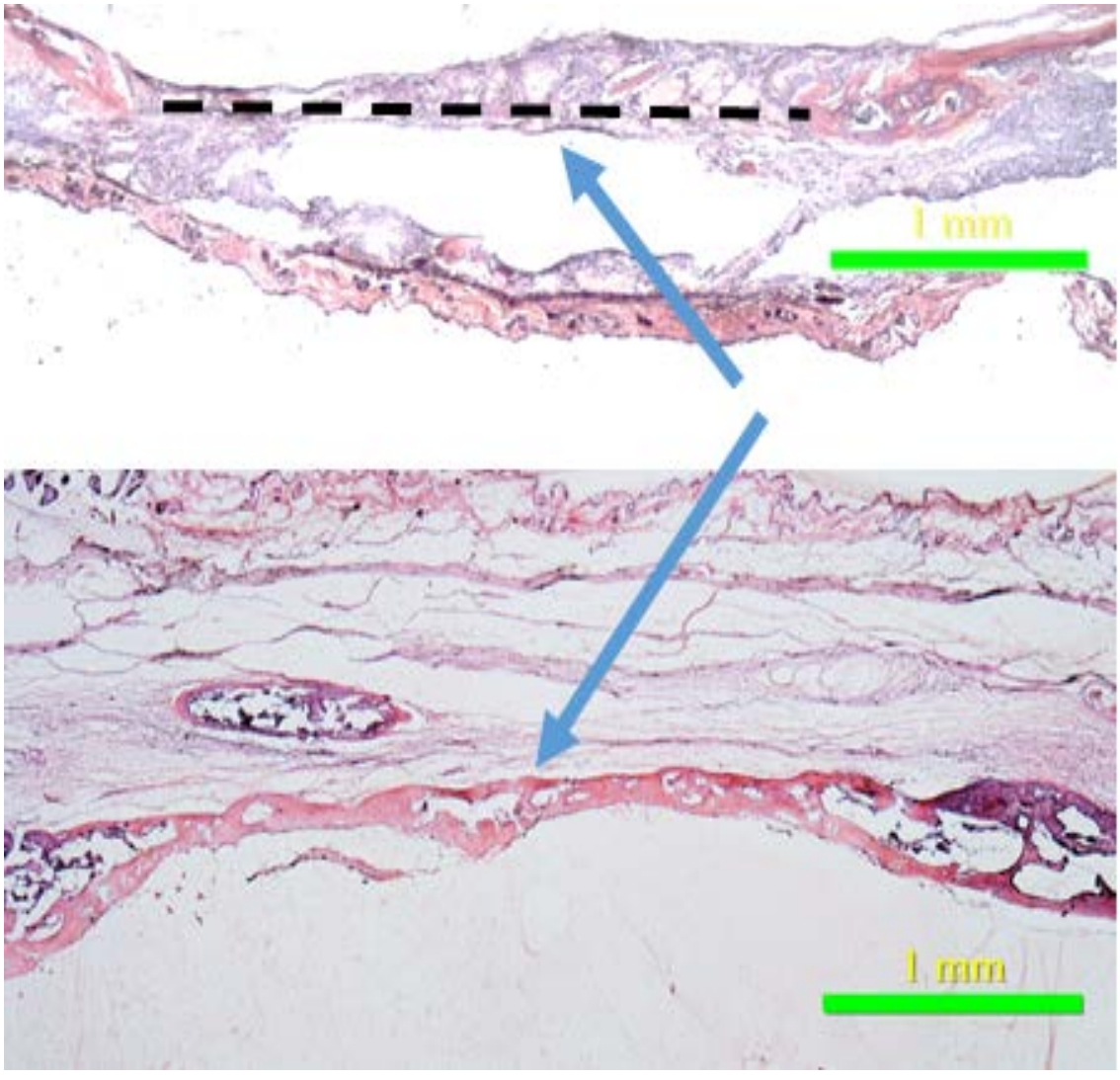

Figure 11: Measurement method using ImagePro

5.8.X-ray analysis

Before decalcification and after fixation, radiographs were taken for each of the collected samples. Using an over-bench X-ray machine and using parallel technique, ordinary X-ray films was taken for each sample (HyBlot CL 5x7 in., Holliston, MA). During X-ray, a standard 1mm metal bar was used to standardize the film magnification.

X-ray films were transferred to a digital format using a manual camera. Each image was calibrated individually with using a standardized metal bar in ImagePro software. Then the surface area of the remaining defect was calculated utilizing the ImagePro shown in Figure 12.

Figure 12: Measurement and calibration bar

5.9. Alkaline Phosphatase Activity Staining and analysis

An alkaline Phosphatase (ALP) activity kit was purchased from Sigma Aldrich (Cat#85L3R, Sigma-Aldrich, St. Louis, MO). Manufacturer recommendations were followed for the staining protocol. Briefly, once the components were mixed, the slides were immersed in the staining cocktail for 30 minutes and then washed in running water. After that, the slides were counterstained with Hematoxylin for 10 seconds, washed and covered using Permount (Fisher Chemical, Fair Lawn, NJ).

Stained samples were analyzed under a light microscope for ALP activity and were scored as follows:

Score of 0: no visible ALP activity

Score of 1: ALP activity around both of the defect edges.

Score of 2: ALP activity around both edges of the defect and in the middle of the defect.

Score of 3: Strong ALP activity around the edges and the newly formed bone is less than 1mm

Score of 4; Strong ALP activity around the defect edges and the newly formed bone is more than 1mm and less than 4.

Score of 5: Strong ALP around the defect edges and the newly formed bone is more than 4mm.

5.10. Statistical Analysis.

All measurements were performed in a blind fashion and double-checked at a one-week interval. Intra-examiner variation was found to be less than 5%. A two-tailed Student's *t*-test was emphasized for comparison between two groups was performed. A *p*-value of <0.05 was considered to be statistically significant.

6. RESULTS

6.1. X-ray Analysis

Our study aimed to compare the four different materials, PGIcNAc, PRP, L-PRF and BMP2. The unhealed areas measured in mm^2 show that untreated mice (negative control) exhibited a 55% healing after six week. However, mice treated with high concentration of BMP2 displayed up to 95% closure of the 5mm defect. At low BMP2 concentration, it allowed for 80-85% closure. Additionally, any treatment combination that contained the BMP2 was sufficient to produce bone healing in CSD. This was statistically significantly higher than in all other treatment groups. All physical forms of PIGcNAc, sheet, crushed powder, gel or any combination of this material was not able to close more than 60-65% of the original CSD. This was not a statistically significant different when compared to the negative control. Groups that received PRP, L-PRF or any combination of this material did not produce a statistically significant difference from the negative control. Representative X-rays are depicted in Figure 16-18 and measurements are shown in Figures 13-15.

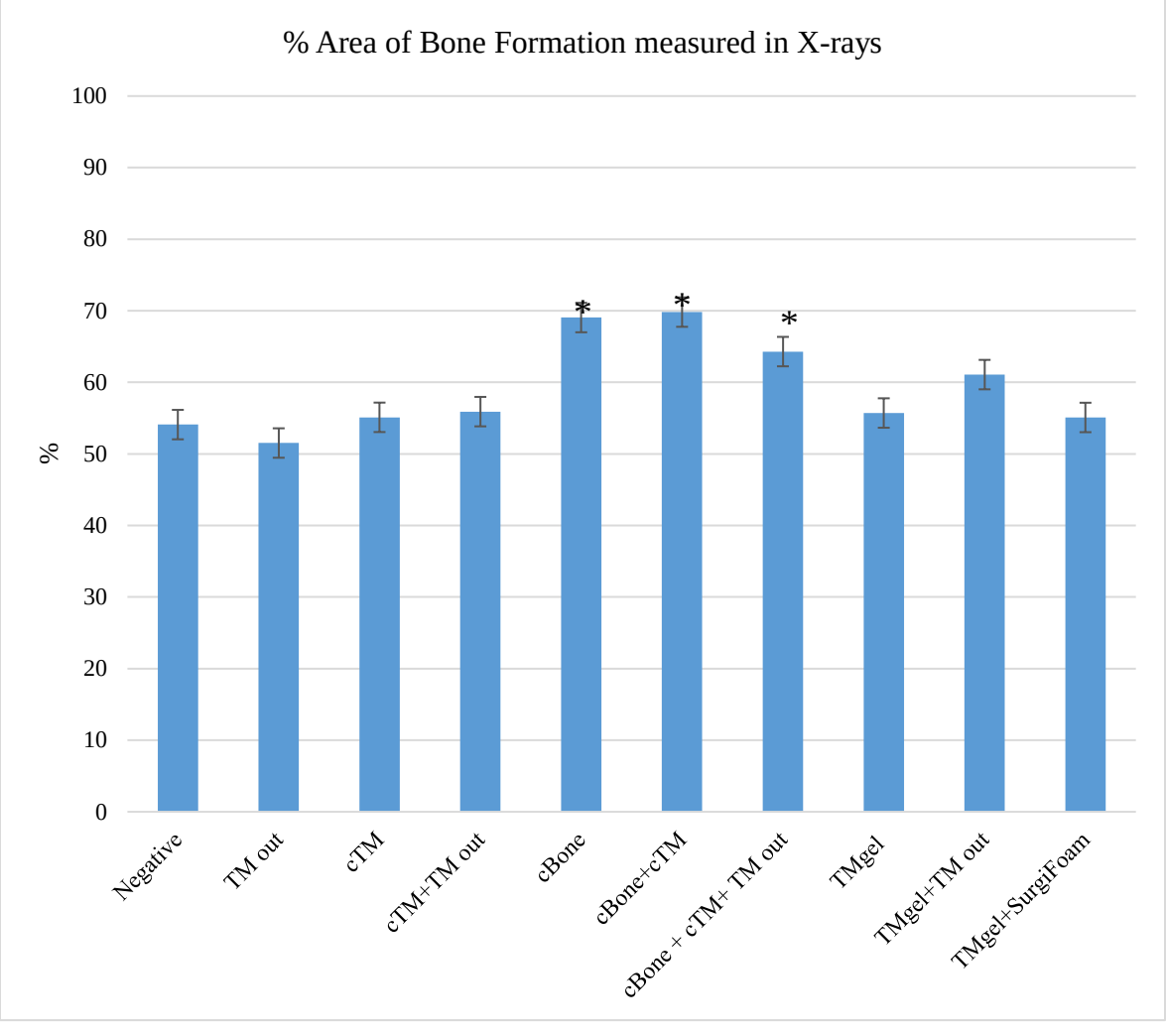

Figure 13 Data represent the percentage of the defect area closed as measure on X-rays. * indicate significant $p<0.05$

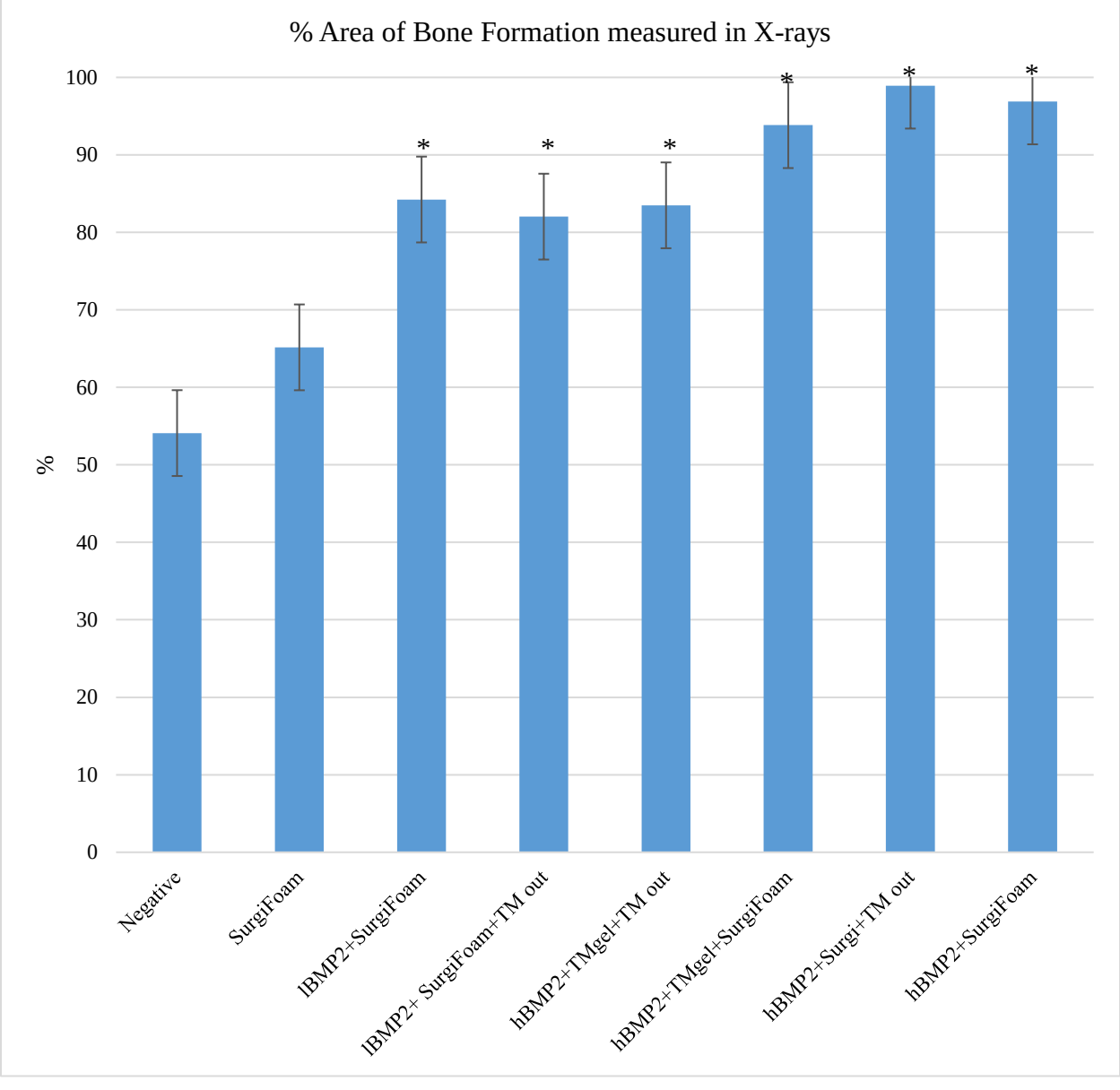

Figure 14 Data represent the percentage of the defect area closed as measure on X-rays. * indicate significant $p<0.05$

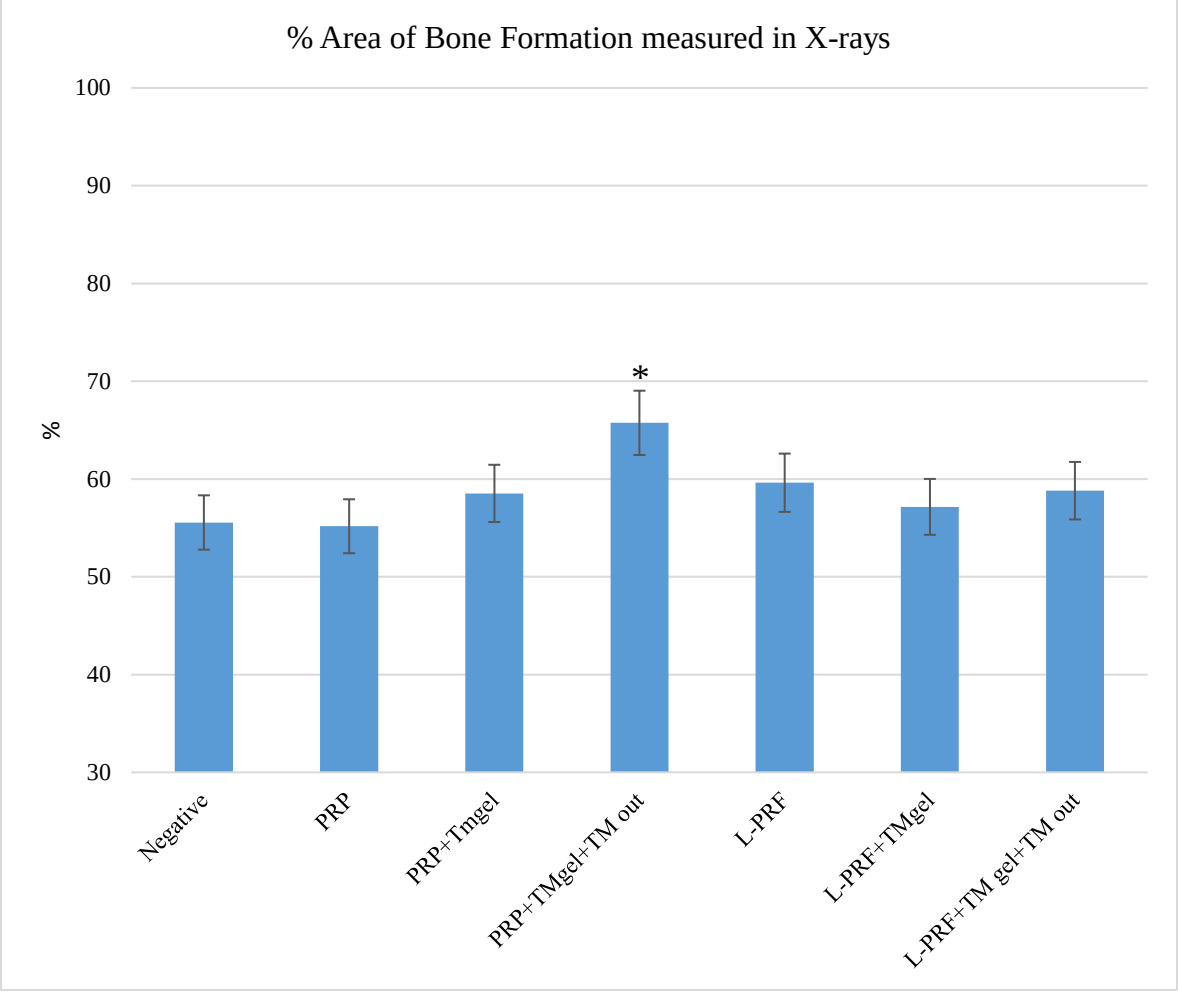

Figure 15 the remaining groups. * indicate significant $p<0.05$

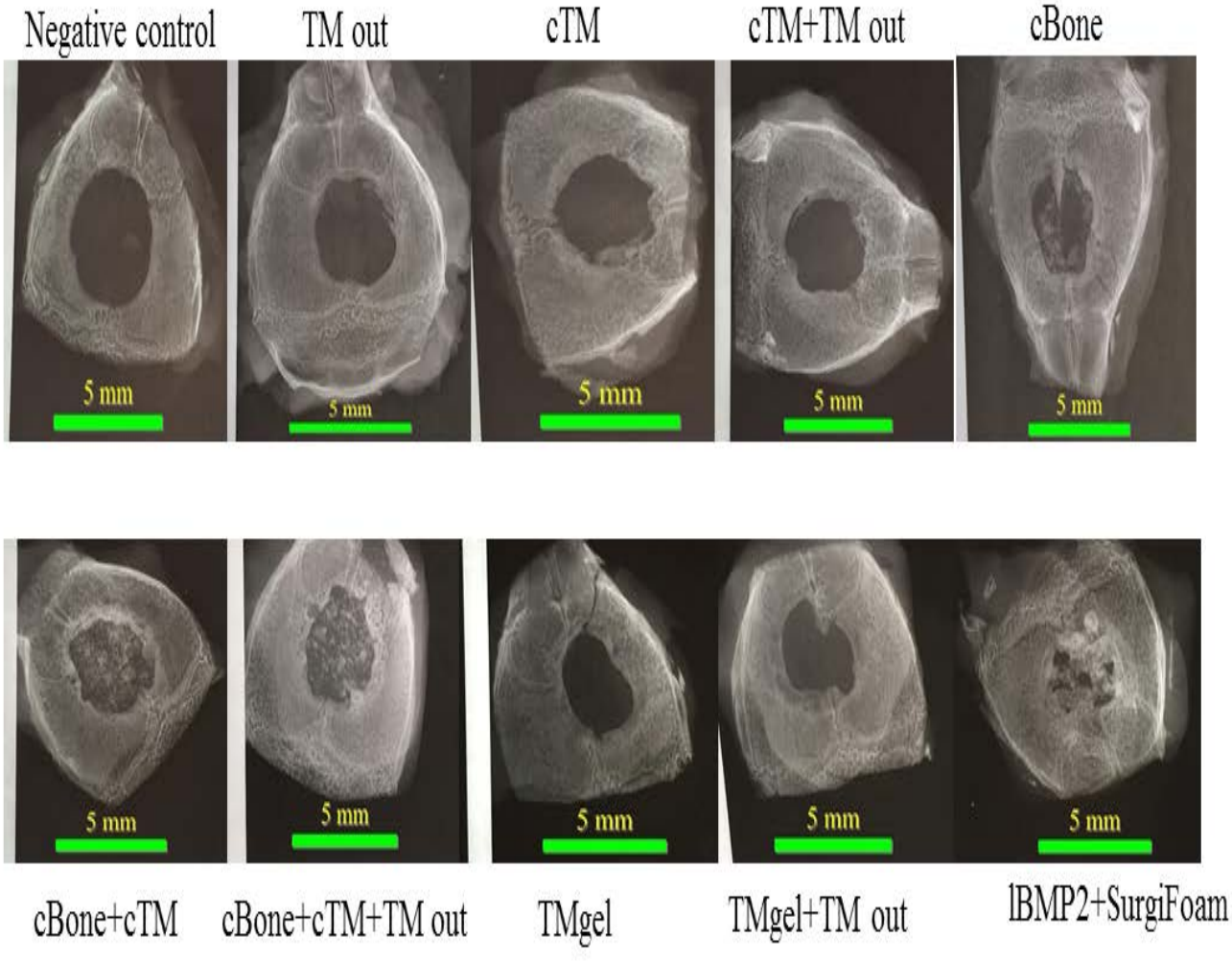

Figure 16 Representative radiographs

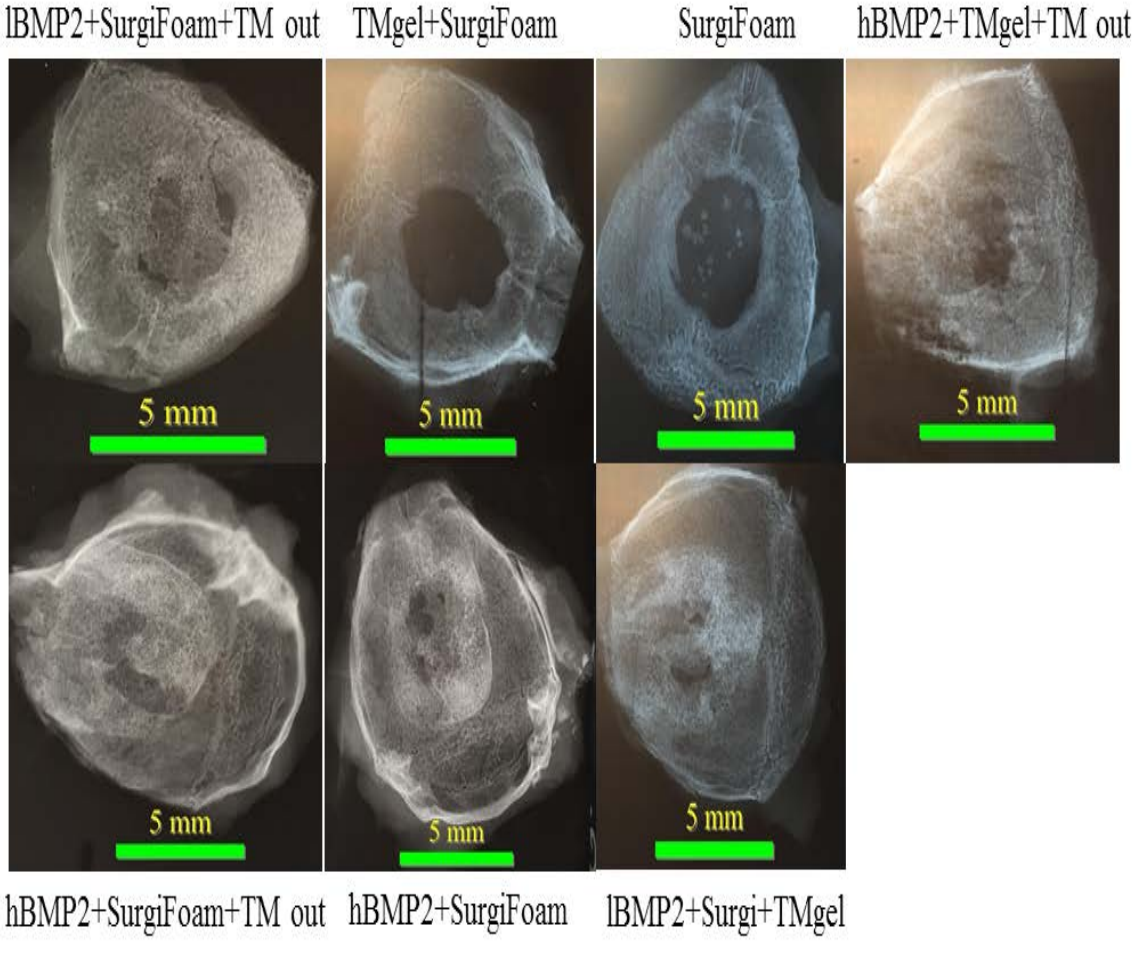

Figure 17 Representative radiographs.

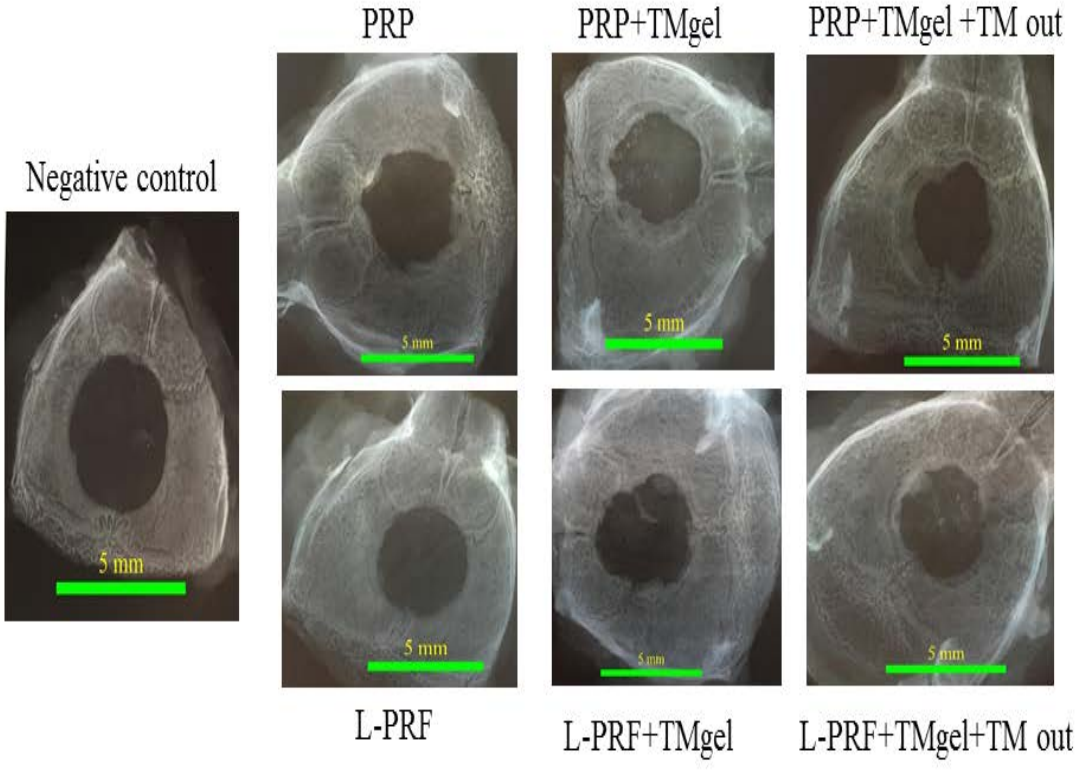

Figure 18 Representative radiographs.

6.2.Histological Analysis

H&E stained slides were analyzed utilizing a light microscope attached camera in an ImagePro Premier program. The results show that groups treated with BMP2 were able to close 90-95% of the original defect, which is statistically significantly higher than all other groups with $p<0.05$. These groups include BMP2 at low or high concentration loaded in SurgiFoam sponge. Additionally, the TMgel BMP2 and TMgel BMP2 and TM-out group showed a similar trend. On the other hand, groups that were treated with PRP, L-PRF, or any combination of the crushed or sheet TM was able to close 60% of the original 5mm CSD. These results were not statistically significant different from the untreated negative control group. Figures 22-29 show representative images from each groups and Figures 19-21 show the quantitative results.

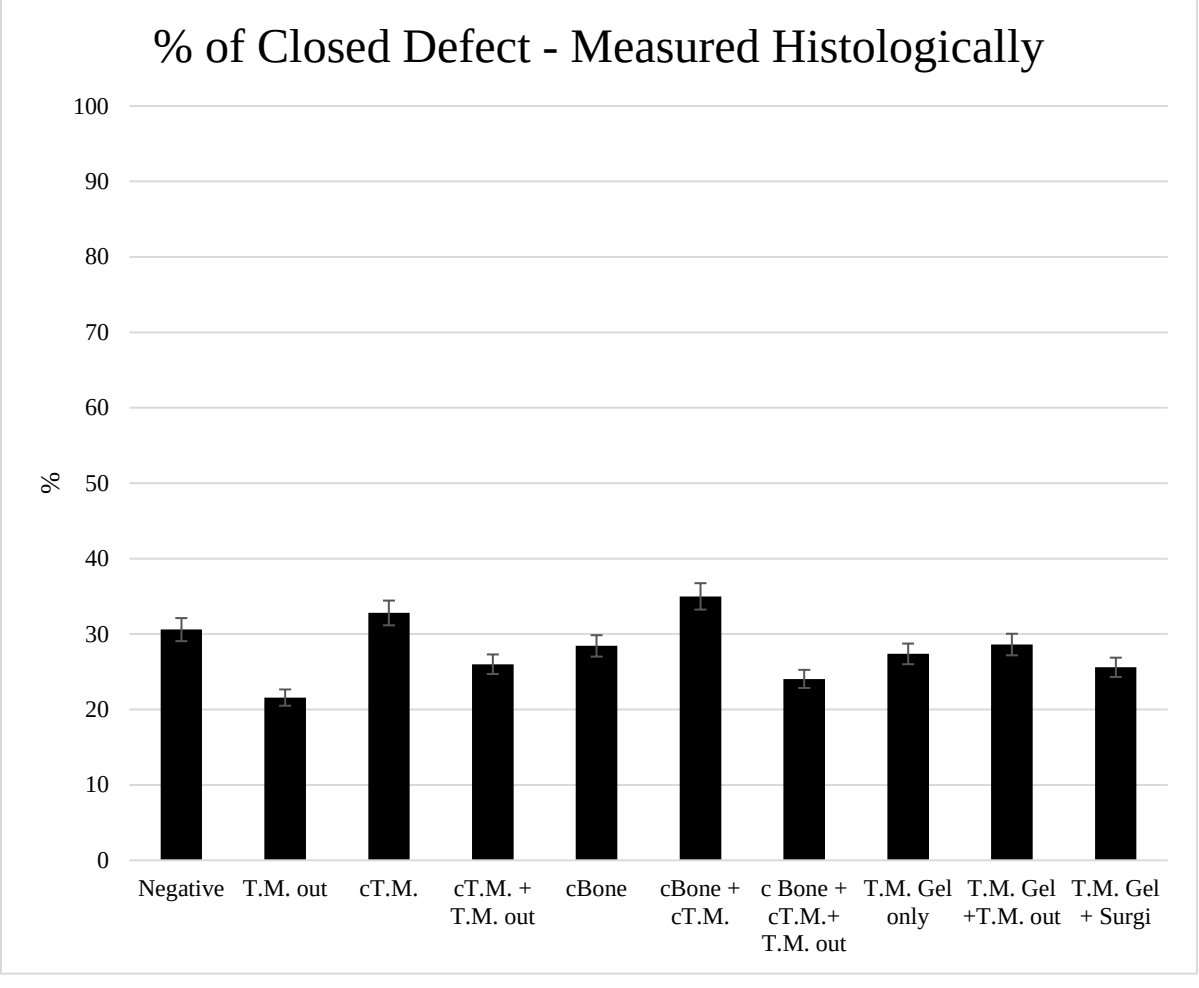

Figure 19 Barograph shows the histological measured sections

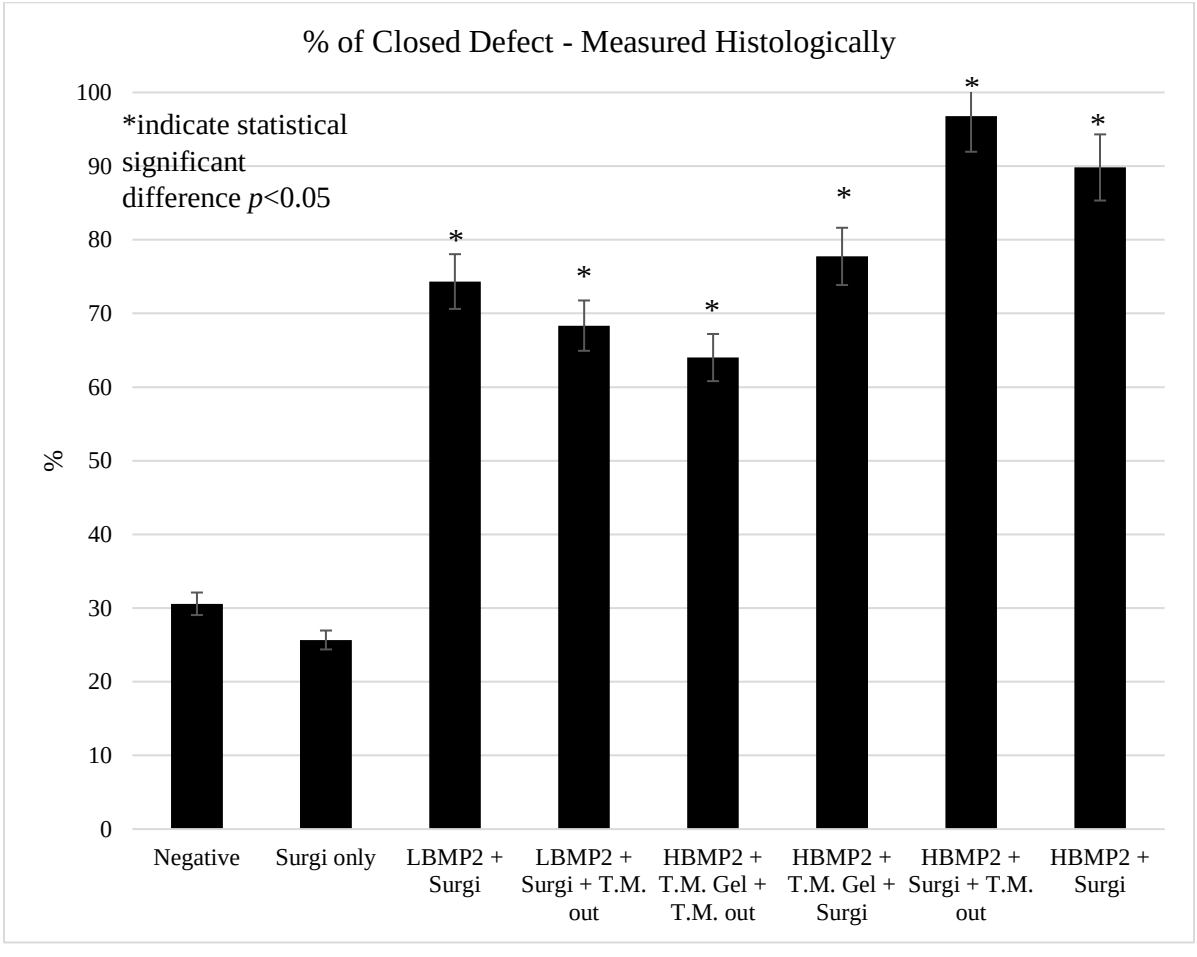

Figure 20 Barograph shows the histological measured sections

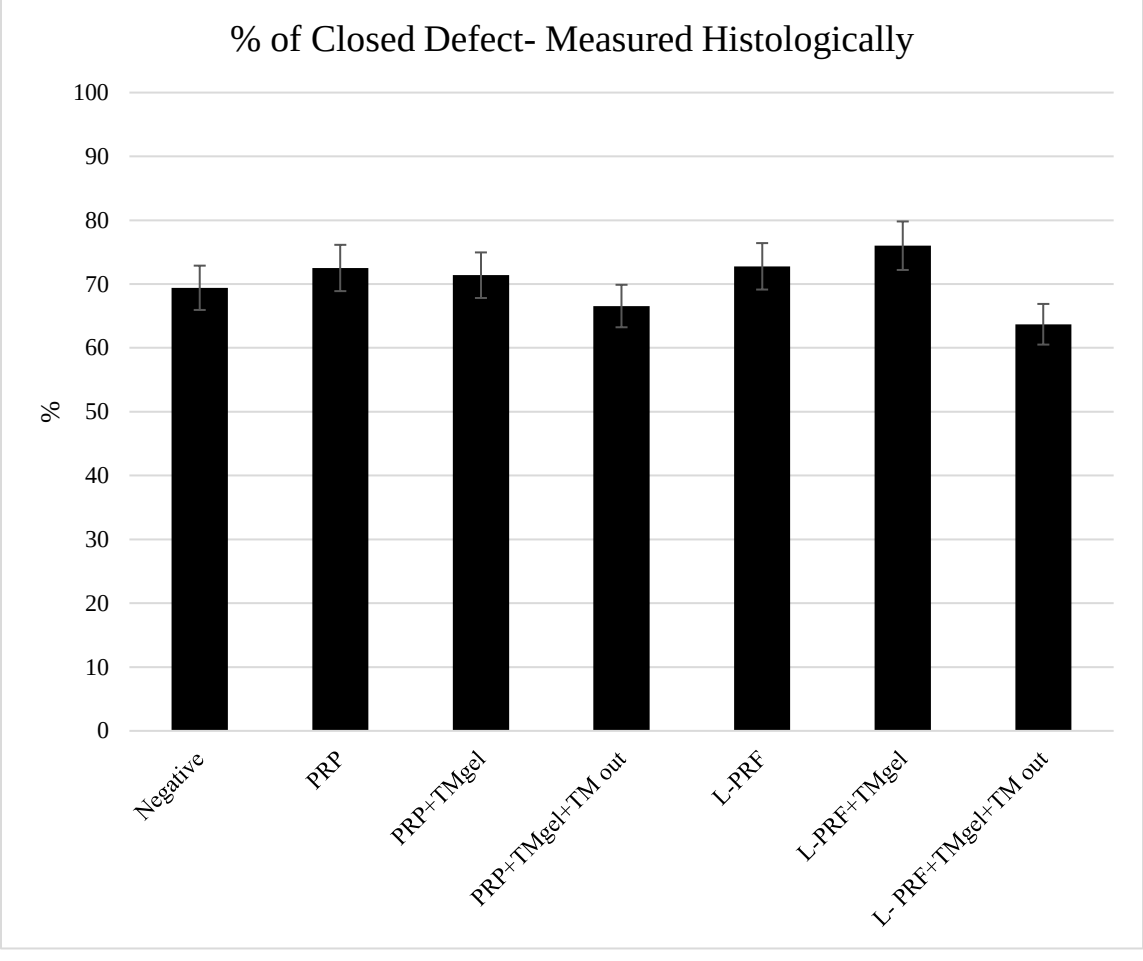

Figure 21 The remaining groups

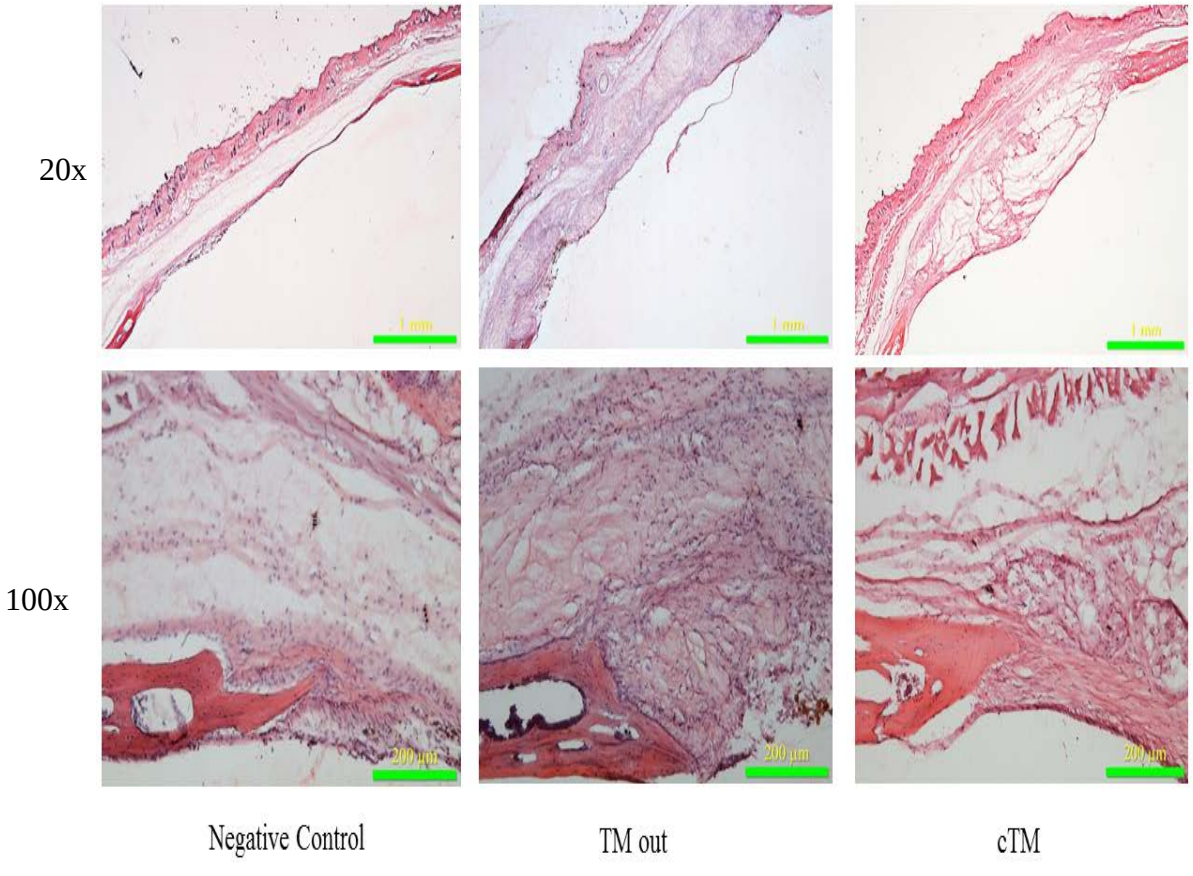

Figure 22 Representative Images G1-3, Top row 20x bottom 100x

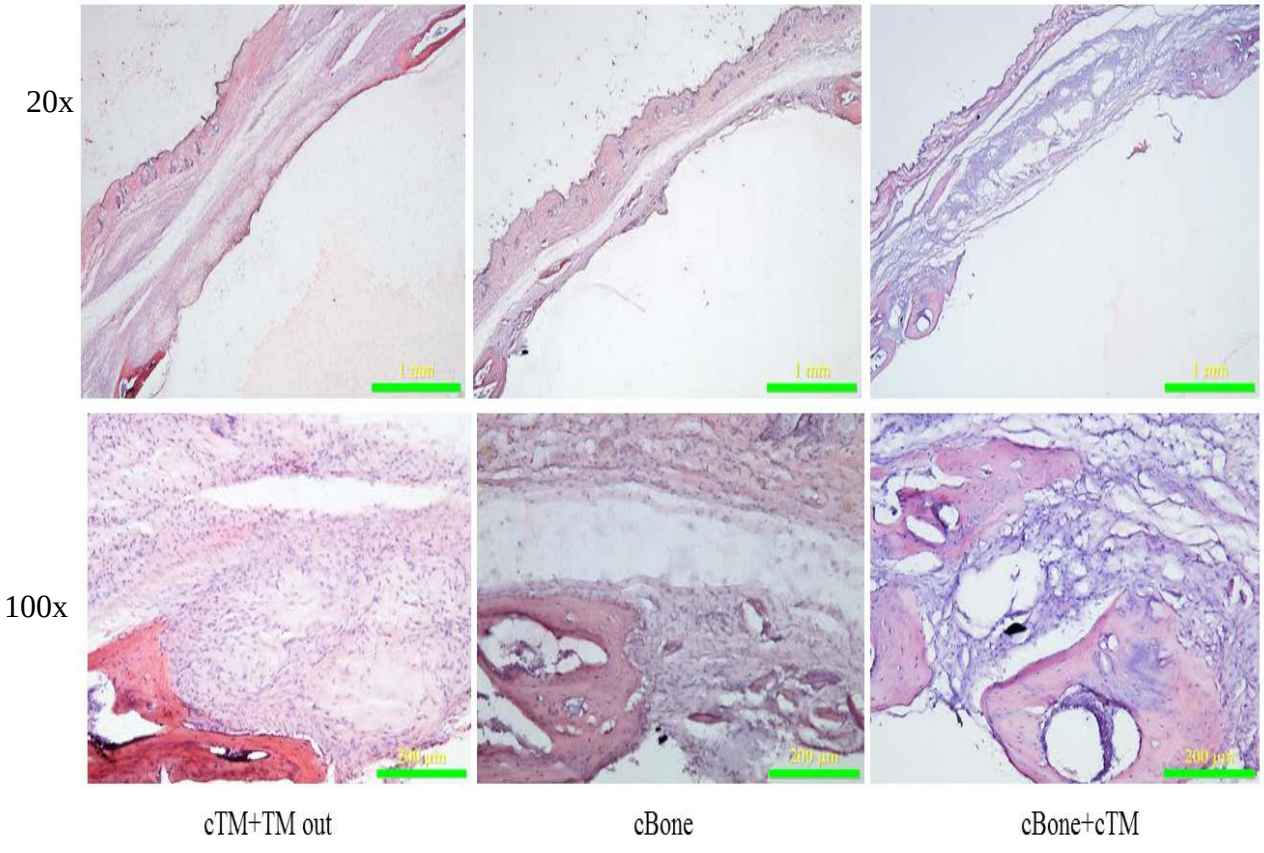

Figure 23 representative images G4-6, Top row 20x bottom 100x

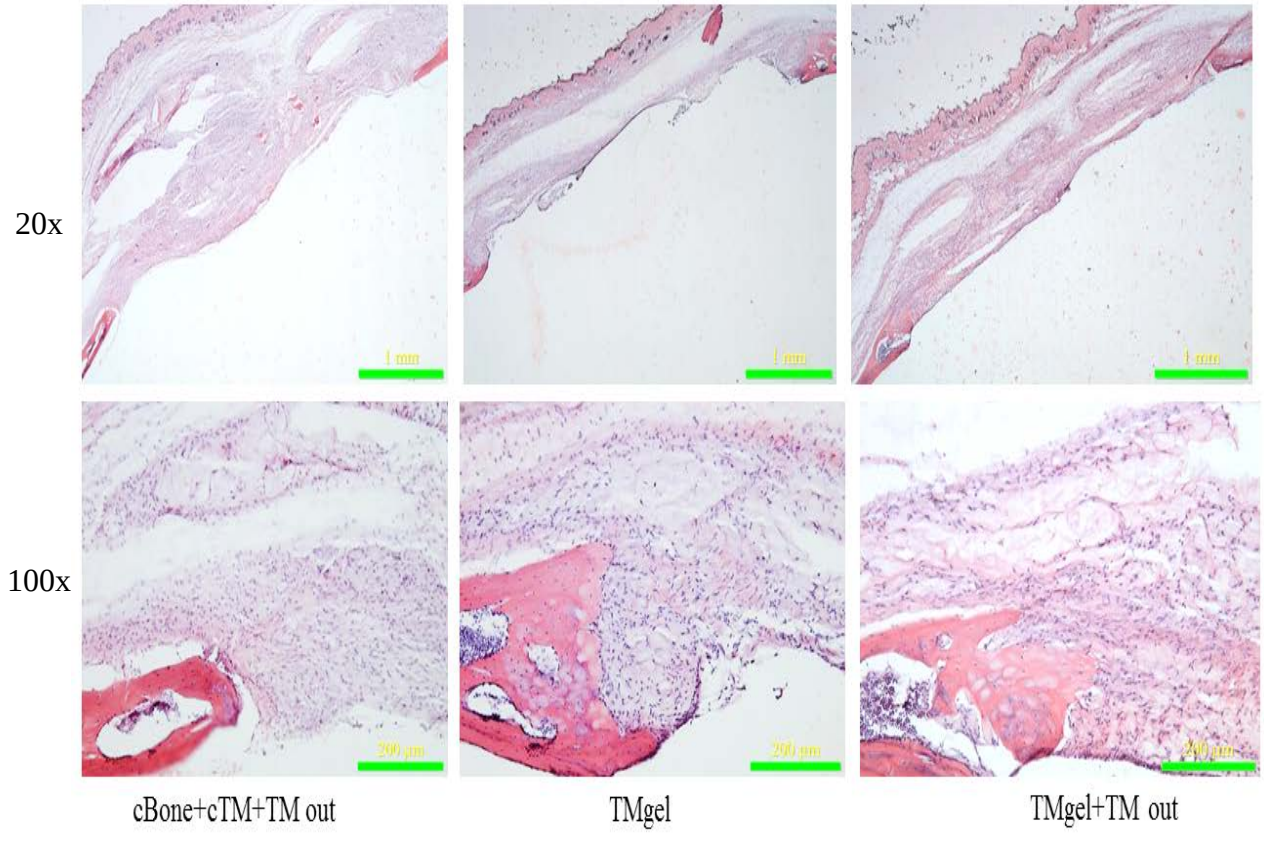

Figure 24 Representative Images G7-9, Top row 20x bottom 100x

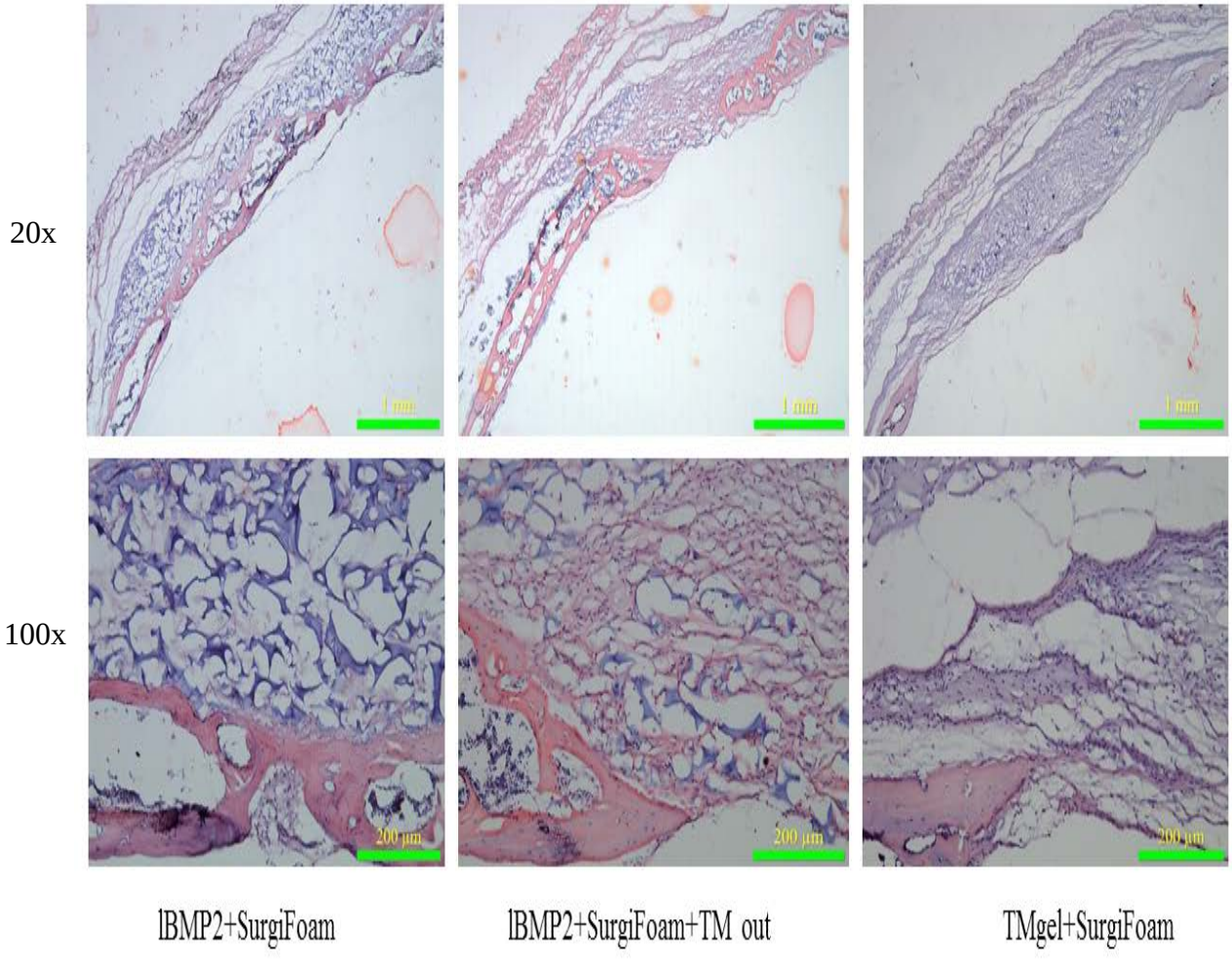

Figure 25 Representative Images G10-12, Top row 20x bottom 100x

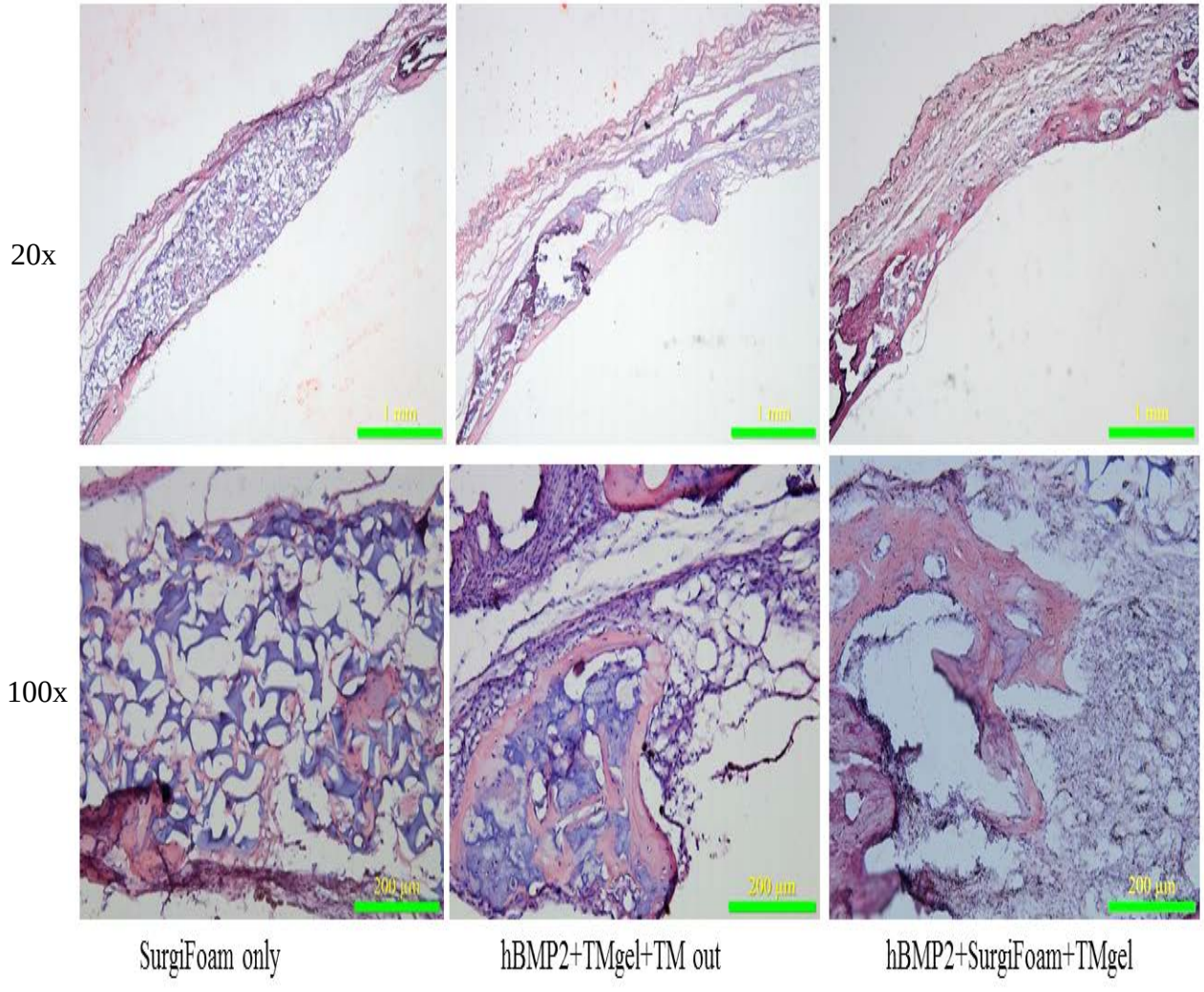

Figure 26 Representative Images G13-15, Top row 20x bottom 100x

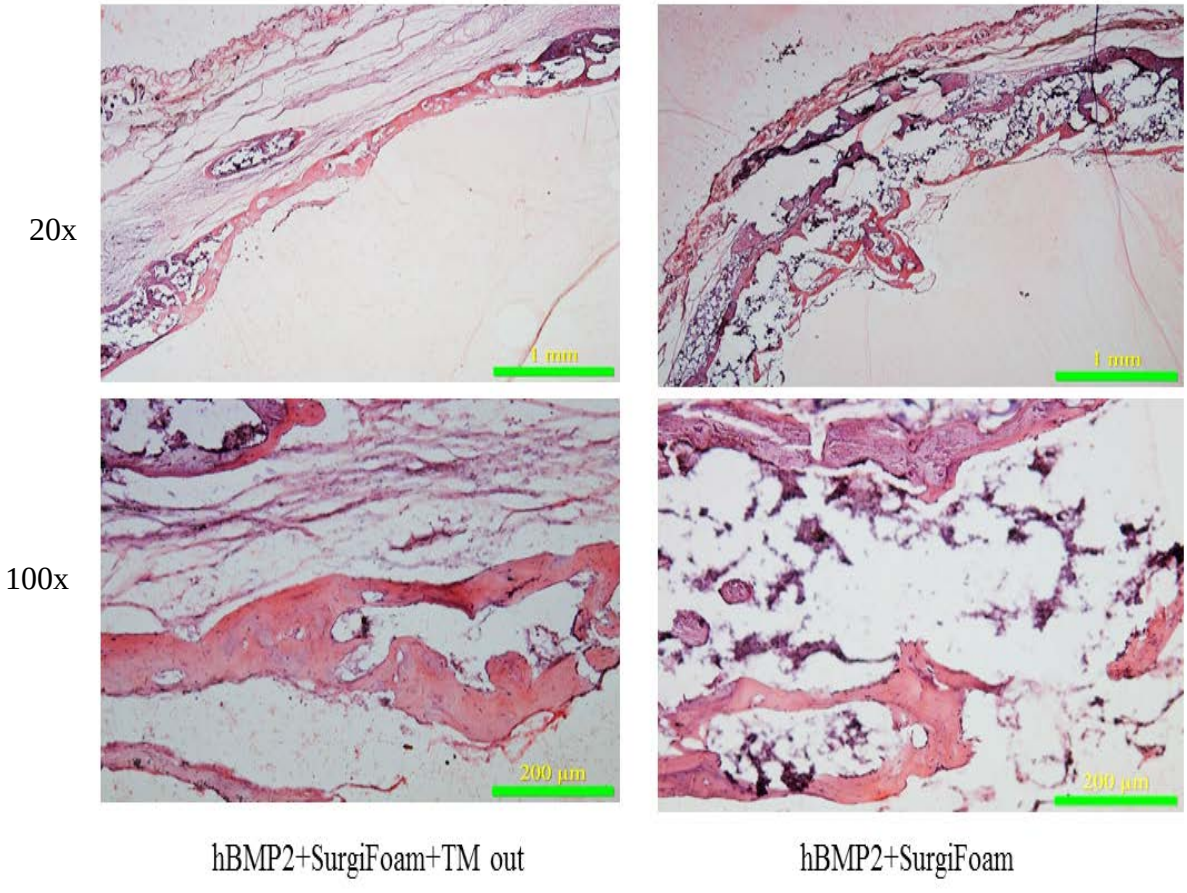

Figure 27 Representative Images G16-17, Top row 20x bottom 100x

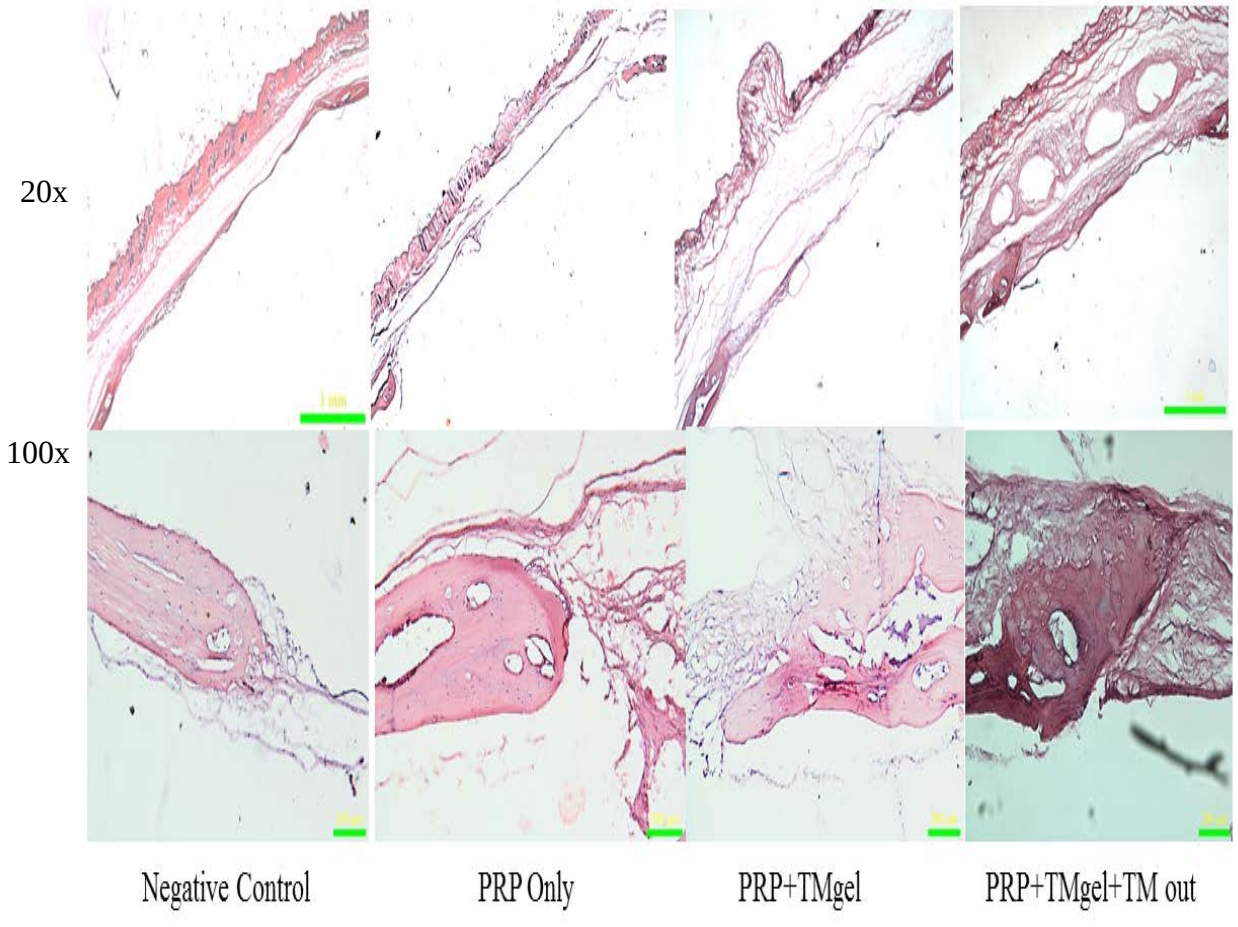

Figure 28 Representative Images G18-20, Top row 20x bottom 100x

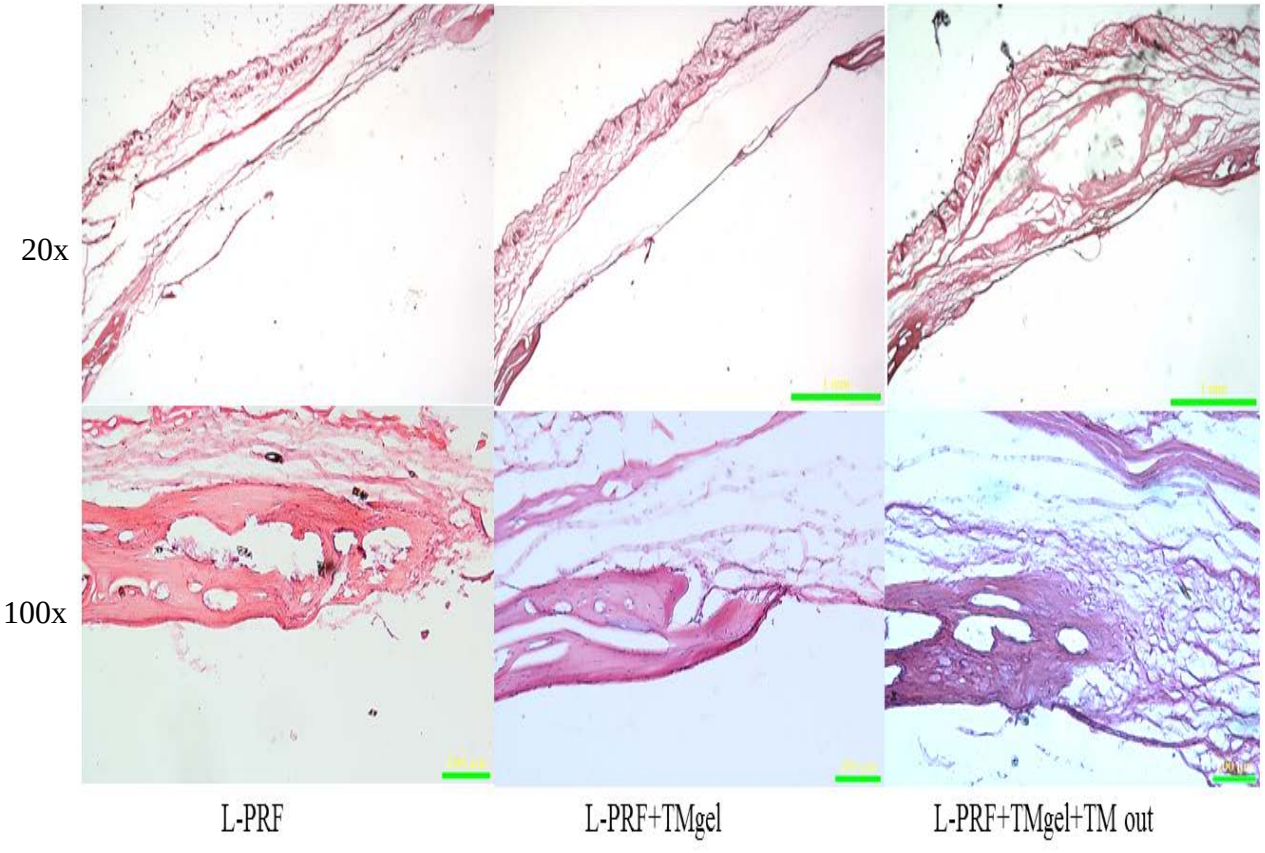

Figure 29 Representative Images G21-23, Top row 20x bottom 100x

Interestingly, the histological analysis showed that the quality of the bone associated with the groups treated with TMgel or TM-out did allow better bone organization. Additionally, the TMgel was a bone-friendly material that did not by any means reduced or interfered with bone formation. In fact, we observed that the TMgel has been engulfed by the newly formed bone. Figures 28-31 depict different combinations of TMgel and TM sheet that demonstrate the compatibility of the materials tested with the bone tissue.

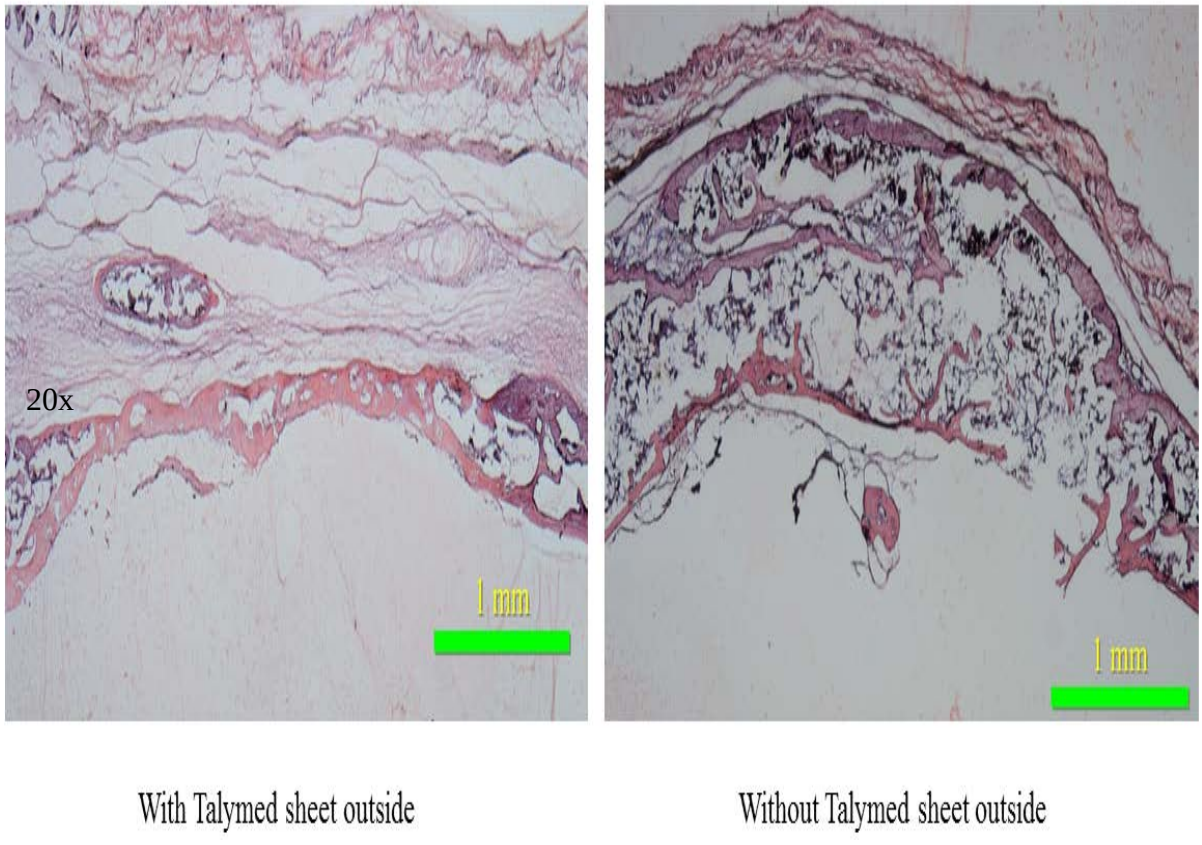

Figure 30 Organization of bone when TM out used versus not TM sheet.

200x

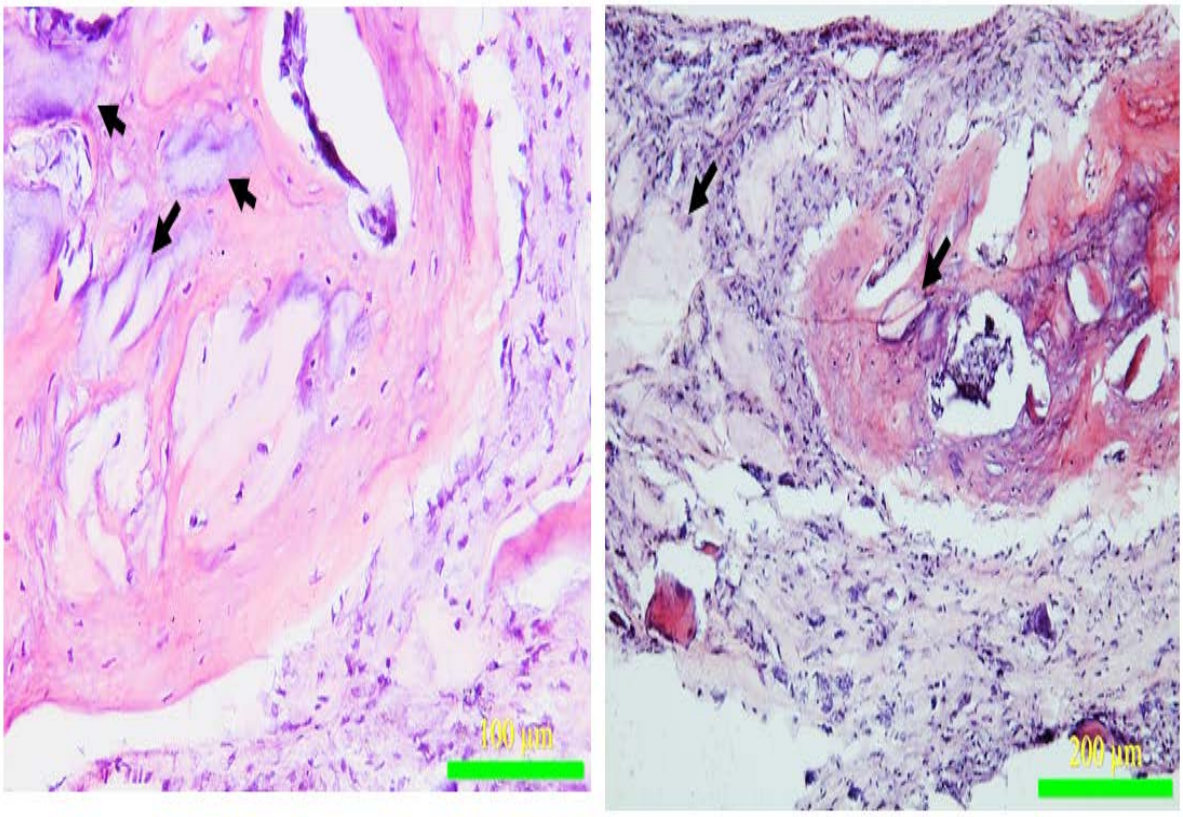

Talymed sheet inside the newly formed bone (images form sample of crushed bone + crushed Talymed)

Figure 31 Arrows point to the TM sheet inserted within the new bone

200x

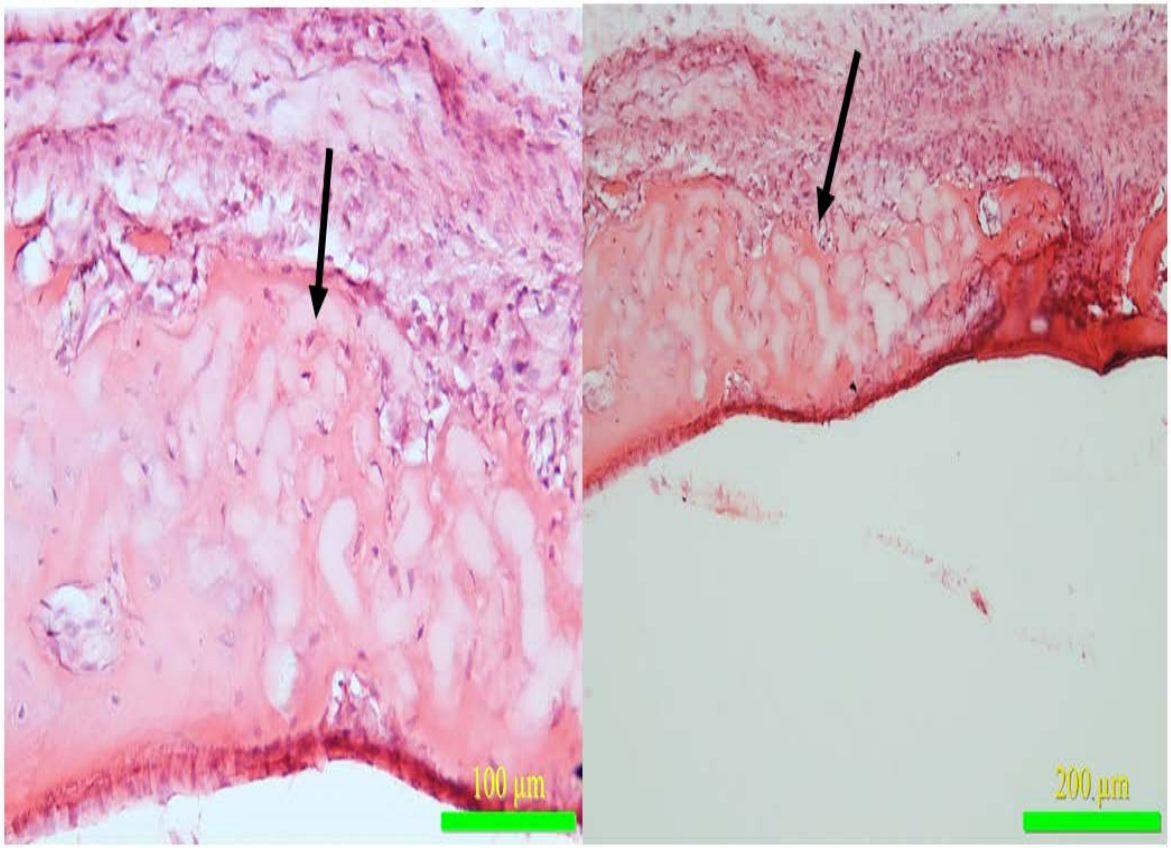

100x

TMgel at 4 weeks

Figure 32 Arrows point to TMgel inside the newly formed bone at 4 weeks

200x

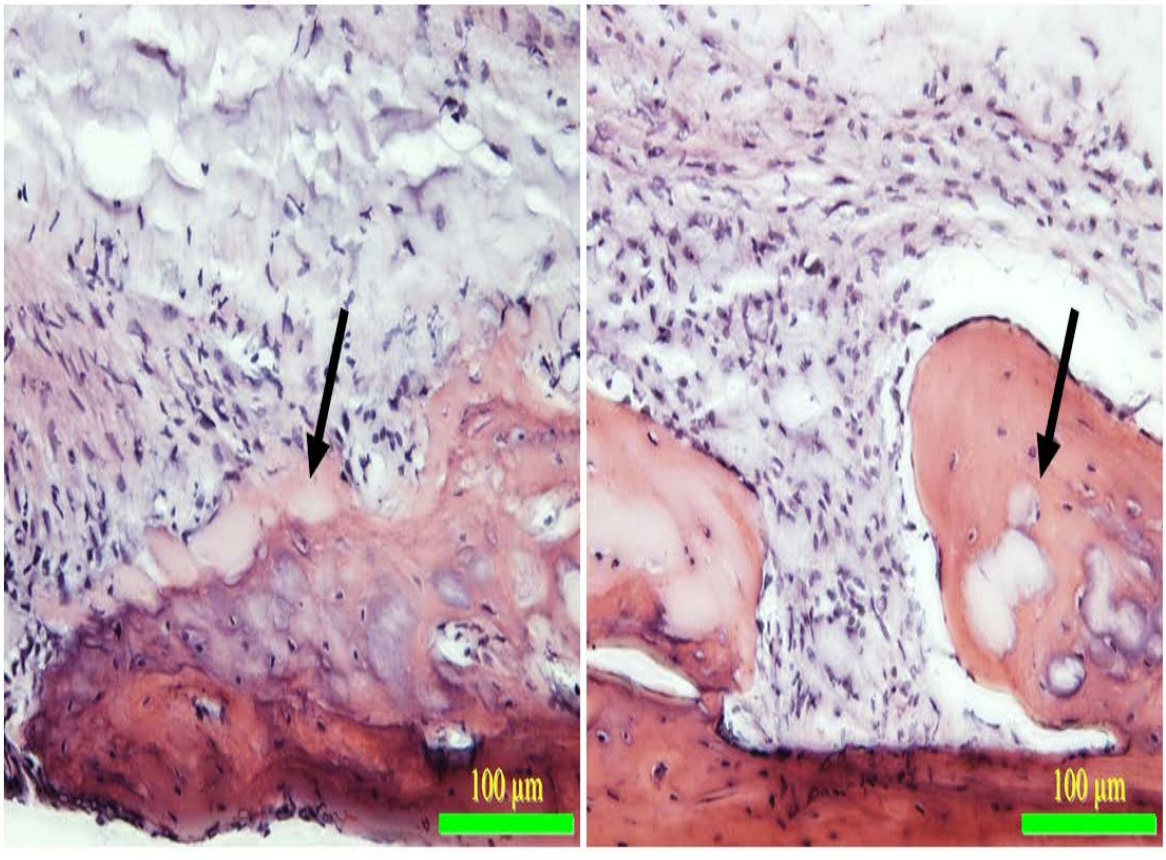

Figure 33 Arrows point to TMgel inside the newly formed bone after 6 weeks

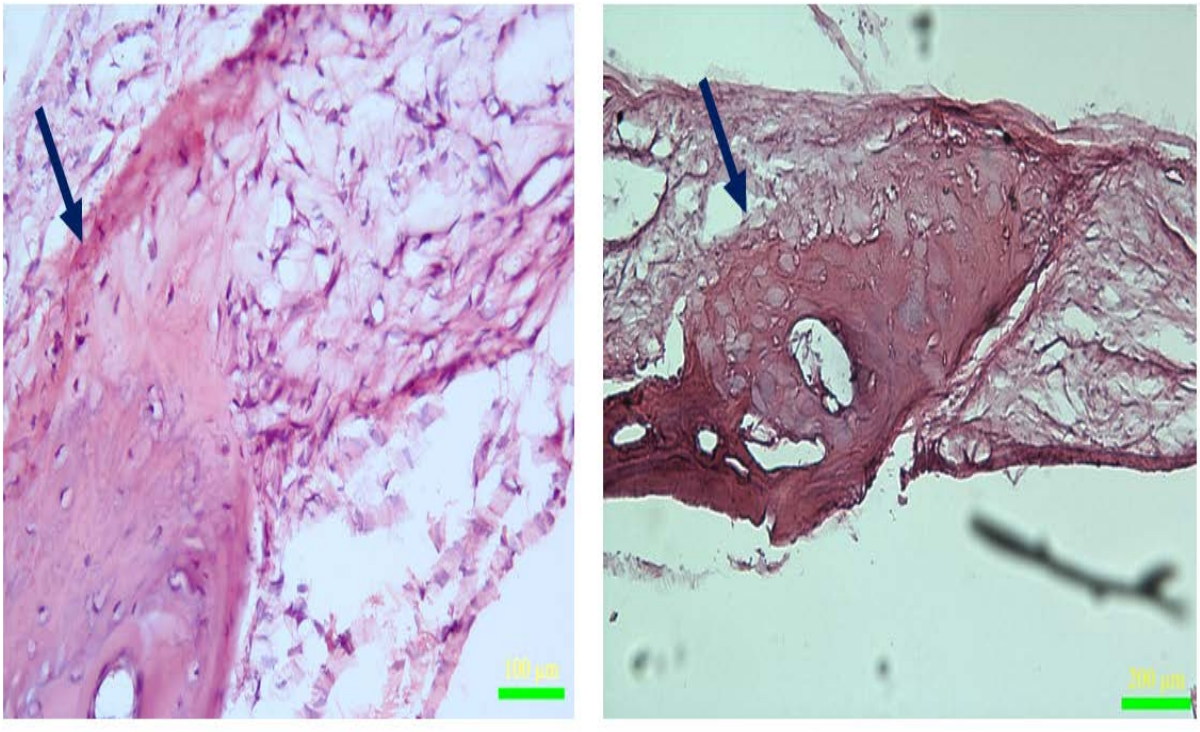

Figure 34 Arrows point to the TMgel inside the newly formed bone, which indicates the TMgel compatibility with bone and other materials

6.3.ALP activity Analysis

The results demonstrate that the BMP2 groups showed significantly higher ALP activity when compared to all other groups. Any combinations that did not contain BMP2 did not present with high ALP activity. Figures 38 and 39 show selected groups for representation and Figure 35-37 shows the quantitative scoring for the ALP activity.

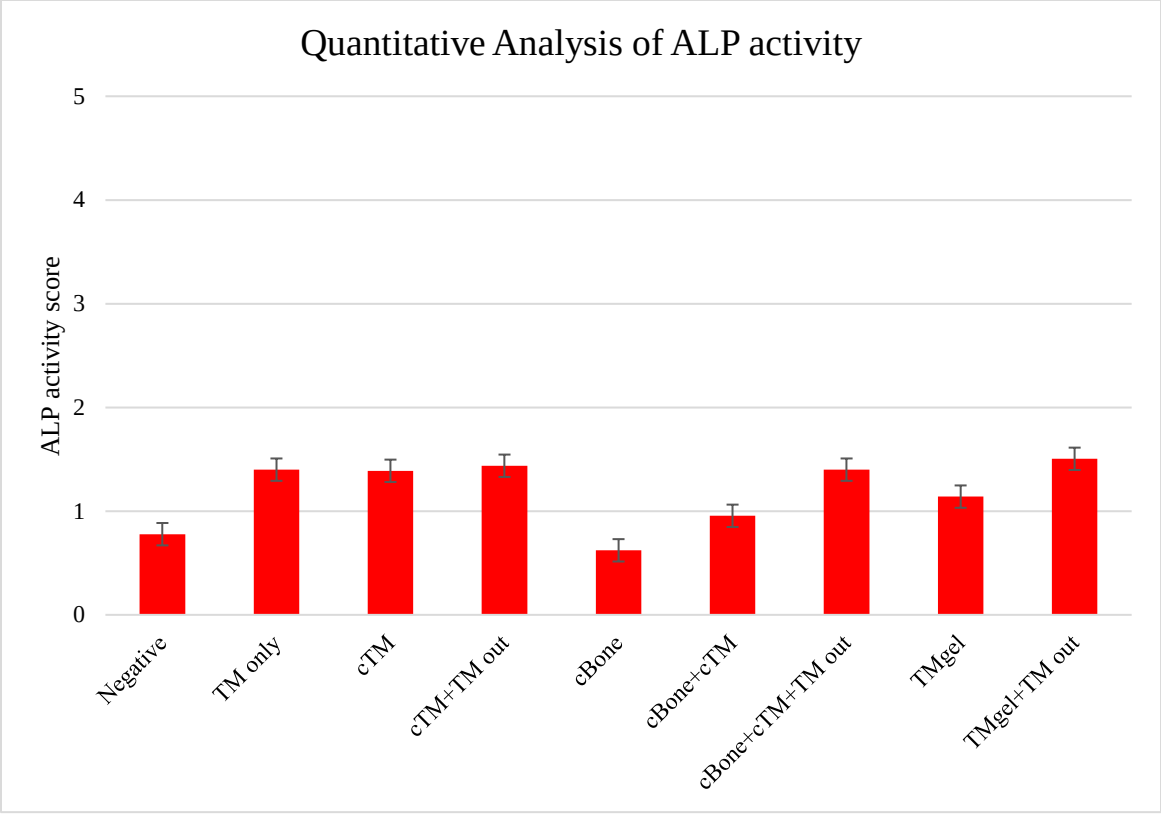

Figure 35 Quantitative ALP activity score

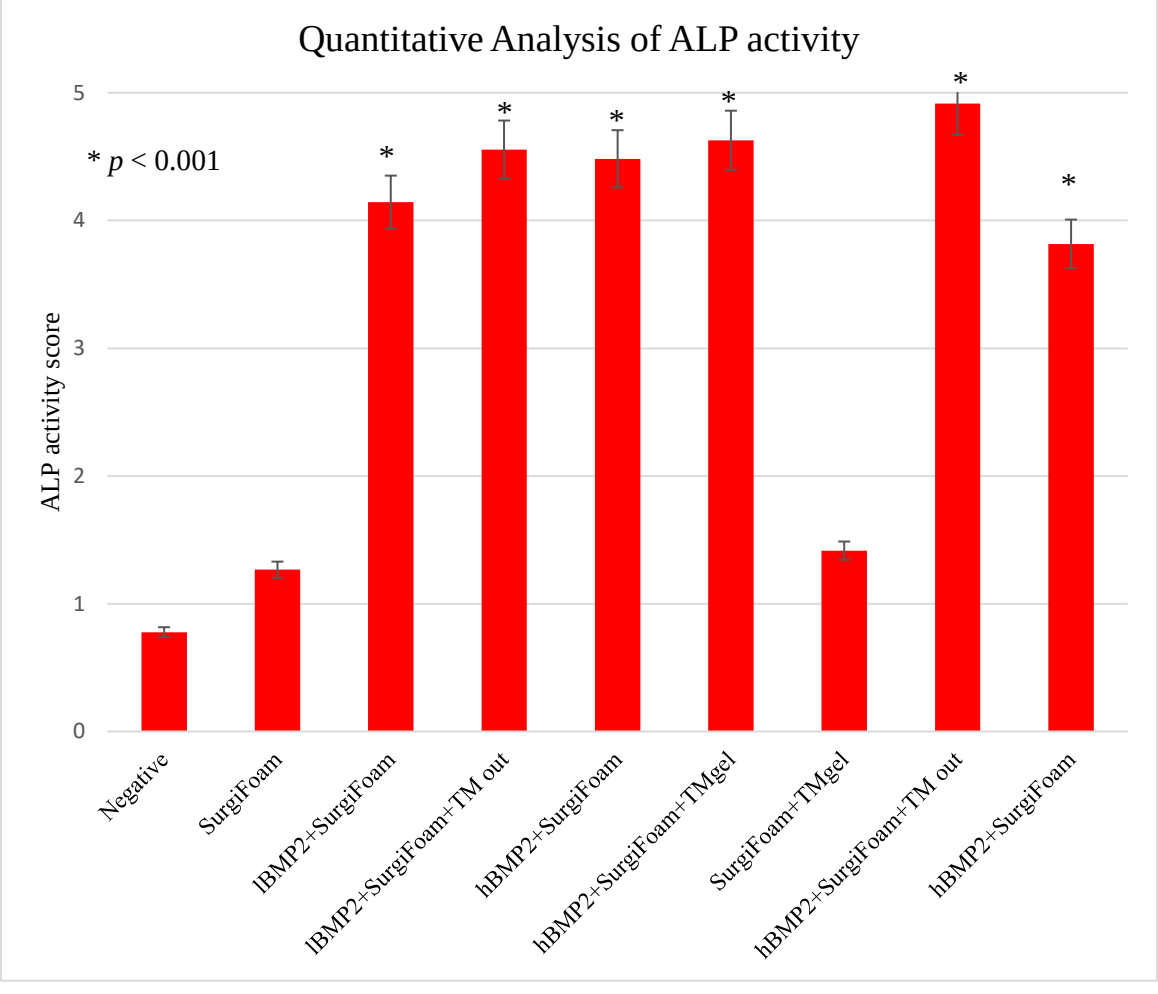

Figure 36 Quantitative analysis of ALP activity $p<0.001$

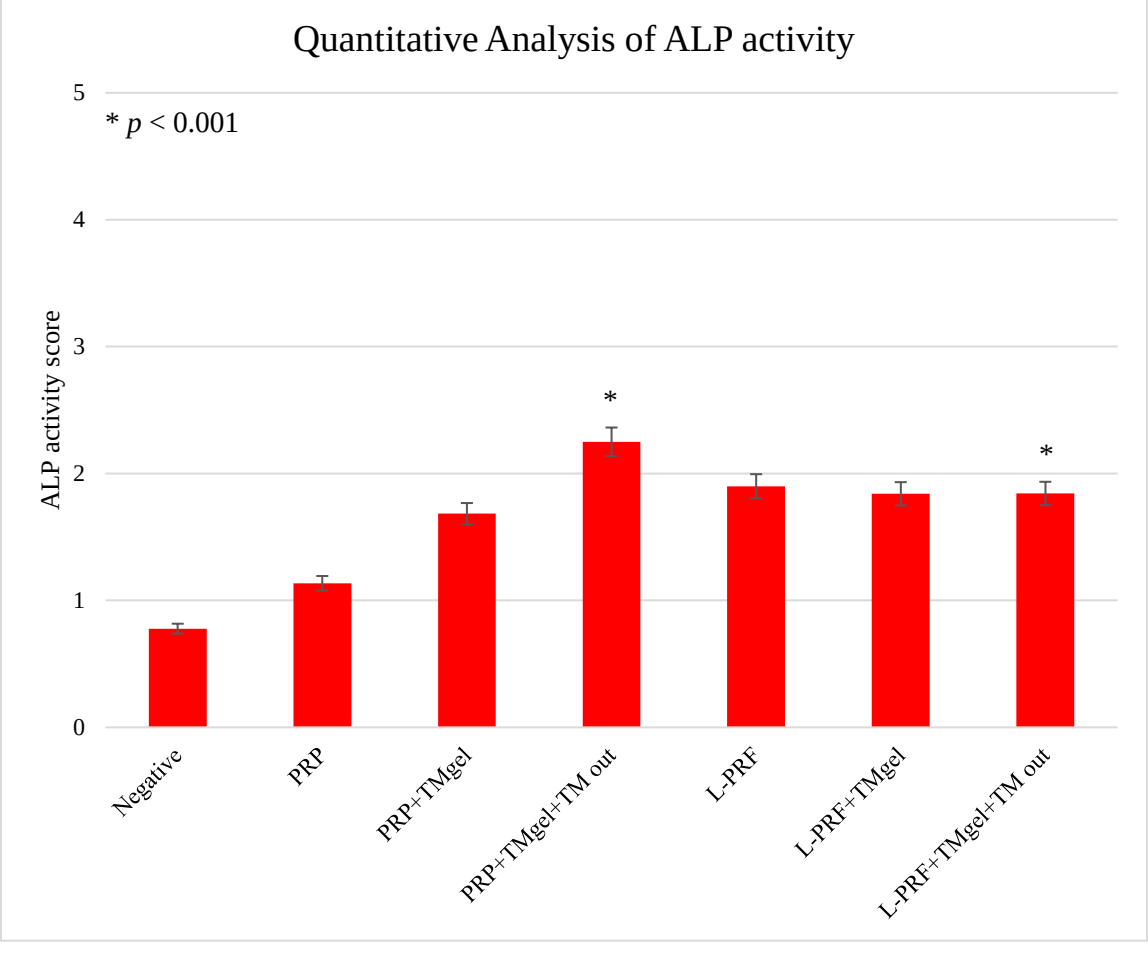

Figure 37 Quantitative analysis of ALP activity $p<0.001$.

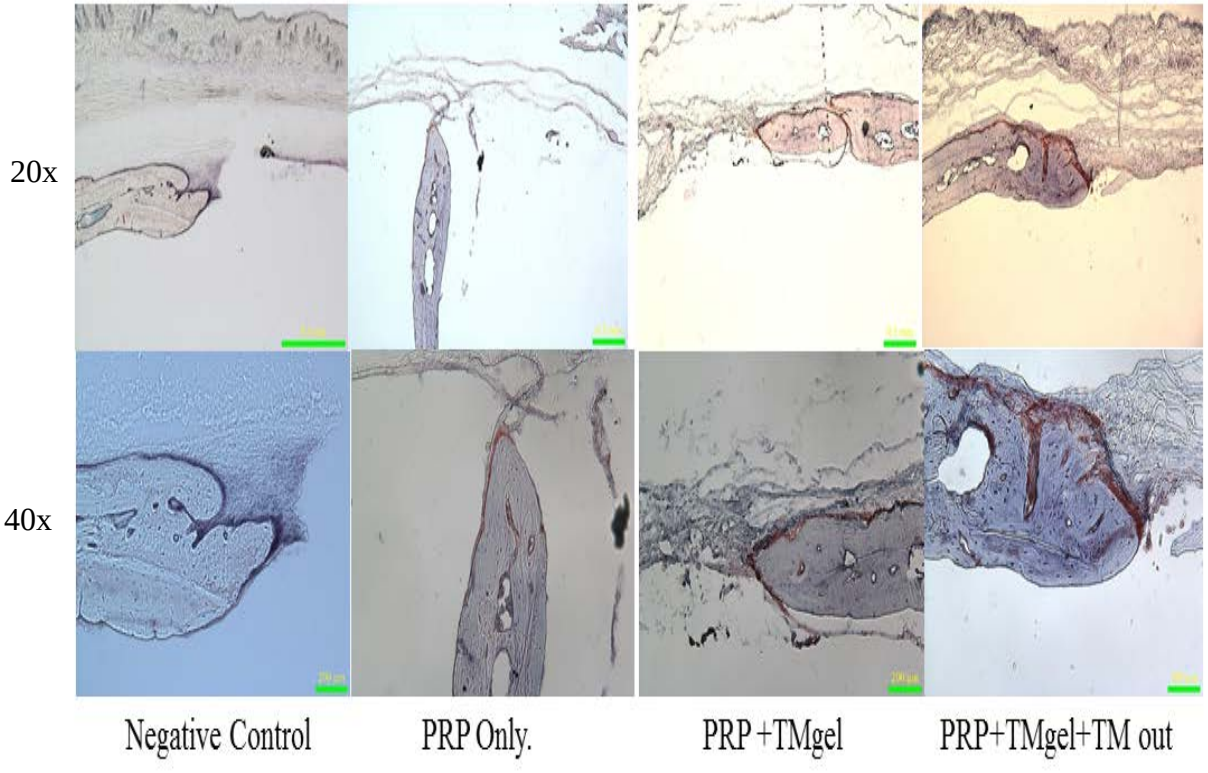

Figure 38 Selected groups showing ALP activity. The ALP levels were evaluated by the increase of red color intensity.

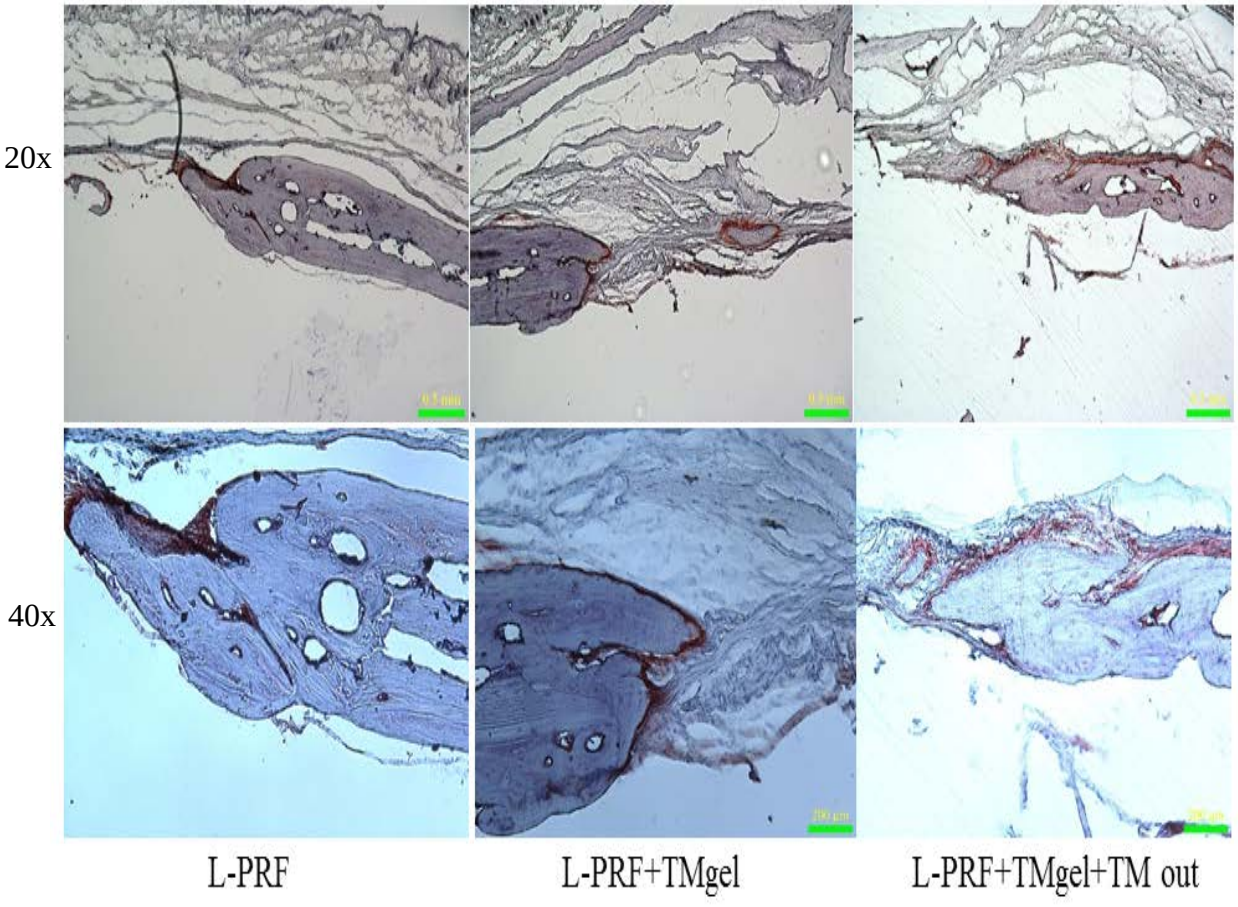

Figure 39 ALP activity images. The ALP levels were evaluated by the increase of red color intensity.

7. DISCUSSION

This study was aimed at evaluating the effects of *Pg* infection on miRNA expression in BMMs and to evaluate their role on the inflammatory host-response *in vitro* and *in vivo*. This wide-scale analysis led to the identification of several miRNAs differentially expressed in infected cells. In order to determine the effects associated to this modulation and potential implication on innate immune response, the focus was placed on miRNAs that had high level of significance. Through bioinformatics prediction and the protein level of cytokines secretion have been conducted suggesting a role for mmu-miR-155-5p, mmu-miR-2137, mmu-miR-7674 and mmu-miR-8109 in *Pg* induced host-response modulation. Interestingly, the present study also showed the potential therapeutic approach of using specific miRNAs to control *Pg* induced inflammatory response in a mouse model of inflammation and bone resorption.

The capacity for modulation of the host-response caused by *Pg* infection is part of the bacterial survival strategy. Several mechanisms have been developed by such bacteria in order to invade and proliferate within the host-cells, whether at the gene (Yu *et al.*, 2010) or protein level (Li *et al.*, 2014; Huck *et al.*, 2015). Regulation of protein expression is critically important in homeostasis and pathology. Because miRNAs have been shown to control 30% of all protein-coding genes and also to participate in the regulation of almost every cellular process (Filipowicz *et al.*, 2008; Simo *et al.*, 2015), miRNAs could be considered as important post-transcriptional regulators. Their expression has been related to the dysregulation of several biological processes in both innate and adaptive immune responses (Kebschull *et al.*, 2015). The impact of infection on miRNA expression has already been described for several bacteria in different cell models. This is especially true for macrophages that play an important role in cytokine secretion, immune response and in early recognition and clearance of bacteria (Silva *et al.*, 2015). For instance, in a model of human macrophages infected with *Mycobacterium*

tuberculosis, it has been observed that the infection leads to the specific expression of several miRNAs that play key roles in immune and inflammatory pathways (Zheng *et al.*, 2015). In the context of PD, up or down-regulation of several miRNAs expression have also been observed such as miR-155, miR-200 or miR-146 that are involved in the regulation of several cellular processes including the control of Toll-like receptor (TLR) sensitivity, cell cycle, apoptosis and autophagy (Kebschull *et al.*, 2015). More specifically, effects on miRNA regulation induced by keystone pathogens such as *Pg* have also been investigated. In macrophages, stimulation by *Pg*-lipopolysaccharide modulates the expression of miR-24, a negative regulator of classical macrophage activation (Fordham *et al.*, 2015). In our model, *Pg* infection down-regulated mmu-miR-211-3p expression; this observation was also visible in an infection model of *Candida albicans,* contributing to the suppression of the host-immune response (Li *et al.*, 2014). Interestingly some other miRNAs have already been described as potential regulator of the host-immune response induced by *Pg* or its virulence factors such as miR-146a that down-regulates pro-inflammatory cytokine secretion through blocking of TLRs pathways *in vitro* (Benakanakere *et al.*, 2009; Jiang *et al.*, 2015) or *in vivo* (Nahid *et al.*, 2011). Several others pathways have been identified as putative targets for *Pg* leading to uncontrolled cytokines secretion such as SOCS3 (Moffatt & Lamont, 2011).

In the study, the effects induced by *Pg* infection were evaluated on 1,908 miRNAs. We observed that the infection leads to the specific modulation of the expression for 8 miRNAs: mmu-miR-155-5p, mmu-miR-211-3p, mmu-miR-2137, mmu-miR-3473b, mmu-miR-3473e, mmu-miR-6975-5p, mmu-miR-7674-5p, and mmu-miR-8109.

MiR-155 expression was up-regulated by *Pg* infection. This miRNA is abundantly expressed in immune cells, such as macrophages, active B and T cells, and in dendritic cells. It is involved in the immune response as well as in the protection against the harmful effects

of inflammation through the modulation of pathways related to apoptosis, proliferation and host-pathogen interaction(s) (Dickey *et al.*, 2016). Interestingly, in human gingival tissues affected by PD, an increase in miR-155 expression has already been observed (Stoecklin-Wasmer *et al.*, 2012), with several pathogens seemingly able to increase it. In a model of macrophages infected with *Helicobacter pylori*, the increased expression of miR-155 acts as an inflammatory promoter, inducing pro-inflammatory cytokines secretion (TNF-α, IL-23, IL-10, IL-8) (Yao *et al.*, 2015). However, in our *in vitro* model of transfection, miR-155 did not modify the secretion of TNF-α while its inhibition increased TNF-α level significantly, demonstrating a potentially differential effect. The observed effect might be dependent on the type of pathogen, cell type or the methods of miRNA delivery.

Interestingly, some bemusing results have been observed regarding the effects of miR-7674 and 8109 and TNF-α secretion while transfection with corresponding mimics and inhibitors induced both an increase of this cytokine secretion. It appears difficult to explain such unspecific modulation as precise targets related to TNF-α are not already described for these miRNAs. Additional experiments are required to fill those gaps of knowledge.

Regarding IL-10, some of the tested miRNAs displayed effects on its secretion in macrophages through the increase of this anti-inflammatory cytokine level. It is important to take into account that this observed increase of IL-10 secretion in transfected BMMs was small, emphasizing the need of confirmatory experiments regarding their impact on specific molecular pathways associated to IL-10 secretion. However, we can hypothesize that this may underline the potential role of these particular miRNAs on the innate immune response, since the down-regulation of miRNA expression by *Pg*-infection is a known bacterial survival strategy (Martin *et al.*, 2003; Yilmaz *et al.*, 2004). Therefore, these effects may contribute to the modulation of the host-response by *Pg* as suggested by the bioinformatics analysis.

Since PD is a chronic disease, infection may occur in already activated cells. Accordingly, the effect of *Pg* infection has been evaluated in pre-treated macrophages. Our results showed that the cell response to infection is modulated by such pre-treatment. For instance, a decrease of TNF- α secretion was observed in cells transfected with miR-155 and infected with *Pg*. Therefore, we hypothesized that the modulation of miR-155 expression by *Pg* is one of the mechanisms developed by the bacteria to restrain host-immune response to *Pg* infection. An anti-inflammatory effect was also observed when macrophages were transfected with anti-miR-2137 and infected with *Pg* resulting in an amplification of anti-inflammatory IL-10 secretion. From a therapeutic point of view, their ability to reduce the pro-inflammatory and to promote anti-inflammatory aspects of the host-response may be an interesting strategy to control the adverse effects induced by *Pg* infection.

Furthermore, our *in vitro* results were confirmed *in vivo* in a proof of concept mouse model. We elected to use the calvarial model for proof of concept to assess the impact of identified miRNAs mimics or inhibitors on the modulation of bone resorption induced by *Pg* (Graves *et al.,* 2012). This model has often been used to study bone repair and soft tissue healing in response to infection and allows the delivery of a precise amount of the miRNAs to a proper location in the context of a monoinfection associated with *Pg*. At the histological level, *Pg* infection induced bone loss, as reported previously (Meka *et al.*, 2010). Interestingly, co-injection with miR-155 or anti-miR-2137 decreased significantly some aspects of the induced lesion, notably by reducing its size. Through their modulation of macrophage polarization, as for miR-155 (Essandoh *et al.*, 2016), the therapeutic potential of miRNAs has already been proposed in the treatment of several inflammation-related diseases. Previously, it was shown that miR-155 was able to affect the expression levels of other miRNAs (Kebschull *et al.*, 2015), which may explain the observed effect *in vivo*. Such a role was already suggested

for miR-155 in a previous study (Zhang *et al.*, 2012) where this miRNA was described as having modulated osteoclastogenesis by targeting SOCS1 and MITF. Interestingly, our *in vivo* model showed that the reduction of TNF-α by miR-155 was not enough to significantly decrease ICI, bone loss or osteoclast activity. Further investigation into the role of miR-155 in inflammation might reveal an alternative pathway. Regarding mmu-miR-2137, *in vitro* results were substantiated *in vivo* when anti-miR-2137 was co-injected with *Pg,* leading to a reduction in osteoclast activity and bone loss. This indicated a potential role in bone metabolism for anti-miR-2137 and revealed that the increase of IL-10 production caused by the miR-2137 inhibition was sufficient to produce a robust reduction in *Pg*-induced inflammatory cell infiltrates, bone loss, or osteoclast activity. However, the injection of the combination group did not affect the size of the lesion associated with *Pg* infection as we had hypothesized. This may be a consequence of the ability of miR-155 to affect the expression of other miRNAs (Kebschull *et al.*, 2015). This could also be attributed to the fact that we used a lower concentration of each miRNA, due to the inherent miRNA toxicity seen at a higher concentration in our *in vivo* model. More importantly, the quantitative histological examination revealed that the effect of miRNA-155 on TNF-α was not sufficient to reduce the strong inflammation produced by *Pg*, which in turn could reverse the robust effect that was produced by anti-miR-2137. However, osteoclast activity was significantly reduced by this combination. These results should be confirmed in a specific model of experimental periodontitis such as oral gavage or with the infected-ligature induced model (Graves *et al.*, 2012) to evaluate precisely the potential therapeutic interest of these miRNAs in the context of a more complex lesion induced by the biofilm multispecies complex present in PD.

Recently, the roles and functions of miRNAs have been more appreciated in the context of PD. However, available studies analyzed miRNA expression between healthy and diseased

gingival biopsies without taking the differences of cell populations into account, leading to biased results (Kebschull *et al.*, 2015). To prevent skewed results due to preactivation of macrophage cells, our study focused on BMMs that can be considered to be naïve cell population. Indeed, the macrophages response to infection is certainly under the influence of several factors including preactivation (Papadopoulos *et al.*, 2016) ruling out using periotoneal macrophages.

Micro-RNA research in the periodontal field is a work in progress as knowledge increases continuously. However, the identification of new miRNA sequences calls for attention. In our study, some of the identified miRNAs were poorly described in the literature and the potential molecular pathways involved in their action could only be approached through bioinformatics analysis. Therefore, further research using other types of immune and periodontal cells but also specific *in vivo* models of periodontitis (Graves *et al.*, 2012) should pave the way for a better understanding of their role in periodontal disease development and to identify their potential use as therapeutics. Their pivotal role in a network of cellular mechanisms may allow us to use them to target specifically well identified pathways with the aim to control infection related process. The development of specific carriers is mandatory to develop highly-selective miR based therapies.

The focus of the second study was to test whether PGIcNAc material can produce a reliable alternative to BMP2 for bone formation. It is known that BMP2 has powerful bone regeneration capability and improves bone formation (Kim *et al.*, 2014). BMP2 can induce ectopic bone formation if expressed at sufficient concentrations at ectopic locations (Tachi *et al.*, 2011). BMP2 belongs to the TGF-β signaling pathway superfamily, which modulates the bone growth and skeletal development (Wang *et al.*, 2014; Wu *et al.*, 2016). As it was shown in X-ray analysis, histological measurements, and ALP activity staining. Namely, all methods

indicate that the addition of BMP2 was sufficient to induce bone formation in CSD. More importantly, BMP2 combination with the TM gel or sheet did not inhibit the strong effect of BMP2 to bone formation. We also noticed that the TM gel could work as a BMP2 carrier material. The physical form of the materials has been demonstrated to revel significant differences biologically. Size, shape and texture of a particular materials can play an important role in the biological response (Hansen *et al.*, 2006; Mitragotri & Lahann, 2009). Importantly, in our study, the different physical forms of the same materials (TM gel, powder and sheet) did not shown increase of bone formation and did not affect the regenerated bone. This indicated that the materials can be safely used as a carrier for osteogenic mediators.

Controversial uses of PRP in bone formation studies were reported in the literature. Many reports have indicated that the PRP enhanced bone formation (Albanese *et al.*, 2013). Other reports showed that PRP was not sufficient to produce bone (Roldan *et al.*, 2004; Sarkar *et al.*, 2006). Our results support that PRP does not inhibit bone formation; however, PRP alone was unable to close the 5mm CSD. This may be due to the size of the defect induced in this study. Many reports have indicated that PRP is a better adjunct for soft tissue healing than for bone (Albanese *et al.*, 2013). In addition, it has been reported that PRP could produce better results when combined with other materials (Albanese *et al.*, 2013).

Multiple studies have also reported that L-PRF induced bone formation in humans and allowed for faster healing (Marenzi *et al.*, 2015). Reports demonstrate that the use of L-PRF can reduce post-surgical pain and enhance soft tissue healing (Munoz *et al.*, 2016). L-PRF was also indicated for enhanced osseointegration after dental implant placement (Öncü *et al.*, 2016). Our data support that L-PRF did not inhibit bone healing; however, it was not sufficient to close the 5mm CSD. This result may be due to the defect size we used in this study. Additionally, L-PRF, as indicated by many studies, is more suited for combined hard and soft

tissue healing instead of CSD regeneration (Marenzi *et al.*, 2015; Munoz *et al.*, 2016; Öncü *et al.*, 2016). This desired effect may be attributed to its use in the oral cavity, where improved blood circulations and sub-critical size bone defect exist.

Results in this study suggest that PGIcNAc material is bone friendly. PGIcNAc can merge with the newly formed bone and would not interfere with or inhibit new bone formation in any physical form. Regardless of the physical form, sheet, powder or gel, PGIcNAc was able to be incorporate within the bone. This indicates that the material can serve as a good candidate for osteogenic substances. Multiple publications have proposed that PGIcNAc material could be used as a blood clotting agent via the induction of platelets, red blood cells aggregations and aiding endothelial cell formation (Ikeda *et al.*, 2002; Thatte *et al.*, 2004; Thatte *et al.*, 2004). It also suggested that the PGIcNAc can help the prevention of bleeding due to varicose veins in animal study (Kulling *et al.*, 1999). Another important use of the material is in antibiotic resistance, detergent resistance, and biofilm forming perio-pathogen (Izano *et al.*, 2007; Izano *et al.*, 2008; Choi *et al.*, 2009). However, no reports have suggested that this material could aid in osteogenic formation. Our study demonstrated that the PGIcNAc does not possess any osteogenic property. However, we did demonstrate that this material can be utilized as a carrier for osteogenic substances due to its bone compatibility.

Future studies utilizing a higher viscosity gel form of TM (PGIcNAc) in combination with osteogenic substances may produce a reliable, non-toxic, and non-carcinogenic bone substitute.

8. BIBLIOGRAPHY

Albanese, A., Licata, M. E., Polizzi, B., & Campisi, G. (2013). Platelet-Rich Plasma (Prp) in Dental and Oral Surgery: From the Wound Healing to Bone Regeneration. *Immunity & Ageing : I & A, 10*, 23-23. doi:10.1186/1742-4933-10-23

Assuma, R., Oates, T., Cochran, D., Amar, S., & Graves, D. T. (1998). Il-1 and Tnf Antagonists Inhibit the Inflammatory Response and Bone Loss in Experimental Periodontitis. *The Journal of Immunology, 160*(1), 403-409.

Baker, P. J. (2000). The Role of Immune Responses in Bone Loss During Periodontal Disease. *Microbes and Infection, 2*(10), 1181-1192. doi:http://doi.org/10.1016/S1286-4579(00)01272-7

Baumann, V., & Winkler, J. (2014). Mirna-Based Therapies: Strategies and Delivery Platforms for Oligonucleotide and Non-Oligonucleotide Agents. *Future medicinal chemistry, 6*(17), 1967-1984. doi:10.4155/fmc.14.116

Benakanakere, M. R., Li, Q., Eskan, M. A., Singh, A. V., Zhao, J., Galicia, J. C., Stathopoulou, P., Knudsen, T. B., & Kinane, D. F. (2009). Modulation of Tlr2 Protein Expression by Mir-105 in Human Oral Keratinocytes. *The Journal of Biological Chemistry, 284*(34), 23107-23115. doi:10.1074/jbc.M109.013862

Benjamini, Y., & Hochberg, Y. (1995). Controlling the False Discovery Rate: A Practical and Powerful Approach to Multiple Testing. *Journal of the Royal Statistical Society. Series B (Methodological), 57*(1), 289-300. doi:citeulike-article-id:1042553 doi: 10.2307/2346101

Bugueno, I. M., Khelif, Y., Seelam, N., Morand, D. N., Tenenbaum, H., Davideau, J. L., & Huck, O. (2016). Porphyromonas Gingivalis Differentially Modulates Cell Death Profile in Ox-Ldl and Tnf-A Pre-Treated Endothelial Cells. *PLoS One, 11*(4), 1-18. doi:10.1371/journal.pone.0154590

Chiang, C. Y., Kyritsis, G., Graves, D. T., & Amar, S. (1999). Interleukin-1 and Tumor Necrosis Factor Activities Partially Account for Calvarial Bone Resorption Induced by Local Injection of Lipopolysaccharide. *Infection and Immunity, 67*(8), 4231-4236.

Choi, A. H., Slamti, L., Avci, F. Y., Pier, G. B., & Maira-Litrán, T. (2009). The Pgaabcd Locus of Acinetobacter Baumannii Encodes the Production of Poly-B-1-6-N-Acetylglucosamine, Which Is Critical for Biofilm Formation. *Journal of bacteriology, 191*(19), 5953-5963.

Cochran, D. L. (2008). Inflammation and Bone Loss in Periodontal Disease. *Journal of Periodontology, 79*(8s), 1569-1576. doi:10.1902/jop.2008.080233

Cordova, L. A., Stresing, V., Gobin, B., Rosset, P., Passuti, N., Gouin, F., Trichet, V., Layrolle, P., & Heymann, D. (2014). Orthopaedic Implant Failure: Aseptic Implant Loosening--the Contribution and Future Challenges of Mouse Models in Translational Research. *Clinical Science (Lond), 127*(5), 277-293. doi:10.1042/cs20130338

Cowan, C. M., Shi, Y.-Y., Aalami, O. O., Chou, Y.-F., Mari, C., Thomas, R., Quarto, N., Contag, C. H., Wu, B., & Longaker, M. T. (2004). Adipose-Derived Adult Stromal Cells Heal Critical-Size Mouse Calvarial Defects. *Nature Biotechnology, 22*(5), 560-567. doi:http://www.nature.com/nbt/journal/v22/n5/suppinfo/nbt958_S1.html

Di Lauro, A. E., Abbate, D., Dell'angelo, B., Iannaccone, G. A., Scotto, F., & Sammartino, G. (2015). Soft Tissue Regeneration Using Leukocyte-Platelet Rich Fibrin after Exeresis of Hyperplastic Gingival Lesions: Two Case Reports. *Journal of Medical Case Reports, 9*, 252-257. doi:10.1186/s13256-015-0714-5

Dickey, L. L., Worne, C. L., Glover, J. L., Lane, T. E., & O'connell, R. M. (2016). Microrna-155 Enhances T Cell Trafficking and Antiviral Effector Function in a Model of Coronavirus-Induced Neurologic Disease. *Journal of Neuroinflammation, 13*(1), 240-252. doi:10.1186/s12974-016-0699-z

Dimitriou, R., Tsiridis, E., & Giannoudis, P. V. (2005). Current Concepts of Molecular Aspects of Bone Healing. *Injury, 36*(12), 1392–1404

Dohan, D. M., Choukroun, J., Diss, A., Dohan, S. L., Dohan, A. J., Mouhyi, J., & Gogly, B. (2006). Platelet-Rich Fibrin (Prf): A Second-Generation Platelet Concentrate. Part I: Technological Concepts and Evolution. *Oral Surg Oral Med Oral Pathol Oral Radiol Endod, 101*(3), e37-44. doi:10.1016/j.tripleo.2005.07.008

Dweep, H., Gretz, N., & Sticht, C. (2014). Mirwalk Database for Mirna-Target Interactions. *Methods in Molecular Biology, 1182*, 289-305. doi:10.1007/978-1-4939-1062-5_25

Enright, A. J., Van Dongen, S., & Ouzounis, C. A. (2002). An Efficient Algorithm for Large-Scale Detection of Protein Families. *Nucleic Acids Research, 30*(7), 1575-1584.

Essandoh, K., Li, Y., Huo, J., & Fan, G. C. (2016). Mirna-Mediated Macrophage Polarization and Its Potential Role in the Regulation of Inflammatory Response. *Shock, 46*(2), 122-131. doi:10.1097/shk.0000000000000604

Filipowicz, W., Bhattacharyya, S. N., & Sonenberg, N. (2008). Mechanisms of Post-Transcriptional Regulation by Micrornas: Are the Answers in Sight? *Nature Review Genetics, 9*(2), 102-114. doi:10.1038/nrg2290

Fordham, J. B., Naqvi, A. R., & Nares, S. (2015). Mir-24 Regulates Macrophage Polarization and Plasticity. *Journal of Clinical and Cellular Immunology, 6*(5), 362-364. doi:10.4172/2155-9899.1000362

Gemmell, E., Mchugh, G. B., Grieco, D. A., & Seymour, G. J. (2001). Costimulatory Molecules in Human Periodontal Disease Tissues. *Journal of Periodontal Research, 36*(2), 92-100.

Giannobile, W. V. (2008). Host-Response Therapeutics for Periodontal Diseases. *Journal of Periodontology, 79*(8 Suppl), 1592-1600. doi:10.1902/jop.2008.080174

Graves, D. T., Kang, J., Andriankaja, O., Wada, K., & Rossa, C., Jr. (2012). Animal Models to Study Host-Bacteria Interactions Involved in Periodontitis. *Frontiers of Oral Biology, 15*, 117-132. doi:10.1159/000329675

Graves, D. T., Naguib, G., Huafei, L., Desta, T., & Amar, S. (2005). Porphyromonas Gingivalis Fimbriae Are Pro-Inflammatory but Do Not Play a Prominent Role in the Innate Immune Response to P. Gingivalis. *Journal of Endotoxin Research, 11*(1), 13-18. doi:10.1177/09680519050110010501

Grossi, S. G., Genco, R. J., Machtet, E. E., Ho, A. W., Koch, G., Dunford, R., Zambon, J. J., & Hausmann, E. (1995). Assessment of Risk for Periodontal Disease. Ii. Risk Indicators for Alveolar Bone Loss. *Journal of Periodontology, 66*(1), 23-29. doi:10.1902/jop.1995.66.1.23

Hajishengallis, G. (2015). Periodontitis: From Microbial Immune Subversion to Systemic Inflammation. *Nature Reviews Immunology, 15*(1), 30-44. doi:10.1038/nri3785

Hajishengallis, G., & Lamont, R. J. (2014). Breaking Bad: Manipulation of the Host Response by Porphyromonas Gingivalis. *European Journal of Immunology, 44*(2), 328-338. doi:10.1002/eji.201344202

Hansen, T., Clermont, G., Alves, A., Eloy, R., Brochhausen, C., Boutrand, J. P., Gatti, A. M., & James Kirkpatrick, C. (2006). Biological Tolerance of Different Materials in Bulk and Nanoparticulate Form in a Rat Model: Sarcoma Development by Nanoparticles. *Journal of the Royal Society Interface, 3*(11), 767-775. doi:10.1098/rsif.2006.0145

Hoodless, P. A., Haerry, T., Abdollah, S., Stapleton, M., O'connor, M. B., Attisano, L., & Wrana, J. L. (1996). Madr1, a Mad-Related Protein That Functions in Bmp2 Signaling Pathways. *Cell, 85*(4), 489-500. doi:http://dx.doi.org/10.1016/S0092-8674(00)81250-7

Hosin, A. A., Prasad, A., Viiri, L. E., Davies, A. H., & Shalhoub, J. (2014). Micrornas in Atherosclerosis. *Journal of Vascular Research, 51*(5), 338-349. doi:10.1159/000368193

Huang, D. W., Sherman, B. T., & Lempicki, R. A. (2008). Systematic and Integrative Analysis of Large Gene Lists Using David Bioinformatics Resources. *Nature Protocols, 4*(1), 44-57. doi:http://www.nature.com/nprot/journal/v4/n1/suppinfo/nprot.2008.211_S1.html

Huck, O., Elkaim, R., Davideau, J. L., & Tenenbaum, H. (2015). Porphyromonas Gingivalis-Impaired Innate Immune Response Via Nlrp3 Proteolysis in Endothelial Cells. *Innate Immunity, 21*(1), 65-72. doi:10.1177/1753425914523459

Ikeda, Y., Young, L. H., Vournakis, J. N., & Lefer, A. M. (2002). Vascular Effects of Poly-N-Acetylglucosamine in Isolated Rat Aortic Rings. *Journal of Surgical Research, 102*(2), 215-220. doi:http://dx.doi.org/10.1006/jsre.2001.6323

Irizarry, R. A., Hobbs, B., Collin, F., Beazer-Barclay, Y. D., Antonellis, K. J., Scherf, U., & Speed, T. P. (2003). Exploration, Normalization, and Summaries of High Density Oligonucleotide Array Probe Level Data. *Biostatistics, 4*(2), 249-264. doi:10.1093/biostatistics/4.2.249

Izano, E. A., Sadovskaya, I., Vinogradov, E., Mulks, M. H., Velliyagounder, K., Ragunath, C., Kher, W. B., Ramasubbu, N., Jabbouri, S., Perry, M. B., & Kaplan, J. B. (2007). Poly-N-Acetylglucosamine Mediates Biofilm Formation and Antibiotic Resistance in Actinobacillus Pleuropneumoniae. *Microbial Pathogenesis, 43*(1), 1-9. doi:http://dx.doi.org/10.1016/j.micpath.2007.02.004

Izano, E. A., Sadovskaya, I., Wang, H., Vinogradov, E., Ragunath, C., Ramasubbu, N., Jabbouri, S., Perry, M. B., & Kaplan, J. B. (2008). Poly-N-Acetylglucosamine Mediates Biofilm Formation and Detergent Resistance in Aggregatibacter Actinomycetemcomitans. *Microbial Pathogenesis, 44*(1), 52-60. doi:http://dx.doi.org/10.1016/j.micpath.2007.08.004

Jämsen, E., Kouri, V.-P., Ainola, M., Goodman, S. B., Nordström, D. C., Eklund, K. K., & Pajarinen, J. (2017). Correlations between Macrophage Polarizing Cytokines, Inflammatory Mediators, Osteoclast Activity, and Toll-Like Receptors in Tissues around Aseptically Loosened Hip Implants. *Journal of Biomedical Materials Research Part A, 105*(2), 454-463. doi:10.1002/jbm.a.35913

Jiang, S. Y., Xue, D., Xie, Y. F., Zhu, D. W., Dong, Y. Y., Wei, C. C., & Deng, J. Y. (2015). The Negative Feedback Regulation of Microrna-146a in Human Periodontal Ligament Cells after Porphyromonas Gingivalis Lipopolysaccharide Stimulation. *Inflammation Research, 64*(6), 441-451. doi:10.1007/s00011-015-0824-y

Joshi Jubert, N., Rodriguez, L., Reverte-Vinaixa, M. M., & Navarro, A. (2017). Platelet-Rich Plasma Injections for Advanced Knee Osteoarthritis: A Prospective, Randomized, Double-Blinded Clinical Trial. *Orthopaedic Journal of Sports Medicine, 5*(2), 1-11. doi:10.1177/2325967116689386

Kato, Y., Hagiwara, M., Ishihara, Y., Isoda, R., Sugiura, S., Komatsu, T., Ishida, N., Noguchi, T., & Matsushita, K. (2014). Tnf-Alpha Augmented Porphyromonas Gingivalis Invasion in Human Gingival Epithelial Cells through Rab5 and Icam-1. *BMC Microbiol, 14*, 229-242. doi:10.1186/s12866-014-0229-z

Kawai, M., Bessho, K., Kaihara, S., Sonobe, J., Oda, K., Iizuka, T., & Maruyama, H. (2003). Ectopic Bone Formation by Human Bone Morphogenetic Protein-2 Gene Transfer to Skeletal Muscle Using Transcutaneous Electroporation. *Human Gene Therapy, 14*(16), 1547-1556. doi:10.1089/104303403322495052

Kebschull, M., & Papapanou, P. N. (2015). Mini but Mighty: Micrornas in the Pathobiology of Periodontal Disease. *Periodontology 2000, 69*(1), 201-220. doi:10.1111/prd.12095

Kim, J. H., Woo, S. M., Choi, N. K., Kim, W. J., Kim, S. M., & Jung, J. Y. (2017). Effect of Platelet-Rich Fibrin on Odontoblastic Differentiation in Human Dental Pulp Cells Exposed to Lipopolysaccharide. *Journal of Endodontics, 43*(3), 433-438. doi:10.1016/j.joen.2016.11.002

Kim, M.-J., Kim, K.-M., Kim, J., & Kim, K.-N. (2014). Bmp-2 Promotes Oral Squamous Carcinoma Cell Invasion by Inducing Ccl5 Release. *PLoS One, 9*(10), 1-8. doi:10.1371/journal.pone.0108170

Kim, S. E., Kim, C. S., Yun, Y. P., Yang, D. H., Park, K., Kim, S. E., Jeong, C. M., & Huh, J. B. (2014). Improving Osteoblast Functions and Bone Formation Upon Bmp-2 Immobilization on Titanium Modified with Heparin. *Carbohydrate Polymers, 114*, 123-132. doi:10.1016/j.carbpol.2014.08.005

Kulling, D., Vournakis, J. N., Woo, S., Demcheva, M. V., Tagge, D. U., Rios, G., Finkielsztein, S., & Hawes, R. H. (1999). Endoscopic Injection of Bleeding Esophageal Varices with a Poly-N-Acetyl Glucosamine Gel Formulation in the Canine Portal Hypertension Model. *Gastrointestinal Endoscopy, 49*(6), 764-771. doi:http://dx.doi.org/10.1016/S0016-5107(99)70298-1

Lennox, K. A., & Behlke, M. A. (2011). Chemical Modification and Design of Anti-Mirna Oligonucleotides. *Gene Therapy, 18*(12), 1111-1120. doi:10.1038/gt.2011.100

Li, X. Y., Zhang, K., Jiang, Z. Y., & Cai, L. H. (2014). Mir-204/Mir-211 Downregulation Contributes to Candidemia-Induced Kidney Injuries Via Derepression of Hmx1 Expression. *Life Science, 102*(2), 139-144. doi:10.1016/j.lfs.2014.03.010

Marenzi, G., Riccitiello, F., Tia, M., Di Lauro, A., & Sammartino, G. (2015). Influence of Leukocyte- and Platelet-Rich Fibrin (L-Prf) in the Healing of Simple Postextraction Sockets: A Split-Mouth Study. *BioMed Research International, 2015*, 1-6. doi:10.1155/2015/369273

Marques-Rocha, J. L., Samblas, M., Milagro, F. I., Bressan, J., Martinez, J. A., & Marti, A. (2015). Noncoding Rnas, Cytokines, and Inflammation-Related Diseases. *Faseb Journal, 29*(9), 3595-3611. doi:10.1096/fj.14-260323

Martin, M., Schifferle, R. E., Cuesta, N., Vogel, S. N., Katz, J., & Michalek, S. M. (2003). Role of the Phosphatidylinositol 3 Kinase-Akt Pathway in the Regulation of Il-10 and Il-12 by Porphyromonas Gingivalis Lipopolysaccharide. *Journal of Immunology, 171*(2), 717-725.

Marx, R. E. (2004). Platelet-Rich Plasma: Evidence to Support Its Use. *Journal of Oral and Maxillofacial Surgry, 62*(4), 489-496.

Marx, R. E., Carlson, E. R., Eichstaedt, R. M., Schimmele, S. R., Strauss, J. E., & Georgeff, K. R. (1998). Platelet-Rich Plasma. *Oral Surgery, Oral Medicine, Oral Pathology, Oral Radiology, and Endodontology, 85*(6), 638-646. doi:http://dx.doi.org/10.1016/S1079-2104(98)90029-4

Maus, E. A. (2012). Successful Treatment of Two Refractory Venous Stasis Ulcers Treated with a Novel Poly-N-Acetyl Glucosamine-Derived Membrane. *BMJ Case Reports, 2012*, 1-3. doi:10.1136/bcr.03.2012.6091

Meka, A., Bakthavatchalu, V., Sathishkumar, S., Lopez, M. C., Verma, R. K., Wallet, S. M., Bhattacharyya, I., Boyce, B. F., Handfield, M., Lamont, R. J., Baker, H. V., Ebersole, J. L., & Kesavalu, L. (2010). Porphyromonas Gingivalis Infection-Induced Tissue and Bone Transcriptional Profiles. *Molecular Oral Microbiology, 25*(1), 61-74. doi:10.1111/j.2041-1014.2009.00555.x

Mitragotri, S., & Lahann, J. (2009). Physical Approaches to Biomaterial Design. *Nature Materials, 8*(1), 15-23.

Moffatt, C. E., & Lamont, R. J. (2011). Porphyromonas Gingivalis Induction of Microrna-203 Expression Controls Suppressor of Cytokine Signaling 3 in Gingival Epithelial Cells. *Infection and Immunity, 79*(7), 2632-2637. doi:10.1128/iai.00082-11

Morandini, A. C., Ramos-Junior, E. S., Potempa, J., Nguyen, K. A., Oliveira, A. C., Bellio, M., Ojcius, D. M., Scharfstein, J., & Coutinho-Silva, R. (2014). Porphyromonas Gingivalis Fimbriae Dampen P2x7-Dependent Interleukin-1beta Secretion. *Journal of Innate Immunity, 6*(6), 831-845. doi:10.1159/000363338

Morris, J. H., Apeltsin, L., Newman, A. M., Baumbach, J., Wittkop, T., Su, G., Bader, G. D., & Ferrin, T. E. (2011). Clustermaker: A Multi-Algorithm Clustering Plugin for Cytoscape. *BMC Bioinformatics, 12*, 436-449. doi:10.1186/1471-2105-12-436

Mountziaris, P. M., & Mikos, A. G. (2008). Modulation of the Inflammatory Response for Enhanced Bone Tissue Regeneration. *Tissue Engineering Part B: Reviews, 14*(2), 179-186.

Munoz, F., Jiménez, C., Espinoza, D., Vervelle, A., Beugnet, J., & Haidar, Z. (2016). Use of Leukocyte and Platelet-Rich Fibrin (L-Prf) in Periodontally Accelerated Osteogenic Orthodontics (Paoo): Clinical Effects on Edema and Pain. *Journal of Clinical and Experimental Dentistry, 8*(2), e119-e124. doi:10.4317/jced.52760

Nahid, M. A., Rivera, M., Lucas, A., Chan, E. K., & Kesavalu, L. (2011). Polymicrobial Infection with Periodontal Pathogens Specifically Enhances Microrna Mir-146a in Apoe-/- Mice During Experimental Periodontal Disease. *Infection and Immunity, 79*(4), 1597-1605. doi:10.1128/iai.01062-10

Okada, H., & Murakami, S. (1998). Cytokine Expression in Periodontal Health and Disease. *Critical Reviews in Oral Biology and Medicine, 9*(3), 248-266.

Olczak, T., Sosicka, P., & Olczak, M. (2015). Hmuy Is an Important Virulence Factor for Porphyromonas Gingivalis Growth in the Heme-Limited Host Environment and Infection of Macrophages. *Biochemical and Biophysical Research Communications, 467*(4), 748-753. doi:10.1016/j.bbrc.2015.10.070

Öncü, E., Bayram, B., Kantarcı, A., Gülsever, S., & Alaaddinoğlu, E.-E. (2016). Posıtıve Effect of Platelet Rich Fibrin on Osseointegration. *Medicina Oral, Patología Oral y Cirugía Bucal, 21*(5), e601-e607. doi:10.4317/medoral.21026

Papadopoulos, G., Shaik-Dasthagirisaheb, Y. B., Huang, N., Viglianti, G. A., Henderson, A. J., Kantarci, A., & Gibson, F. C. (2016). Immunologic Environment Influences Macrophage Response to Porphyromonas Gingivalis. *Molecular Oral Microbiology, 32*(3), 250-261. doi:10.1111/omi.12168

Pihlstrom, B. L., Michalowicz, B. S., & Johnson, N. W. (2005). Periodontal Diseases. *Lancet, 366*(9499), 1809-1820. doi:10.1016/s0140-6736(05)67728-8

Rodrigues, P. H., Reyes, L., Chadda, A. S., Belanger, M., Wallet, S. M., Akin, D., Dunn, W., Jr., & Progulske-Fox, A. (2012). Porphyromonas Gingivalis Strain Specific Interactions with Human Coronary Artery Endothelial Cells: A Comparative Study. *PLoS One, 7*(12), 1-10. doi:10.1371/journal.pone.0052606

Roldan, J. C., Jepsen, S., Miller, J., Freitag, S., Rueger, D. C., Acil, Y., & Terheyden, H. (2004). Bone Formation in the Presence of Platelet-Rich Plasma Vs. Bone Morphogenetic Protein-7. *Bone, 34*(1), 80-90.

Sarkar, M. R., Augat, P., Shefelbine, S. J., Schorlemmer, S., Huber-Lang, M., Claes, L., Kinzl, L., & Ignatius, A. (2006). Bone Formation in a Long Bone Defect Model Using a Platelet-Rich Plasma-Loaded Collagen Scaffold. *Biomaterials, 27*(9), 1817-1823.

Shannon, P., Markiel, A., Ozier, O., Baliga, N. S., Wang, J. T., Ramage, D., Amin, N., Schwikowski, B., & Ideker, T. (2003). Cytoscape: A Software Environment for Integrated Models of Biomolecular Interaction Networks. *Genome Research, 13*(11), 2498-2504. doi:10.1101/gr.1239303

Silva, N., Abusleme, L., Bravo, D., Dutzan, N., Garcia-Sesnich, J., Vernal, R., Hernandez, M., & Gamonal, J. (2015). Host Response Mechanisms in Periodontal Diseases. *Journal of Applied Oral Science, 23*(3), 329-355. doi:10.1590/1678-775720140259

Simo, G., Lueong, S., Grebaut, P., Guny, G., & Hoheisel, J. D. (2015). Micro Rna Expression Profiles in Peripheral Blood Cells of Rats That Were Experimentally Infected with Trypanosoma Congolense and Different Trypanosoma Brucei Subspecies. *Microbes and Infection, 17*(8), 596-608. doi:10.1016/j.micinf.2015.03.004

Spicer, P. P., Kretlow, J. D., Young, S., Jansen, J. A., Kasper, F. K., & Mikos, A. G. (2012). Evaluation of Bone Regeneration Using the Rat Critical Size Calvarial Defect. *Nature Protocols, 7*(10), 1918-1929.

Stoecklin-Wasmer, C., Guarnieri, P., Celenti, R., Demmer, R. T., Kebschull, M., & Papapanou, P. N. (2012). Micrornas and Their Target Genes in Gingival Tissues. *Journal of Dental Research, 91*(10), 934-940. doi:10.1177/0022034512456551

Szklarczyk, D., Franceschini, A., Wyder, S., Forslund, K., Heller, D., Huerta-Cepas, J., Simonovic, M., Roth, A., Santos, A., Tsafou, K. P., Kuhn, M., Bork, P., Jensen, L. J., & Von Mering, C. (2015). String V10: Protein-Protein Interaction Networks, Integrated over the Tree of Life. *Nucleic Acids Research, 43*(Database issue), D447-452. doi:10.1093/nar/gku1003

Tachi, K., Takami, M., Sato, H., Mochizuki, A., Zhao, B., Miyamoto, Y., Tsukasaki, H., Inoue, T., Shintani, S., Koike, T., Honda, Y., Suzuki, O., Baba, K., & Kamijo, R. (2011). Enhancement of Bone Morphogenetic Protein-2-Induced Ectopic Bone Formation by Transforming Growth Factor-Beta1. *Tissue Engineering Part A, 17*(5-6), 597-606. doi:10.1089/ten.TEA.2010.0094

Thatte, H. S., Zagarins, S., Khuri, S. F., & Fischer, T. H. (2004). Mechanisms of Poly-N-Acetyl Glucosamine Polymer–Mediated Hemostasis: Platelet Interactions. *Journal of Trauma and Acute Care Surgery, 57*(1), S13-S21.

Thatte, H. S., Zagarins, S. E., Amiji, M., & Khuri, S. F. (2004). Poly-N-Acetyl Glucosamine–Mediated Red Blood Cell Interactions. *Journal of Trauma and Acute Care Surgery, 57*(1), S7-S12.

Thomas, M. V., & Puleo, D. A. (2011). Infection, Inflammation, and Bone Regeneration: A Paradoxical Relationship. *Journal of Dental Research, 90*(9), 1052-1061. doi:10.1177/0022034510393967

Varghese, M. P., Manuel, S., & Surej Kumar, L. K. (2017). Potential for Osseous Regeneration of Platelet-Rich Fibrin-a Comparative Study in Mandibular Third Molar Impaction Sockets. *Journal of Oral and Maxillofacial Surgery*. doi:10.1016/j.joms.2017.01.035

Wang, R. N., Green, J., Wang, Z., Deng, Y., Qiao, M., Peabody, M., Zhang, Q., Ye, J., Yan, Z., Denduluri, S., Idowu, O., Li, M., Shen, C., Hu, A., Haydon, R. C., Kang, R., Mok, J., Lee, M. J., Luu, H. L., & Shi, L. L. (2014). Bone Morphogenetic Protein (Bmp) Signaling in Development and Human Diseases. *Genes & Diseases, 1*(1), 87-105. doi:http://dx.doi.org/10.1016/j.gendis.2014.07.005

Weibrich, G., Kleis, W. K. G., Hafner, G., & Hitzler, W. E. (2002). Growth Factor Levels in Platelet-Rich Plasma and Correlations with Donor Age, Sex, and Platelet

Count. *Journal of Cranio-Maxillofacial Surgery, 30*(2), 97-102. doi:http://dx.doi.org/10.1054/jcms.2002.0285

Wu, M., Chen, G., & Li, Y.-P. (2016). Tgf-B and Bmp Signaling in Osteoblast, Skeletal Development, and Bone Formation, Homeostasis and Disease. *Bone Research, 4*, 1-21. doi:10.1038/boneres.2016.9

Yao, Y., Li, G., Wu, J., Zhang, X., & Wang, J. (2015). Inflammatory Response of Macrophages Cultured with Helicobacter Pylori Strains Was Regulated by Mir-155. *International Journal of Clinical and Experimental Pathology, 8*(5), 4545-4554.

Yilmaz, O., Jungas, T., Verbeke, P., & Ojcius, D. M. (2004). Activation of the Phosphatidylinositol 3-Kinase/Akt Pathway Contributes to Survival of Primary Epithelial Cells Infected with the Periodontal Pathogen Porphyromonas Gingivalis. *Infection and Immunity, 72*(7), 3743-3751.

Yu, W. H., Hu, H., Zhou, Q., Xia, Y., & Amar, S. (2010). Bioinformatics Analysis of Macrophages Exposed to Porphyromonas Gingivalis: Implications in Acute Vs. Chronic Infections. *PLoS One, 5*(12), 1-8. doi:10.1371/journal.pone.0015613

Zara, J. N., Siu, R. K., Zhang, X., Shen, J., Ngo, R., Lee, M., Li, W., Chiang, M., Chung, J., Kwak, J., Wu, B. M., Ting, K., & Soo, C. (2011). High Doses of Bone Morphogenetic Protein 2 Induce Structurally Abnormal Bone and Inflammation in Vivo. *Tissue Engineering Part A, 17*(9-10), 1389-1399. doi:10.1089/ten.tea.2010.0555

Zhang, J., Zhao, H., Chen, J., Xia, B., Jin, Y., Wei, W., Shen, J., & Huang, Y. (2012). Interferon-Beta-Induced Mir-155 Inhibits Osteoclast Differentiation by Targeting Socs1 and Mitf. *Febs Letters, 586*(19), 3255-3262. doi:10.1016/j.febslet.2012.06.047

Zhang, X., Goncalves, R., & Mosser, D. M. (2008). The Isolation and Characterization of Murine Macrophages. *Current Protocols in Immunology, Chapter 14*, Unit 14.11. doi:10.1002/0471142735.im1401s83

Zheng, L., Leung, E., Lee, N., Lui, G., To, K. F., Chan, R. C., & Ip, M. (2015). Differential Microrna Expression in Human Macrophages with Mycobacterium Tuberculosis Infection of Beijing/W and Non-Beijing/W Strain Types. *PLoS One, 10*(6), 1-16. doi:10.1371/journal.pone.0126018

Zhou, Q., & Amar, S. (2007). Identification of Signaling Pathways in Macrophage Exposed to Porphyromonas Gingivalis or to Its Purified Cell Wall Components. *Journal of Immunology, 179*(11), 7777-7790.

9. CURRICULUM VITAE